

AD-A230 590



MEASURING THE EFFECTIVENESS OF SPACE:
SATELLITE WEATHER SYSTEMS

THESIS

Steven Trent Wilson
Captain, USAF

AFIT/GSO/ENS/90D-18

DISTRIBUTION STATEMENT A

Approved for public release;
Distribution Unlimited

DEPARTMENT OF THE AIR FORCE
AIR UNIVERSITY
AIR FORCE INSTITUTE OF TECHNOLOGY

Wright-Patterson Air Force Base, Ohio

91 1 3 113

1

AFIT/GSO/ENS/90D-18

DTIC
ELECTE
JAN 07 1991
S D D

MEASURING THE EFFECTIVENESS OF SPACE:
SATELLITE WEATHER SYSTEMS

THESIS

Steven Trent Wilson
Captain, USAF

AFIT/GSO/ENS/90D-18

Approved for public release; distribution unlimited

THESIS APPROVAL

STUDENT: Captain Steven T. Wilson

CLASS: GSO 90-D



THESIS TITLE: Measuring the Effectiveness of Space:
Satellite Weather Systems

DEFENSE DATE: 03 DEC 90

Accession For	
NTIS CRA&I	<input checked="" type="checkbox"/>
DTIC TAB	<input type="checkbox"/>
Unannounced	<input type="checkbox"/>
Justification	
By	
Distribution	
Availability Codes	
Dist	Available or Special
A-1	

COMMITTEE:

NAME/DEPARTMENT

SIGNATURE

Advisor

Major Bruce W. Morlan/ENS

B. W. Morlan

Reader

Major Kenneth W. Bauer, Jr./ENS

Kenneth W. Bauer, Jr.

AFIT/GSO/ENS/90D-18

MEASURING THE EFFECTIVENESS OF SPACE:
SATELLITE WEATHER SYSTEMS

THESIS

Presented to the Faculty of the School of Engineering
of the Air Force Institute of Technology

Air University

In Partial Fulfillment of the
Requirements for the Degree of
Master of Science in Space Operations

Steven Trent Wilson, B.S.

Captain, USAF

December, 1990

Approved for public release; distribution unlimited

Acknowledgments

To Major Bruce W. Morlan; I wish to thank you for talking me into the most difficult of the thesis topics we discussed, and for helping to make the impossible seem only excruciating. Seriously, thanks for everything.

Lieutenant Colonel William P. Baker provided invaluable assistance with both the physics and the calculus used in the model. Any errors in the math, however, are mine.

Mr. Norm Baker and Captain Mark Storz, of the 4th Weather Wing (MAC), have my sincere appreciation for taking the time from their busy schedules to provide me with data and insight into this problem. A special thanks goes to Colonel William B. Freeman, Vice Commander, 4th Weather Wing, for acting as expert decision maker and lending his considerable expertise to the project.

Captains Brad Shaffer, Bill Gaught, and Maurice Martin each rendered their own type of assistance when I needed it most. Without them, I never would have finished on time.

Captain Jay Payne is simply the finest friend a man could have.

As much as I'm indebted to the others, I reserve my greatest appreciation for my wife, Jody, for enduring this demanding period of our life together. There can be few trials more perilous for a new bride than following a wedding and out-of-state move by chronic separation from her new husband. Your belief and support went way beyond the call of duty, and I hope I have a chance to make it up to you some time.

Steven Trent Wilson

Table of Contents

	Page
Acknowledgments	ii
Table of Contents	iii
List of Figures	vii
List of Tables	ix
Abstract	x
 I. Introduction and Background	 1-1
1.1 Background	1-1
1.2 Specific Objective	1-1
1.3 Problem Solving Approach.	1-2
1.4 Overview	1-3
 II. Review of Pertinent Literature	 2-1
2.1 Introduction and Overview	2-1
2.2 Measures of Effectiveness	2-1
2.2.1 General Considerations.	2-1
2.2.2 Common MOEs.	2-5
2.3 Utility Theory.	2-7
2.3.1 Value and Utility.	2-7
2.3.2 Definitions.	2-7
2.3.3 Uncertainty.	2-8
2.3.4 Rational Utility.	2-10
2.3.5 Functional Forms.	2-11
2.4 Summary.	2-11

	Page
III. Methodology	3-1
3.1 Introduction.	3-1
3.2 Define the space meteorological mission.	3-1
3.2.1 Limiting the scope of the problem.	3-1
3.2.2 Limiting assumptions.	3-3
3.2.3 Choose a decision maker.	3-3
3.2.4 Present operational mission scenario to decision maker.	3-5
3.3 Identify factors which influence mission accomplishment.	3-5
3.3.1 Develop list of attributes.	3-5
3.3.2 Refine list of attributes.	3-6
3.3.3 Attribute vector listing.	3-6
3.3.4 Area Factors.	3-7
3.4 Generate a discrete earth model.	3-8
3.4.1 Assumptions.	3-8
3.4.2 Shell definition.	3-9
3.5 Identify relationships between attributes.	3-19
3.5.1 Assign weights to attributes.	3-19
3.5.2 Attribute vector reduction.	3-20
3.5.3 Remaining Attributes.	3-22
3.6 Choose a functional form.	3-22
3.6.1 Independence.	3-22
3.6.2 Additive vs. multiplicative value.	3-23
3.7 Express the value of each attribute over all points of the model.	3-24
3.7.1 Geographic area importance weights.	3-24
3.7.2 Sampling rate.	3-31
3.7.3 Timeliness.	3-32
3.7.4 Resolution.	3-34

	Page
IV. Results and Analysis	4-1
4.1 Introduction.	4-1
4.2 Relative Value curves.	4-1
4.2.1 Sampling rate.	4-1
4.2.2 Timeliness.	4-4
4.2.3 Resolution.	4-6
4.3 MOEs for various subpoints.	4-7
4.4 Significance of the MOE.	4-10
4.4.1 Unit analysis.	4-10
4.4.2 Limits of MOE.	4-11
4.5 Sensitivity to changes in sampling rate attribute.	4-11
4.6 Sensitivity to changes in timeliness attribute.	4-11
4.7 Sensitivity to changes in resolution attribute.	4-14
4.8 Summary.	4-14
V. Conclusion and Recommendations	5-1
5.1 Conclusion.	5-1
5.2 Shortcomings of the model and recommendations for further research.	5-1
Appendix A. Meteorological Satellite (METSAT) Utility Survey	A-1
Appendix B. User Response to METSAT Utility Survey	B-1
Appendix C. Shell model generation file	C-1
Appendix D. Actual Area of shells $s_{i,j}$ for all Values of i	D-1
Appendix E. Approximate Area of shells $s_{i,j}$ for all Values of i	E-1
Appendix F. MathStation file to assign importance weights of shells $s_{i,j}$ for all Values of i at example METSAT subpoint of 5°E	F-1

	Page
Appendix G. MOE generation file	G-1
Appendix H. MathStation file which assigned area scaling factors and perceived areas of shells $s_{i,j}$ for all Values of i , for example METSAT subpoint of 5°E	H-1
Appendix I. MathStation file to find resolution values of of shells $s_{i,j}$, for all Values of i , at example METSAT subpoint of 5°E	I-1
Appendix J. MathCad file to generate value function for sampling rate attribute	J-1
Appendix K. Relative value of sampling rate generation file	K-1
Appendix L. MathCad file to generate value function for timeliness at- tribute	L-1
Appendix M. Relative value of timeliness generation file	M-1
Appendix N. MathCad file to generate value function for resolution at- tribute	N-1
Bibliography	BIB-1
Vita	VITA-1

List of Figures

Figure	Page
2.1. Mission Level Hierarchy for Damage Expectancy	2-6
3.1. Mission Level Hierarchy for the Satellite Meteorological Mission .	3-2
3.2. Discrete Shell Model Shown in Mercator Projection	3-10
3.3. Discrete Shell Model Shown in Conic Projection	3-11
3.4. Relationship between geodetic latitude (ϕ) and geocentric latitude (ϕ'), on an ellipsoid of revolution.	3-13
3.5. ECF location of a point on the reference ellipsoid.	3-15
3.6. Differential arc length dl on a cross-section of the ellipsoid. . . .	3-17
3.7. Differential area dA on the ellipsoid.	3-18
3.8. Vector from satellite to earth location at subpoint is antiparallel to local surface normal.	3-26
3.9. Tangent vector from satellite to earth location is perpendicular to local surface normal.	3-27
3.10. Range vector from METSAT to earth point, $\rho_{i,j}$ is the third leg of triangle including radius vectors to satellite and earth location $p_{i,j}$	3-29
3.11. Resolution of a Pixel at the Satellite Subpoint	3-35
3.12. Resolution of a Pixel at Point $p_{i,j}$	3-37
4.1. Graphic representation of sampling rate data provided by the decision maker.	4-2
4.2. Relative Values of Various Sampling Rates	4-3
4.3. Graphic representation of timeliness data provided by the decision maker.	4-4
4.4. Relative Values of Timeliness	4-5
4.5. Graphic representation of resolution data provided by the decision maker.	4-6

Figure	Page
4.6. Relative Values of Resolution	4-7
4.7. Graphic representation of calculated values of the MOE as a function of satellite subpoint.	4-9
4.8. Graphic representation of sensitivity of MOE to changes in sampling rate attribute	4-12
4.9. Graphic representation of sensitivity of MOE to changes in timeliness attribute	4-13
4.10. Graphic representation of sensitivity of MOE to changes in resolution attribute	4-15
F.1. Reproduction of Geographical Area Importance Data Provided by the Decision Maker	F-4

List of Tables

Table	Page
2.1. Order relations on decision choices and outcomes	2-8
3.1. Initial Decision Attributes and Relative Weights	3-20
3.2. Final Decision Attributes and Relative Weights	3-22
3.3. Sampling rates of various operational METSATs	3-31
3.4. Relative values of various levels of sampling rate	3-32
3.5. Timeliness values for DMSP imagery received on 8 Nov 1990 . . .	3-33
3.6. Relative values of various levels of timeliness	3-34
3.7. Subpoint resolutions of various operational METSATs	3-38
3.8. Relative values of various levels of resolution	3-39
4.1. Calculated values of the MOE for geostationary METSATs as a function of satellite subpoint	4-8
4.2. Calculated values of the MOE for geostationary METSATs at 265E, as a function of sampling rate	4-12
4.3. Calculated values of the MOE for geostationary METSATs at 265E, as a function of timeliness	4-13
4.4. Calculated values of the MOE for geostationary METSATs at 265E, as a function of resolution	4-14

Abstract

Using concepts from multivariate utility theory, basic orbital mechanics, and information regarding operational and planned meteorological satellites, this thesis develops a meaningful MOE to support high-level decision making regarding the allocation, acquisition, and operational deployment of space meteorological satellite (METSAT) assets. Satellite meteorological systems were chosen because of the ready availability of pertinent unclassified data. However, the methodology presented may be applied to any type of space system.

MEASURING THE EFFECTIVENESS OF SPACE: SATELLITE WEATHER SYSTEMS

I. Introduction and Background

1.1 Background

The current global situation is marked by reduced superpower military tensions and concurrent increased economic constraints on military budgets, especially in the United States. At the same time, space programs are growing in proliferation, share of federal budgets, and importance to our national defense. Consequently, there exists a growing need for techniques to help high-level planners make allocation and acquisition decisions regarding space assets. These types of decisions require a simple yet comprehensive way to discriminate between complex choices. One such decision-making aid commonly used throughout the military is the Measure of Effectiveness (MOE). However, there currently exist no commonly accepted MOEs for space operations at the force structure level.

1.2 Specific Objective

Using concepts from multivariate utility theory, basic orbital mechanics, and information regarding operational and planned meteorological satellites, this thesis develops a meaningful MOE to support high-level decision making regarding the allocation, acquisition, and operational deployment of space meteorological satellite (METSAT) assets. Satellite meteorological systems were chosen because of the ready availability of pertinent unclassified data. However, the methodology presented may be applied to any type of space system.

Completion of the objective requires that the student become proficient in and synthesize multivariate utility theory and principles of MOEs, bringing the two together in order to fashion an MOE which can be used by space planners and operators in real world situations. A broad general knowledge of astrodynamics and satellite meteorological systems and applications is also necessitated by the methodology chosen.

1.3 Problem Solving Approach.

A specific mission scenario is chosen as the focus of the study in order to limit the scope of the problem. A decision maker with specific expertise in the chosen mission area is also chosen. Mission accomplishment is then defined according to published sources and the decision maker's understanding of the problem.

Initial research into various satellite meteorological systems revealed several factors which appeared to have an impact on accomplishment of the defined mission. The list is next modified by the decision maker to reflect his own references and understanding, removing from the list unnecessary entries and adding those omitted by the analyst. Finally, precise definitions for each system characteristic on the list are researched and agreed on by the decision maker and analyst.

An oblate spheroid earth model is created in order to evaluate the values of the system attributes at different locations on the earth. The model partitions the spheroid into discrete shells of specified latitude and longitude. Each shell is also assigned a relative importance factor to mission accomplishment based on the decision maker's inputs.

Weights are assigned to each of the system parameters according to the decision maker's preference. The existence of utility independence among attributes is assumed. This data and additional preference information supplied by the decision maker is used to derive the functional relationship among attributes.

The information regarding the relationships between and among the attributes is then used to obtain a simple mathematical expression for the utility of a particular meteorological satellite system, in terms of the parameters identified earlier as influential.

For those attributes which are considered to be constant over all geographical points of the model, the specific value for that attribute was determined for each satellite tested. For all other attributes, algorithms to generate values for all points are constructed and run. The result of this procedure is the assembly of a database for each satellite, wherein each point in the model is associated with a vector of values, one for each attribute.

The completed model is next used to generate MOEs for several operational and hypothetical cases. Inferences regarding the usefulness of the MOE for various applications are made as well. Finally, specific weaknesses of the methodology are discussed, and recommendations for correcting them are presented.

1.4 Overview

A description of the methodology employed in reaching the objectives described above constitutes Chapter III. Discussion of experimental results and the usefulness of the MOE comprises Chapter IV, and Chapter V contains concluding remarks.

II. Review of Pertinent Literature

2.1 Introduction and Overview

To properly address the tasks outlined in the previous chapter, it will first be necessary to review the professional literature pertaining to MOEs and value assessment, in order to better understand the terminology, methodology, and state of the art.

2.2 Measures of Effectiveness

2.2.1 General Considerations. In the broadest sense, a measure of effectiveness (MOE) is simply any convenient gauge of an item's performance or desirability on some scale. As applied to military operations, Battilega (4:38) describes it as an index or set of indices used to quantitatively measure all of the dimensions of some process relevant to mission accomplishment. Further, they typically relate the degree of mission accomplishment to the details of force composition (4:39).

The descriptions in the previous paragraph imply several key points regarding MOEs. Those concepts are developed in detail in sections 2.2.1.1 through 2.2.1.4.

2.2.1.1 Mission Accomplishment. The fundamental requirement for any MOE stems from the need for some measure of the degree of actual mission accomplishment achieved by an alternative of interest. However, in some cases it may not be possible or desirable to evaluate mission accomplishment directly. In such a case it may be assumed that some other performance measure (i.e., command and control functionality) contributes directly and monotonically to mission accomplishment and thus force effectiveness. However, the nature of this contribution is usually unknown. For example, the presence of linearity is rare. More often, the familiar concept of "diminishing returns" is observed. Therefore, whenever possible, it is preferable to have the MOE directly quantify how well a combat or support mission is performed

(4:39). Thus, the nature of the mission modeled will be of prime importance to the analyst in creating an MOE.

2.2.1.2 Levels of MOEs. The mission for which the MOE serves as an index can be either generalized or specific, depending on the need of the analyst. An example of a broadly defined mission is air superiority. A specific mission might be to shoot down a single enemy aircraft in a one-on-one dogfight. Hughes (17:112) classifies combat-oriented MOEs by the numbers of opposing units, which could be individuals, tanks, satellites, etc. An MOE which describes one-on-one combat is described as being at the "micro" level; few-versus-few combat is at the "medial" level, and many-versus-many MOEs are at the "macro" level.

A good MOE at one level of combat may not necessarily be useful at another. In the examples given above, an analyst studying the dogfight would be interested in the individual probability of kill of the two opposing aircraft. However, this figure carries little information for the direct measurement of the degree of attainment of air superiority at, say, a theater level of operations. Although a higher individual probability of kill will likely contribute to the goal of air superiority, it is only one dimension of the broader mission. Other factors may overshadow it, and in fact there may even be an unknown tradeoff which causes the degree of air superiority to decrease with increasing individual probability of kill (If, for example, the greater kill probability is tied to the fact that there is a very small number of highly expensive aircraft available).

These examples illustrate the fact that, at higher levels of abstraction (i.e., force structuring), the mission itself becomes harder to define. When the scope is large, Battilega states that an MOE is still "considered useful if it is an indicator that, in connection with its use in the analysis, is consistent with the overall goals of the potential decision makers (4:40)."

These different levels of MOEs can be shown to be a dependent hierarchy.

A useful MOE to compare different types of artillery might be the probability of striking a target (inside a given circular error) within a given number of volleys. An MOE used to compare entire artillery batteries might be the exchange ratio versus a standard enemy artillery battery. But as in the air superiority example, the individual kill probability that is the output of the lower-level model serves as input to the higher-level model (4:43).

Temporal effects also influence MOEs. It is generally assumed that decision-makers will prefer to obtain things of value sooner than later, although this is not always the case(21:30). For example, if profit from a capital investment is the thing of value that a decision maker wishes to maximize, it may be in his or her best interest to obtain the profit at a later time, so that the investment has sufficient time to mature, and a greater profit may be obtained. For the single aircraft duel mentioned in Section 2.2.1.2, the individual probability of kill remains a useful MOE. But for several successive engagements, the expected exchange ratio (the ratio of the expected number of enemy losses to expected friendly losses) is more appropriate. If sustained combat were being modeled, aircraft maintenance and logistics would need to be considered (10:120).

2.2.1.3 Combined MOEs. Especially apparent in more complex situations is the multidimensionality of the mission to be modeled. An MOE which adequately describes mission accomplishment must then also contain all of the dimensionality which influences mission outcome. Any effectiveness-oriented MOE can also be used in conjunction with cost criteria. Alternative systems to achieve a given mission at a fixed level of effectiveness can be compared on the basis of lowest cost in terms of one or more resources. Alternatively, fixed-cost systems can be compared on the basis of highest effectiveness in one or more mission areas (4:46).

In addition, temporal considerations can be taken into account in conjunction with other criteria. For a given fixed cost and effectiveness, the system which could

complete the mission in the shortest period of time – or closest to some specified time – might be considered superior. In a similar manner, any number of criteria of various types can be alternatively considered.

2.2.1.4 Quantitative versus Qualitative MOEs. Because the end result of an MOE is a subjective report on a process or object's ability to fulfill some military mission, it is required that the MOE be measurable on some absolute or relative scale. Because the model may contain many dimensions of incompatible measure, some means of equating these inconsistent units must be found. The method used in this thesis is called multiattribute utility theory, and is discussed in Section 2.3. Once all facets of the model are considered, it is necessary to be able to compare different systems against some index or scale. It is desirable that this scale be an absolute, ordinal one, so that the "distance" between any two systems may be determined for analytical purposes. However, some applications do not allow any more than an ordering of choices. In such a case, it may be sufficient to state that one alternative is in some well-defined sense "better" than another.

2.2.1.5 Pitfalls of MOEs. As one would expect, there exist many ways in which improper selection of an MOE can lead to poor decision making. An MOE is a simplification of a complex situation. Since it is, in essence, a distillation of many facets into one measure, the analyst must take care that the MOE is a true measure of the modeled system. Failure to include relevant details lead to models which are too global in nature, or which simply don't reflect all of the dynamics of the system. However, including too many variables can lead to an MOE which is confusing, computationally inefficient, and (most significantly) misunderstood by the decision-maker and others (4:56-57), (3:247).

A related pitfall associated with MOEs is their incorrect use by decision makers (26:354). While the analyst must be careful that the measure constructed is an accurate reflection of the mission of interest – that is, it answers the question being

asked – all users of the MOE should be aware of the class of problems for which it is and is not valid. For instance, assume that a well-known measure of effectiveness for comparing missile defense systems is used in the post-cold war era for procurement purposes. However, this MOE was constructed during a period of high levels of defense spending. As such, fiscal considerations were much less strongly stressed than they would be today. Such a model might choose a weapon system based primarily on wartime effectiveness that would simply be unaffordable and in fact infeasible in the current political climate.

2.2.2 Common MOEs. Because of its ability to assess that which is difficult to measure, the MOE has long been a favorite tool of the military analyst. In the business world, well defined concepts such as cost and profit are easily understood and calculated by newcomers to the field. Yet military planners must make decisions based on less well-defined, if not more complex, alternatives and variables. Two MOEs which have been used with considerable success and frequency are described in the sections below.

2.2.2.1 Damage Expectancy. Damage Expectancy is an MOE commonly used by the U.S. Air Force's Strategic Air Command and others interested in problems of strategic nuclear force requirements to assess the effectiveness of nuclear attacks. Damage expectancy is a high-level MOE which serves to summarize damage done to a target set by nuclear weapons. According to Seiler (29:11), damage expectancy is "... a statistical expected value that the weapon will arrive, detonate, and cause a certain level of damage — light, moderate, or severe." It is calculated as

$$DE = PA \times PD \quad (2.1)$$

where PA is the statistical probability that a particular weapon will arrive on target and detonate, and PD is the probability of damage to the target (assuming arrival and detonation). Both of these terms are subsequently broken down into components

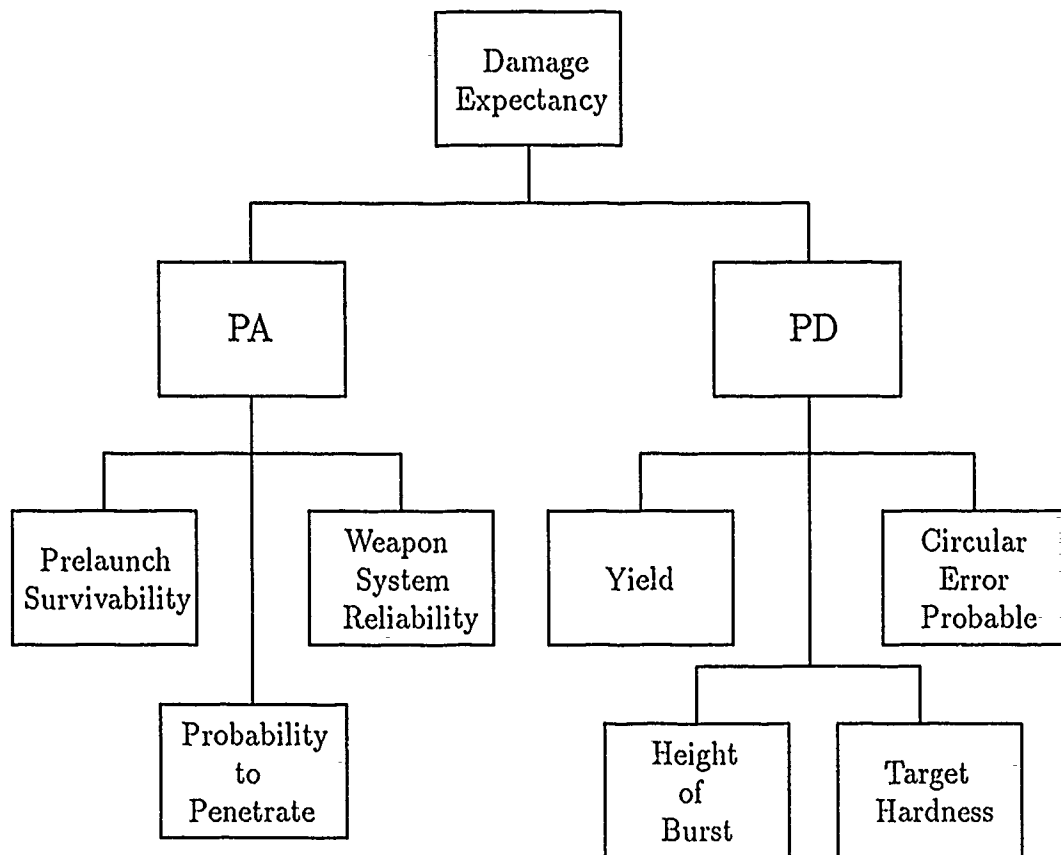


Figure 2.1. Mission Level Hierarchy for Damage Expectancy

and subcomponents, in a hierarchy of levels as discussed in Section 2.2.1.2. This hierarchy is shown in Figure 2.1.

2.2.2.2 Ton-Miles Per Day. This MOE is used by Military Airlift Command and other agencies interested in measuring strategic airlift capabilities. Unlike many common MOEs, this one is completely described by its name. It indicates the expected total tonnage moved on a particular day by the entire airlift force (or some subset of interest), and the total distance flown in miles.

2.3 Utility Theory.

The second major concept used in developing the methodology is that of utility theory. Although this thesis will not assess the risky elements of the problem, those concepts are treated in this section for completeness.

2.3.1 Value and Utility. Measures of value and utility are subsets of the broader classification of measuring preference. If risk (probability) is not involved, a *value function* completely describes the decision-maker's preference structure. However, virtually every practical decision contains a substantial degree of uncertainty. Therefore, a *utility function* must be used in order to model the decision-maker's assessment of risk in conjunction with "pure" value judgments. Often, the utility function is directly assessed because of the difficulty in separating the decision maker's risk preference from value assessment. However, it is possible in certain well-behaved cases to construct the utility function directly from the less complex value function. This two-step construction of the utility function also allows analysis of the riskless preference characteristics described by the value function.

2.3.2 Definitions. The construction of utility and/or value functions presupposes (1) a decision between choices, and (2) a decision maker, whose decision-making process we are modeling. To accomplish this construction, the decision maker is first questioned regarding the available choices and information, and the decision maker's preferences. This information is referred to as the *decision set* of the problem. The decision set consists of *decision vectors* and *outcome vectors* in addition to the utility function. The fact that we are allowing each choice to possess multiple (n) attributes requires that the functions created be defined on an n -dimensional euclidean vector space \mathbb{R}^n . Each of the choices being considered in the decision process, and their multiattribute nature are represented as an n -dimensional decision vector x from the

set of all possible decisions \mathcal{X} ; where

$$\mathbf{x} = \{x_1, x_2, \dots, x_n\} \quad (2.2)$$

Each of the possible outcomes (any number is possible) of the decision process is displayed in the form

$$\mathbf{r} = \{r_1, r_2, \dots, r_n\} \quad (2.3)$$

The n subscripts represent each of the n attributes, defined by Keefer (18:115) as measuring the degree with which each objective is met by an individual outcome \mathbf{r} . Here we will use the following notation to indicate the attribute itself, as opposed to its level in any given decision vector:

$$\mathbf{R} = \{R_1, R_2, \dots, R_n\} \quad (2.4)$$

Order between decision vectors or outcomes is denoted by the three transitive and connected order relations given in Table 2.1.

Symbol	Interpreted as
\succ	is preferred to (by the decision maker)
\sim	(the decision maker) is indifferent to
\succeq	is preferred to or indifferent to

Table 2.1. Order relations on decision choices and outcomes

2.3.3 Uncertainty. Uncertainty is a part of every decision. Numerous studies (15:12), (34:109), (30:39) have demonstrated that human perceptions of probability are far from reliable. Even highly intelligent people and those schooled in probability often make probabilistic errors (15:13), (12:5). The need to overcome this natural weakness is one of the chief concerns of the decision maker, and one of his or her

greatest challenges as well. Essentially, there are two types of uncertainty. Primary uncertainty occurs when only a finite amount *can* be known about an event. This is also called the state of information (23:206). Secondary uncertainty stems from the fact that no one can know all there is *to know* about an event, that an event is always incompletely considered. If ϵ represents the primary uncertainty of an event r , Tani (33:1502) describes the *authentic probability* of the event as

$$p_a = \Pr(r \mid \epsilon) \quad (2.5)$$

The right side of this equation can be interpreted as "what the decision maker would calculate as the probability of an event r occurring, given that he or she perfectly knows the state of the world as it exists."

Since we know this to be an unattainable goal, the term *operative probability* is used to reflect probability in the face of imperfect consideration $\mathcal{C}(\epsilon)$. The operative probability for the same event is then

$$p_o = \Pr(r \mid \mathcal{C}(\epsilon)) \quad (2.6)$$

Which may be interpreted as "what the decision maker would calculate as the probability of an event r occurring, given our current incomplete understanding of the state of the world."

One objective of the analyst in this stage of problem formulation is to aid the decision maker in bringing the operative probability as close to the authentic probability as possible. Through introspection and research into the nature of the mission scenario, the analyst can limit unknown factors, bringing p_o closer to p_a . (33:1502) However, there is always some cost (in time at least, or also in terms of other resources) associated with this process, as well as a point at which the information gained is no longer worth the expense of obtaining it (6:B-165). This is referred to by Ravindran (28:229) as the *expected value of perfect information*.

2.3.4 *Rational Utility.* Next, the decision maker describes a multiattribute utility function on the outcome vector, $\mathcal{U}(\mathbf{r})$. Such an expression of utility is possible if and only if the decision maker's personal utility-assigning process meets certain axioms of rational utility (11:26), (20:333-340), (27:123), (23:203), (16:213-214). All of the authors prefer different notation and expression, but Szidarovsky (32) shows them all to be functionally equivalent. Fundamentally, they all state that the decision maker must be rational and consistent (11:26) in his or her individual preference structure. An adaptation of Goicoechea's interpretation is given below.

Axiom 1 (Order) *For two alternative outcomes x and y , one of the following must be true: $x \succ y$, $y \succ x$, or $x \sim y$, where " \succ " means "is preferred to (by the decision maker)," and " \sim " means "(the decision maker) is indifferent to."*

Axiom 2 (Transitivity) *If $x \succ y$ and $y \succ z$, then $x \succ z$.*

Axiom 3 (Continuity) *If $x \succ y$ and $y \succ z$, then \exists some probability p , $0 \leq p \leq 1$, \in that the decision maker is indifferent between the certainty of outcome y and the probability p of getting outcome x vice the probability $(1 - p)$ of getting outcome z . In other words, there is a certainty equivalent to any gamble, and vice versa.*

Axiom 4 (Consistency) *Let $x \sim y$. Then for any z , the decision maker will be indifferent between the following two gambles: Gamble 1 offers a probability p of receiving x and a probability $(1 - p)$ of receiving z , and Gamble 2 offers y at probability p and z at probability $(1 - p)$.*

If the axioms of rational choice described above are met, then the decision should be chosen to maximize the expected utility, given by (18:115)

$$\mathcal{E}[\mathcal{U}(\mathbf{r} \mid \mathbf{x})] = \int_{\mathbf{R}} \mathcal{U}(\mathbf{r}) \mathcal{F}(\mathbf{r} \mid \mathbf{x}) d\mathbf{r} \quad (2.7)$$

Maximizing Equation 2.7 results in a (usually) nonlinear mathematical programming problem, for which several solution techniques are available. A discrete model may be utilized to approximate the integral by a sum, thereby reducing the complexity of the computation.

2.3.5 Functional Forms. A major step in determining the final utility function is specifying the relationship between each of the variables in the value and utility functions. The simplest relationships are additive and multiplicative. Thus, if $\mathbf{x} = \{x_1, x_2, \dots, x_n\}$ is the multiattribute decision vector and \mathcal{V}_i is the i th single attribute value function on \mathfrak{R}^n , and \mathcal{V} is the conjoint (total) value function, the additive relation is expressed

$$\mathcal{V}(\mathbf{x}) = \mathcal{V}_1(x_1) + \mathcal{V}_2(x_2) + \dots + \mathcal{V}_n(x_n) \quad (2.8)$$

Likewise, the multiplicative relationship is given as

$$\mathcal{V}(\mathbf{x}) = \mathcal{V}_1(x_1)\mathcal{V}_2(x_2)\dots\mathcal{V}_n(x_n) \quad (2.9)$$

Equations 2.8 and 2.9 both assume the independence of each of the attributes (5:1060).

2.4 Summary.

The concepts involved in assessing MOEs are different from those relating to multiattribute utility theory. However, they are complimentary in that they may both be applied to different aspects of the task of assessing the worth of complex systems. These principles will now be incorporated into the solution of the problem defined in Chapter 1.

III. Methodology

3.1 Introduction.

This chapter develops the techniques required to complete each of the tasks listed in Chapter 1. Specific application to the problem, as well as general concepts, are presented. Intermediate data is also listed where necessary to the understanding of the method.

3.2 Define the space meteorological mission.

3.2.1 Limiting the scope of the problem. As mentioned in the preceding chapter, understanding the level of abstraction of the problem is important to obtaining the correct MOE. As pointed out by Buede (7:2), multiattribute utility (or value) models are hierarchical in nature. Beginning with the specified top level factor for which an overall evaluation is desired, each factor is decomposed into successively more specific sublevels. This process is continued until a sufficiently precise level is achieved that allows for the prediction or direct observation of system characteristics.

The hierarchical model for the satellite meteorological mission, modeled after Buede's tree structure (7:3), is given in Figure 3.1. It begins at the mission accomplishment level, which is what we wish the MOE to measure. It then breaks the meteorological mission down into several levels of factors, including information on the operational environment, and probable uses for the gathered data. These levels constitute the various possible mission scenarios. The finest level of detail consists of performance parameters. These include the measurable and/or predictable system characteristics whose values will be aggregated in the final value function. It should be noted that at this point in the analysis, the performance parameters given are only examples, and are not necessarily those which will form the value function.

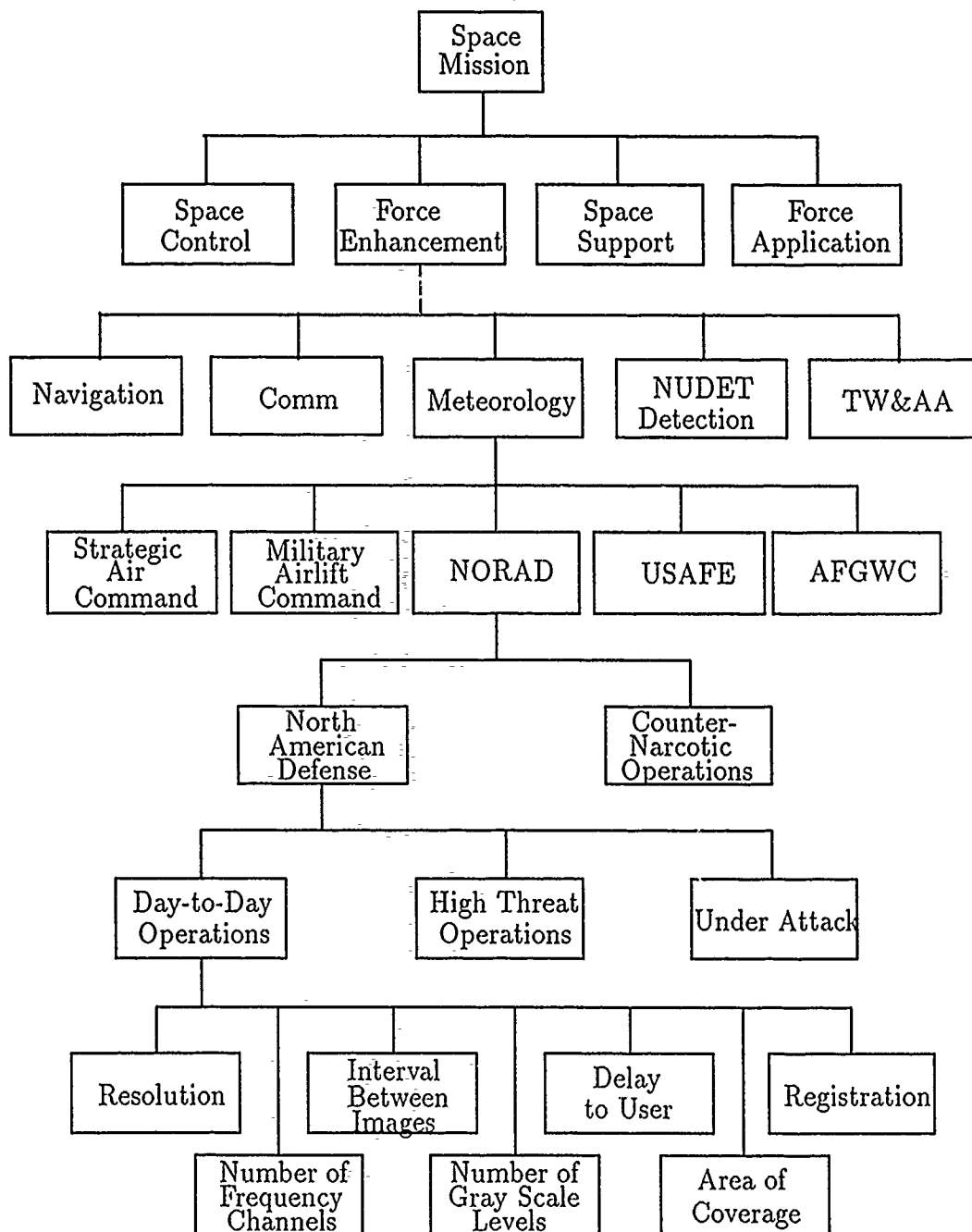


Figure 3.1. Mission Level Hierarchy for the Satellite Meteorological Mission

3.2.2 *Limiting assumptions.* Only geostationary meteorological satellites were considered in order to develop the methodology presented. However, the concepts presented may be applied to sun-synchronous METSATS as well, and may also be adapted for application to any other type of space asset. To further simplify the problem, risk will not be considered in the analysis. Thus, the effectiveness of the systems studied will be measured in terms of value, as opposed to utility.

3.2.3 *Choose a decision maker.* In order to perform an adequate analysis of the scenario treated in this paper, an expert decision maker must be consulted in order to gather information and preferences. What makes a given decision maker "expert" encompasses several factors, not all of which are easily recognizable or available.

3.2.3.1 *Accuracy.* One necessary qualification for an expert is that the individual be capable of making correct decisions in his or her area of specialty. The term "making correct decisions" is meant here to mean that, based on past performance, the decision maker has chosen the correct alternative of those available with a high degree of frequency. That is, he or she is usually right. This paper will refer to this quality as *accuracy*.

3.2.3.2 *Precision.* However, it may be the case that any layperson could arrive at a similar record of accuracy in the field due to the simplistic nature of the field. Helmer gives the following examples:

...in a region of very constant weather, a layman can prognosticate the weather quite successfully by always predicting the same weather for the next day as for the current one. Similarly, a quack who hands out bread pills and reassures his patients of recovery "in due time" may prove right more often than not and yet have no claim to being classified as a medical expert. (14:11)

Highly uncertain situations may also be less sensitive to expert decision making. The tourist with no knowledge of the laws of probability (or for that matter, the rules of the game) may nonetheless win big at roulette, a game in which chance plays a major part. Thus, precision tends to reflect the quality of decisions made, as opposed to the frequency of merely acceptable decisions.

In addition to precision and accuracy, other factors must be considered in choosing an expert. Academic qualifications, experience, and technical knowledge all account for an individual's qualification as an expert (25:326). These factors combine to make the decisions reached by the individual of a higher fidelity in terms of how closely, in retrospect, they match what would have been the "best" decision in whatever sense is applicable to the problem.

Using the guidelines presented above, the following traits were determined to be desirable in the decision maker.

1. Knowledge of technical aspects of satellite meteorological systems.
2. Knowledge of operational aspects of satellite meteorological systems.
3. Access to operational parameters of satellite meteorological systems.
4. Familiarity with the military procurement process for space systems.
5. Experience with making force structure-level procurement decisions.
6. Availability to the analyst for several in-depth interviews.
7. Ready access in terms of geographical proximity to the analyst.

The choice of a decision maker in this analysis was constrained primarily by the availability of high-ranking decision makers for lengthy interviews. Consequently, the responses of a test subject were used in order to develop the methodology presented here (35). In any case, the methodology presented here is equally applicable to any expert decision maker and is more important than the actual data collected.

The developed methodology was in turn applied to the case of the actual expert, Colonel William B. Freeman, NORAD Deputy Assistant for Weather, and Vice Commander of MAC's 4th Weather Wing. Colonel Freeman (hereafter referred to as *the decision maker*) meets all of the qualifications listed above, save that he has no experience in making extremely high-level procurement decisions. However, fulfilling that requirement would have necessitated interviewing at the general officer level, which was deemed inappropriate for this project.

3.2.4 Present operational mission scenario to decision maker. The scenario for which this analysis was conducted was chosen for the decision maker's familiarity and expertise, in order to facilitate the interview process. It is only one of the many presented in the mission hierarchy given in Table 3.1. The scenario was described to the decision maker as "day-to-day peacetime weather reporting over the NORAD defended area in support of military aircraft operations."

3.3 Identify factors which influence mission accomplishment.

3.3.1 Develop list of attributes. The analyst next developed a list of measurable operational variables which may impact accomplishment of the mission described in Section 3.2.4. While the analyst is less qualified than the decision maker to construct such a list, the effort was made in order to provide a starting point for discussion during the interviews. As mentioned in Section 2.2.1.5, the analyst remained alert against guiding the discourse of the interviews toward his own preconceptions. The list developed in this manner was:

- Resolution
- Orbital parameters
- Registration error
- Interval between images

- Time delay to user
- Area of coverage
- Number of gray scale levels
- Number of frequency channels

Note that this list is not well defined at this point in the analysis. This is intentionally done in order to permit freer input by the decision maker, whose own personal interpretation of the attributes will be used in the analysis.

3.3.2 Refine list of attributes. At the first interview, the initial list of attributes was presented to the decision maker on the form shown in Appendix A. The decision maker was asked to consider the list in regard to the mission statement, and add any variables he felt were not listed, but would be relevant to mission accomplishment. Similarly, he was asked to remove any elements of the list he felt were unrelated to mission accomplishment. At this time, the decision maker was asked to provide precise definitions for each of the decision variables. He was prompted to refer to whatever technical references required to obtain those definitions. The decision maker's response is provided in Appendix B, and the resulting list is given in Section 3.3.3.

3.3.3 Attribute vector listing. The following list constitutes all those attributes of the given satellite meteorological mission scenario which, in the judgement of the decision maker, affect mission accomplishment. This correlates to the attribute vector \mathcal{R} given in Equation 2.4. Where the decision maker provided a different name for an attribute mentioned above, both are shown.

1. (Sampling rate)/Interval between images: During normal operations, the number of times a particular shell is imaged in any 24-hour period.
2. (Timeliness)/Time delay to User: Number of processing intervals per hour, or the reciprocal of the average number of hours that elapses between scanning

an area and receipt of that imagery by 4th Weather Wing/NORAD Weather Directorate personnel.

3. (Resolution)/spot size: At any point on the imaged surface, the number of pixels at the image plane per square kilometer of imaged geography.
4. (Spectral coverage)/Number of frequency channels: Frequency range, in units of dbHz, of the imaging sensor. Limited to visual and infrared bands.
5. (Registration error)/Location accuracy: Average error between a pixel's actual and calculated geographical location, measured in kilometers.
6. ("Dynamic" range of imagery system): The dynamic range of the entire gray scale. Units recommended are the (base ten) logarithm of the maximum flux minus the logarithm of the minimum flux.
7. (Number of gray shades)/Number of gray scale levels: Number of gray shades available per unit dynamic range.

Note that the attribute for coverage area was deemed to be unimportant by the decision maker, once the scenario was limited to geostationary METSATs only. The decision maker also shows the attribute for number of gray scale levels as being broken down into two components, where the total number of gray shades is the product of dynamic range and the last attribute listed. All other attributes remained the same except for minor changes in the definitions.

3.3.4 Area Factors. In addition to the characteristics of the METSATs themselves, two characteristics of the area imaged must be considered. The first is the relative importance of an area's location on the earth. This factor, the *geographical area importance weight*, will be assigned the variable name GeoWt. Because of the perspective of the METSAT, a given shell may be seen obliquely, or not at all, due to the curvature of the geoid. This effect makes it necessary to represent the portion of a shell viewed by the variable PerArea, for *perceived area*.

3.4 Generate a discrete earth model.

3.4.1 Assumptions. The earth model used for this project assumes two-body satellite motion only. The earth's shape was approximated as an oblate spheroid (explained in detail in Section 3.4.1.1), and the effects of nodal precession, nutation, and time-variant rotation rate were ignored. The limitation to geostationary satellites allowed the use of Earth-centered fixed, versus geocentric inertial coordinate systems. It also obviated the necessity to integrate any factors over time, since the satellites do not change their position with respect to the earth over time. Because of the extremely limited value of weather information south of the equator for the mission scenario given, only the Northern Hemisphere is included in this model. This is equivalent to assigning each point in the Southern Hemisphere an importance weight of zero.

3.4.1.1 The reference ellipsoid. As mentioned above, the earth is modeled as an oblate spheroid, or ellipsoid of revolution. This may be described as a sphere which has been "flattened" so that any cross-section parallel to the line of poles is an ellipse. All cross sections parallel to the equator are circles. The semi-major axis of the ellipse is given as the equatorial radius a , and the semi-minor axis, b , is the polar radius of the earth (2:93). Simple geometry then gives the eccentricity, e , of the elliptical sections as

$$e = \frac{\sqrt{a^2 - b^2}}{a} \quad (3.1)$$

The values used for these measurements are taken from *The Fundamentals of Astrodynamics*, by Bate, Mueller, and White (2:94). The equatorial radius is

$$a = 6378.145\text{km} \quad (3.2)$$

The value for the polar radius is

$$b = 6356.785\text{km} \quad (3.3)$$

The values of a and b are taken as exact for the purposes of the model. They do, in fact, generate a close approximation to the earth's mean sea level. The value of e is calculated from these values in the model, but is given here to five significant figures as

$$e = 0.081772 \quad (3.4)$$

3.4.2 Shell definition. The Northern Hemisphere of the earth was divided into 32,400 *shells*, or sections of the surface. Each shell is defined as having sides of one arc degree of latitude, and one of longitude. A mercator projection (a projection of the earth onto a cylinder (9:x)) would show the shells as rectangular boxes, as in Figure 3.2.

Another perspective of the shape of the shells, showing how the areas decrease with increasing latitude, is given by the conic projection in Figure 3.3 (9:x).

Mathematically, each shell $s_{i,j}$ is defined in terms of its associated latitude (ϕ) and longitude (λ) as follows:

$$s_{i,j} : \left. \begin{array}{l} \phi = (2i - 1) \cdot 0.5^\circ N \pm 0.5^\circ \\ \lambda = (2j - 1) \cdot 0.5^\circ E \pm 0.5^\circ \end{array} \right\} i \in [1, 90], j \in [1, 360] \quad (3.5)$$

Equivalently, each shell $s_{i,j}$ is the region of geodetic latitude and longitude whose lower left corner is at $\phi = (i - 1)^\circ$, $\lambda = (j - 1)^\circ$ and whose upper right corner is at $\phi = i^\circ$, $\lambda = j^\circ$. Note also that all longitudes have units of degrees east from the Greenwich Meridian ($0^\circ E$). Also, an input given in terms of west longitude is converted to the form used here by the relation

$$(360 - n)^\circ W = {}^\circ E \quad (3.6)$$

Each shell may also be associated with the point $p_{i,j}$ at its geometric center. This is the point for which all calculations and measurements will be made. That is,

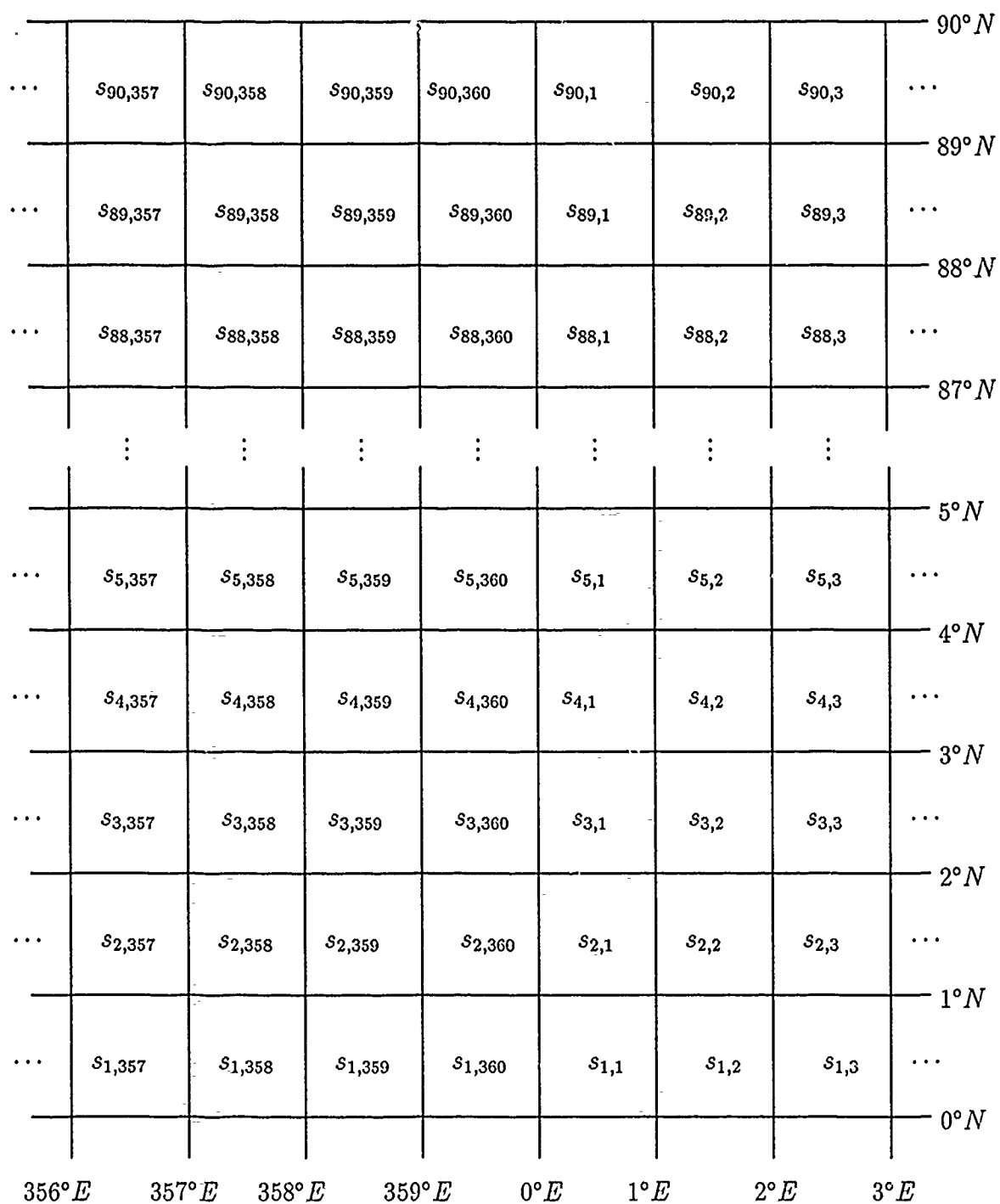


Figure 3.2. Discrete Shell Model Shown in Mercator Projection

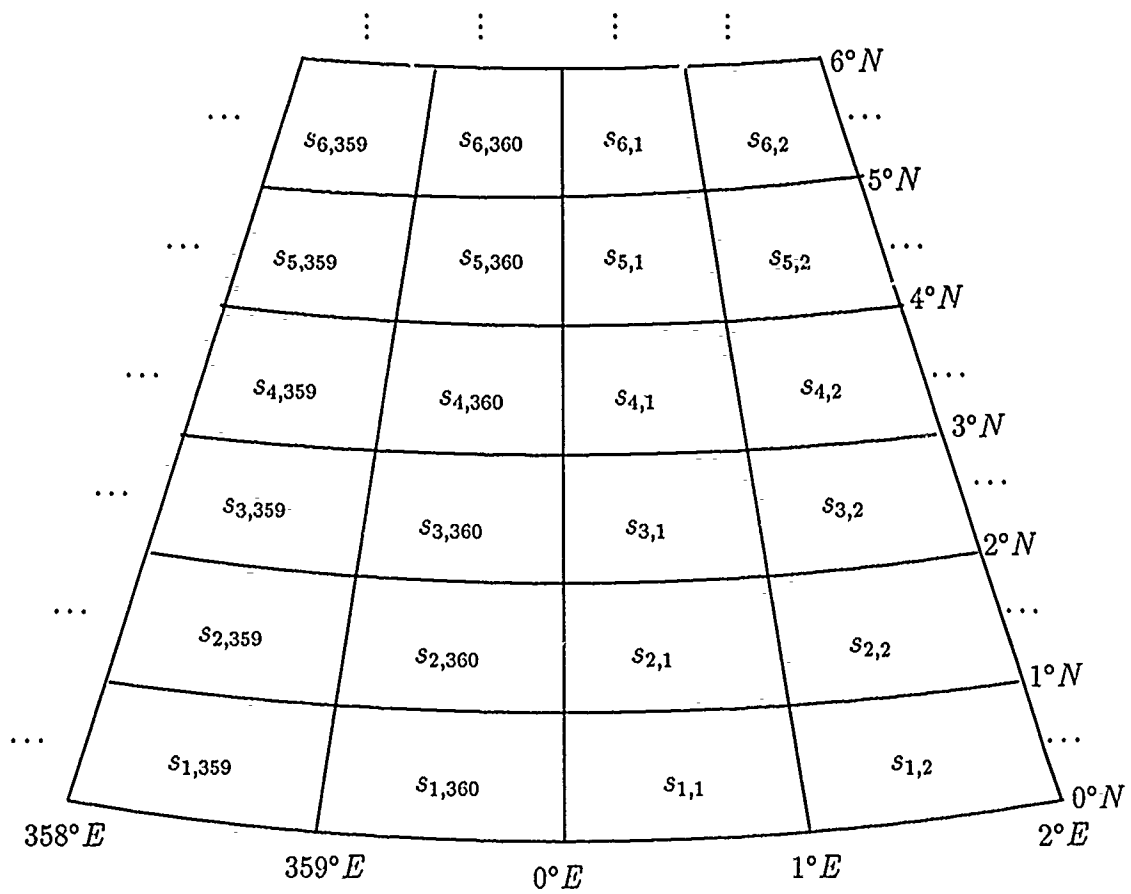


Figure 3.3. Discrete Shell Model Shown in Conic Projection

the value for every attribute is considered to be constant over the entire shell, and is taken as the value at the center point. The points may be more precisely defined than the shells in terms of their geodetic coordinates. These are generated by the relation

$$p_{i,j} = \begin{bmatrix} \phi_i \\ \lambda_j \end{bmatrix}, \text{ where } \left. \begin{array}{l} \phi_i = 0.5(2i - 1) \\ \lambda_j = 0.5(2j - 1) \end{array} \right\} i \in [1, 90], j \in [1, 360] \quad (3.7)$$

It will be assumed that the units for each point $p_{i,j}$ when expressed in this manner are degrees latitude and longitude.

3.4.2.1 Shape and location of shells. The double subscript notation used in defining each shell allows its location on the ellipsoid to be easily determined. All shells with a given first (i) subscript lie along a line of constant latitude, the exact geodetic latitude of the center point $p_{i,j}$ in degrees north given by the relationship in Equation 3.7. Similarly, every shell with a given second (j) subscript lies along a line of constant longitude, with the exact longitude of the center point in degrees east also given by Equation 3.7. For example, the center point $p_{4,2}$ of shell $s_{4,2}$ is located at $\phi = 3.5^\circ N$, $\lambda = 1.5^\circ E$.

All shells $s_{i,j}$ for a given value of i (latitude) have the same size and shape. To determine the area of a particular shell, and in order to compute the performance parameters over each shell, it was first necessary to convert the point coordinates from geodetic to earth-centered fixed (ECF) coordinates.

3.4.2.2 Conversion from geodetic to ECF coordinates. First, each geodetic latitude is converted to geocentric. As shown in Figure 3.4, geodetic latitude is that angle between the equator and a vector normal to the surface of the ellipsoid.

Geocentric latitude, by contrast, is the angle between the equator and a line from the geocenter to the surface point. Letting ϕ' denote geocentric latitude, the

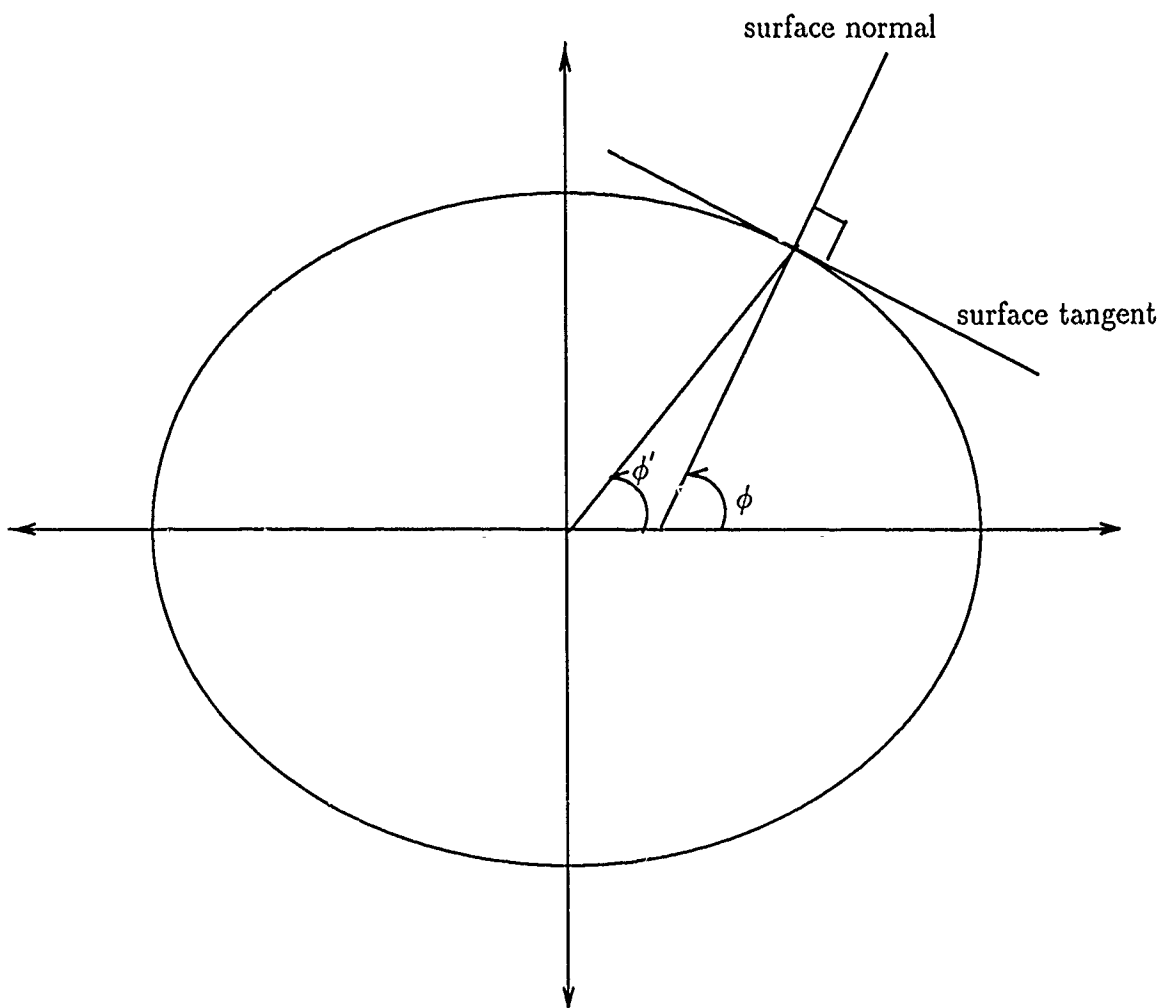


Figure 3.4. Relationship between geodetic latitude (ϕ) and geocentric latitude (ϕ'), on an ellipsoid of revolution.

conversion relation is

$$\phi'_i = \phi_i - \arctan \left[\frac{e^2 \sin \phi_i \cos \phi_i}{1 - e^2 \sin^2 \phi_i} \right] \quad (3.8)$$

The radius to any point on the geoid is dependent only on that point's latitude. The following relation is expressed in terms of geocentric latitude (24:16).

$$r_i = \frac{ab}{\sqrt{b^2 \cos^2 \phi'_i + a^2 \sin^2 \phi'_i}} \quad (3.9)$$

The quantities derived in Equations 3.8 and 3.9 can now be used to express the vector of ECF coordinates as (2:98)

$$\begin{bmatrix} x_{i,j} \\ y_{i,j} \\ z_{i,j} \end{bmatrix} = \begin{bmatrix} r_i \cos \phi'_i \cos \lambda_j \\ r_i \cos \phi'_i \sin \lambda_j \\ r_i \sin \phi'_i \end{bmatrix} \quad (3.10)$$

The MathStation file which generated the model developed in Sections 3.4.2 through 3.4.2.2 is displayed in Appendix C.

3.4.2.3 Actual area of shells. The actual area of each shell (as opposed to the perceived area as viewed from the METSAT, which is calculated in Section 3.7.1.1) is calculated as follows. We begin by examining the geoid located on the x - y - z plane, as shown in Figure 3.5.

Revising Equation 3.10 in order to make use of geodetic latitudes, the ECF location of a point on the geoid can be expressed parametrically as (2:98)

$$x(\phi, \lambda) = r \cos \phi \cos \lambda \quad (3.11)$$

$$y(\phi, \lambda) = r \cos \phi \sin \lambda \quad (3.12)$$

$$z(\phi, \lambda) = r(1 - e^2) \sin \phi \quad (3.13)$$

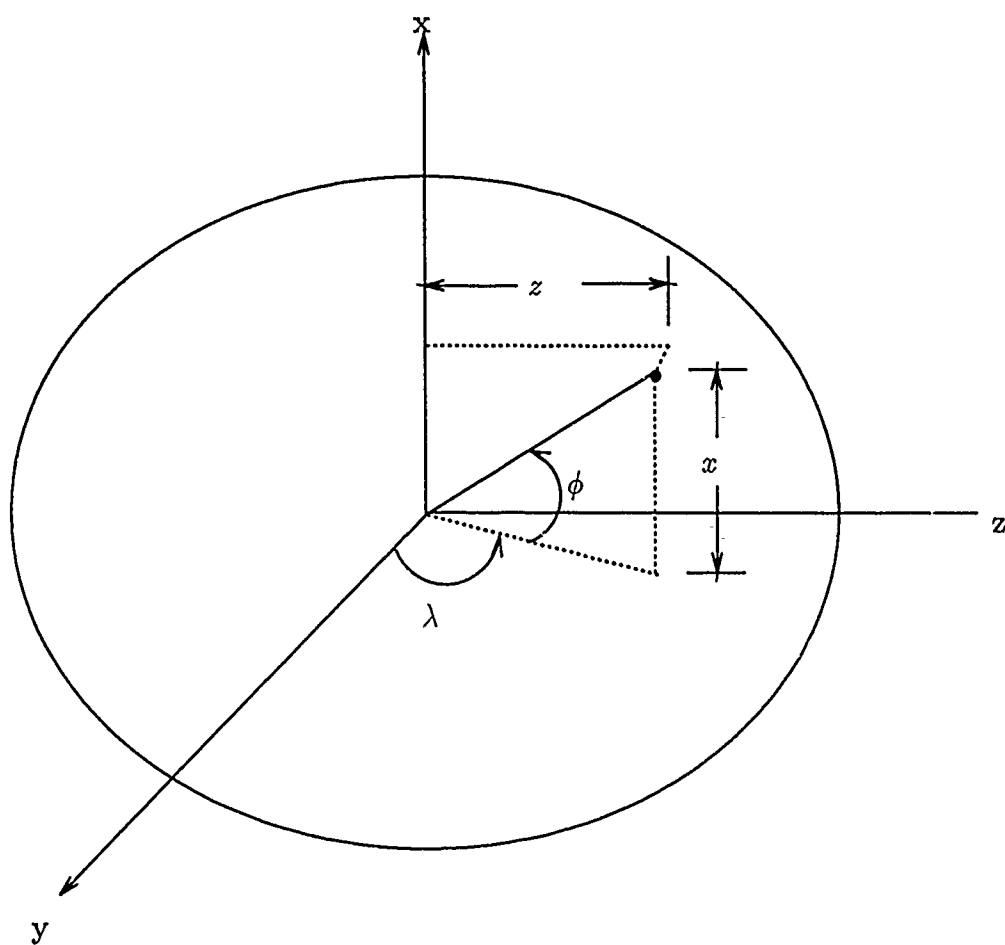


Figure 3.5. ECF location of a point on the reference ellipsoid.

where

$$r(\phi) = \frac{a}{\sqrt{1 - e^2 \sin^2 \phi}} \quad (3.14)$$

Looking next at a cross-section of the ellipsoid mapped onto the x - z plane (Figure 3.6), we consider the arc length dl swept out by a differential change in latitude $d\phi$. This is expressed

$$dl = \sqrt{dx^2 + dz^2}, \quad (3.15)$$

where the partial derivatives of x and z with respect to ϕ are given by

$$dx = \frac{\partial}{\partial \phi} \left[\frac{a \cos \phi \cos \lambda}{\sqrt{1 - e^2 \sin^2 \phi}} \right] d\phi \quad (3.16)$$

and

$$dz = \frac{\partial}{\partial \phi} \left[\frac{a(1 - e^2) \sin \phi}{\sqrt{1 - e^2 \sin^2 \phi}} \right] d\phi \quad (3.17)$$

Setting $g1x(\phi, \lambda) = \frac{\partial x}{\partial \phi}$ and $g1z(\phi, \lambda) = \frac{\partial z}{\partial \phi}$ simplifies the notation, allowing us to express the differential arc length as

$$dl = \sqrt{g1x(\phi, \lambda)^2 + g1z(\phi, \lambda)^2} \cdot d\phi \quad (3.18)$$

If we now rotate this arc dl through a differential change in longitude $d\lambda$, as shown in Figure 3.7, the differential area dA swept out is given by

$$dA = r(\phi) \cos \phi \cdot d\lambda \cdot dl \quad (3.19)$$

where the cosine term is needed because we are rotating about a circle of constant latitude (parallel to the equator) instead of the geocenter.

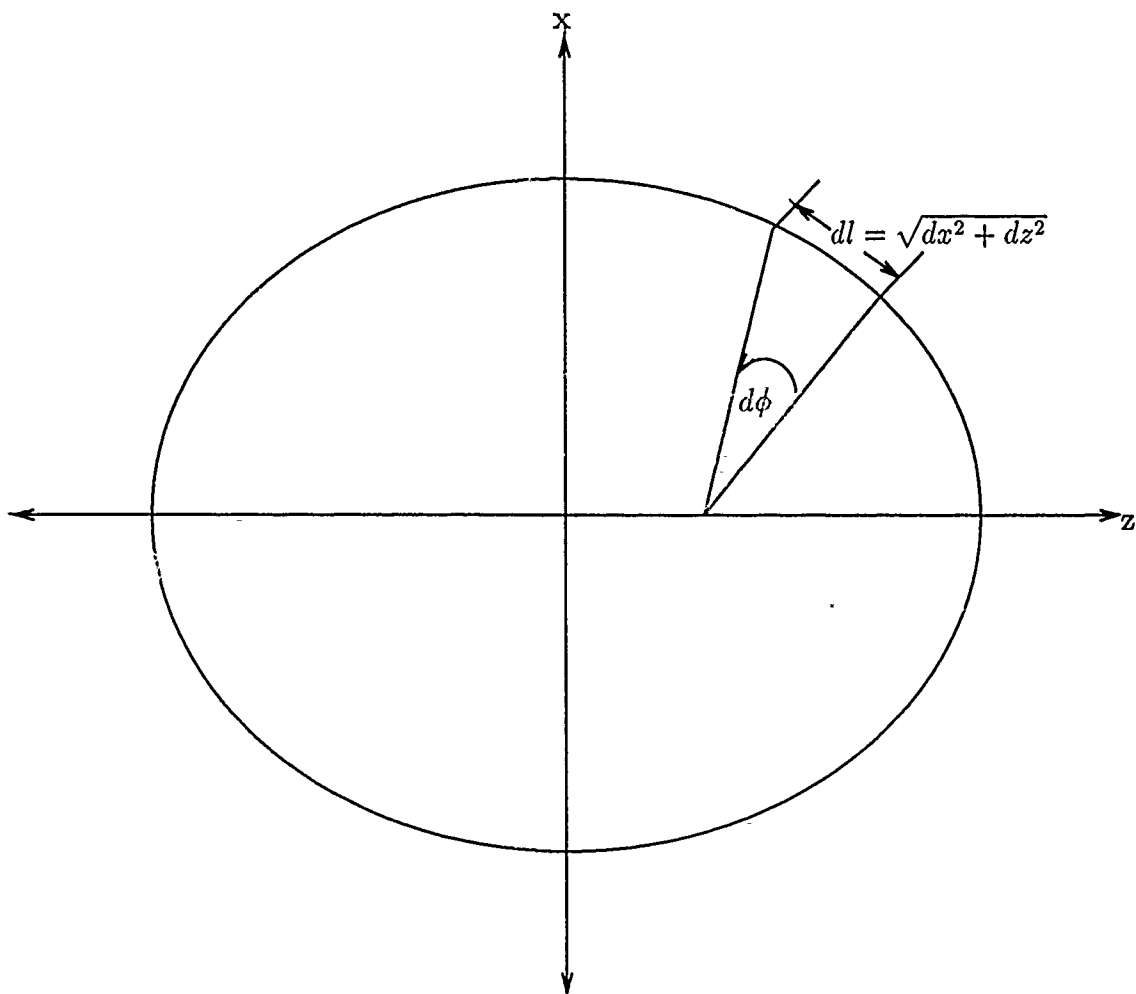


Figure 3.6. Differential arc length dl on a cross-section of the ellipsoid.

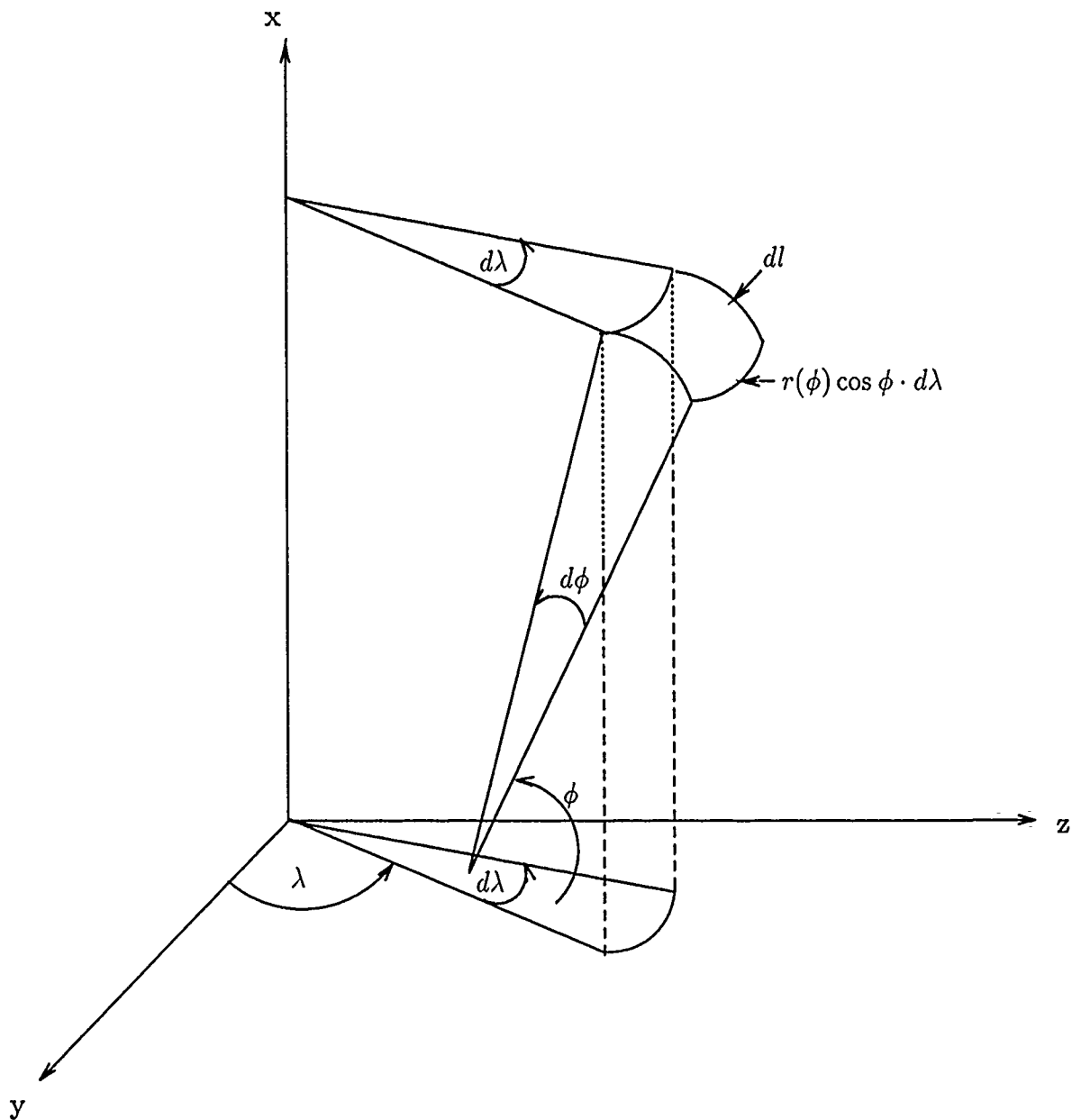


Figure 3.7. Differential area dA on the ellipsoid.

Substituting Equation 3.18 into Equation 3.19 and integrating over one degree each of latitude and longitude, the actual area A_i of shell $s_{i,j}$ (for any value of j , by symmetry) is

$$A_i = \int_{\phi=(i-1)^\circ}^{\phi=i^\circ} \int_{\lambda=0^\circ}^{\lambda=1^\circ} r(\phi) \cos \phi \sqrt{g1x(\phi, \lambda)^2 + g1z(\phi, \lambda)^2} \cdot d\lambda \cdot d\phi \quad (3.20)$$

Calculated values of A_i for each value of i from 1° to 90° , and the MathStation file which generated them, are given in Appendix D.

3.4.2.4 Validation of methodology. In order to validate the methodology and calculations presented above, a trapezoidal approximation of each shell's area was computed. For each latitude, the length of one arc degree of longitude was calculated. A local spherical approximation allowed us to assume that within each arc degree of latitude, the geocentric radius was constant at the value of the midpoint radius. Letting the variable "top" be the length of the upper longitudinal arc, "side" be the length of the sides of the shell, and "bottom" be the length of the lower longitudinal arc, we can approximate the area of the shell as

$$\text{ApproxArea} = \frac{(\text{top} + \text{bottom})}{2} \text{side} \quad (3.21)$$

Calculated values of this approximation for each value of i , and the MathStation file which generated them, are given in Appendix E. The approximate values compare favorably with those integrated by the previous technique.

3.5 Identify relationships between attributes.

3.5.1 Assign weights to attributes. The decision maker was next asked to assign relative weights to the attributes. The decision maker was presented with a list of the attributes and their definitions identical to that given in Section 3.3.3. The decision maker was asked to rank order the attributes from most to least important

to mission accomplishment (within the given scenario); assigning the number 1 to the most important attribute, 2 to the next most important, and so on. Ties in importance were allowed. This method will be referred to as *ranking*.

Next, a separate sheet of paper (Appendix A) was given to the expert containing the ordered list of attributes. To the right of the list was a scale from 0 to 100, marked off in units of ten. The decision maker was asked to draw a line from each attribute to the point on the scale which he thought best indicated that attribute's relative importance to mission accomplishment. The decision maker was permitted to select points between numbers, or to assign two or more attributes the same point on the scale. This method is similar to the *rating* method given by Eckenrode (8:181), whose scale was from 0 to 10 in single units.

The data given by the decision maker in each of the methods above was collated and checked for continuity and transitivity. The resulting weights, normalized to a total weight (sum) of one unit, are given in Table 3.1.

Attribute	Relative Weight
Sampling rate	.258
Timeliness	.226
Resolution	.194
Spectral coverage	.161
Registration error	.097
Dynamic range	.032
Number of gray shades	.032

Table 3.1. Initial Decision Attributes and Relative Weights

3.5.2 Attribute vector reduction. The procedures in sections 3.3.1 through 3.5.1 generated a total of seven attributes. Some reduction was required in order to assure computational efficiency and ease of comprehension of the final value function. But the proper degree of simplification was a significant issue, in order to avoid the pitfalls discussed in Section 2.2.1.5. For reasons discussed in detail in the following

sections, the four lowest-ranking attributes were discarded from consideration in the final MOE. Their total weight, from Table 3.1, was 0.322, or about one-third of the total weight.

3.5.2.1 Spectral coverage. Because this model is limited to assessing METSAT performance only on the basis of visual and infrared imagery, all satellites are assumed to have identical performance throughout this bandpass. This assumption was determined to be valid by the decision maker because of the inclusion of this type of sensor on all current operational METSATS. Therefore, this attribute is not included in the model. The low value of importance placed on this attribute by the decision maker (Appendix B) indicates that little information will be lost by its omission.

3.5.2.2 Registration error. Registration error is a complex phenomenon involving many factors, including range, frequency, and the satellite's accuracy in determining its own position (22). The range to each shell in the model is known. As mentioned in Section 3.5.2.1, the same bandwidth is assumed for all METSATS. However, an expression relating frequency and registration error was not available at the time of this writing. Also, the assumption that each METSAT maintains its nominal geostationary orbit perfectly eliminates any registration error due to inaccurate position determination. For all of these reasons, registration error will not be included in the model.

3.5.2.3 Dynamic range and number of gray shades. These two attributes, rated lowest in relative importance to mission accomplishment, were also omitted from the MOE model. The two attributes, which are actually different representations of the same parameter, measure the number of quantized levels available for display of the imagery. According to the decision maker, the number of levels differs insignificantly from one imagery system to another. Had data other than imagery

been included in the model, this attribute would have had to have been included.

3.5.3 Remaining Attributes. The three remaining attributes, along with their new normalized weights, are given in Table 3.2. Throughout the remainder of this

Attribute	Relative Weight
Sampling rate	.381
Timeliness	.333
Resolution	.286

Table 3.2. Final Decision Attributes and Relative Weights

document, the level of the attribute will be assigned a variable name that is simply the name of the attribute. The relative value assigned that level, on a scale from zero to one, will be assigned the subscripted variable R (following the notation from Chapter 2, Section 2.3.2), with the subscript matching the attribute's name. Thus, the attribute levels are *Sampling_Rate*, *Timeliness*, and *Resolution*. Their respective relative values are $R_{\text{Sampling_Rate}}$, $R_{\text{Timeliness}}$, and $R_{\text{Resolution}}$.

3.6 Choose a functional form.

3.6.1 Independence. As mentioned in Chapter 2, the existence of independence among all attributes implies either an additive or multiplicative form for the value function. For the purpose of demonstrating the technique, this quality was assumed to exist between each of the remaining three attributes. However, it should be noted that the independence was not statistically or otherwise proven. It could be the case, for example, that a significant increase in the level of resolution of a METSAT system would require a greater density of data transmission, increasing the amount of time required to process and deliver an image to the user. This would manifest itself in a decrease in the level of the timeliness attribute. However, such a relationship did not appear to be the case in the operational systems studied.

Most likely this is due to the large-bandwidth, high speed data transmission systems employed by all current operational systems.

3.6.2 Additive vs. multiplicative value. For any shell in the model, if the level of any of the attributes is zero, then the total value for that shell would be zero. For example, if the level of resolution was so low as to produce unintelligible imagery, there would be no value in the images whatsoever, regardless of the frequency with which they were received (sampling rate) or how quickly they were delivered (timeliness). Similarly, a zero value of sampling rate (no images received) drives the total value to zero, and the same is true for timeliness. Therefore, the form of the value function for this case should be multiplicative within each shell. Furthermore, each attributes' value for a particular shell shall be raised to an exponent appropriate to its relative weight to the decision maker, as shown in Figure 3.2. However, since the relative values are all numbers between zero and one, the relative weight is subtracted from one in the exponent in order to weight the more important attributes more heavily.

Between shells, however, the value function is additive. This is because the value gained in each shell is unaffected by the value in any other shell. Some MET-SATs will deliver very high value levels for a small number of shells and low or zero value elsewhere, while others will provide a lower level of value over a greater area. Summing the values over all shells will reflect this tradeoff.

On the basis of the preceding analysis, the value function within each shell $s_{i,j}$ was determined to be

$$\text{MOE}_{i,j} = \text{GeoWt}_{i,j} \cdot \text{PerArea}_{i,j} \cdot (R_{\text{Sampling_Rate}}^{(1-0.381)} \cdot R_{\text{Timeliness}}^{(1-0.333)} \cdot R_{\text{Resolution}}^{(1-0.286)})_{i,j} \quad (3.22)$$

The total value for the METSAT is found by averaging the value for all shells in the model. This value is the measure of effectiveness for that satellite.

$$MOE = \frac{\sum_{i=1}^{90} \sum_{j=1}^{360} MOE_{i,j}}{90 \cdot 360} \quad (3.23)$$

The MathStation file used to calculate the value of the MOE from the input data files is shown in Appendix G.

3.7 Express the value of each attribute over all points of the model.

3.7.1 Geographic area importance weights. The decision maker was provided with a map of the Northern Hemisphere and asked to rank order each shell in the model in its geographic importance to mission accomplishment. For example, the decision maker places a high priority on knowing the weather over the east coast of the United States, where most of the NORAD interceptors are located. A much lower priority is given to knowing the weather in the Pacific broad ocean area. The results received from the decision maker were color coded, and cannot be represented here. However, a black-and-white reproduction of the same chart, along with the MathStation file used to enter the data into the model, is given in Appendix F. The geographic area importance weight for shell $s_{i,j}$ is given as $GeoWt_{i,j}$.

Although a given shell in the model may have a particular importance to the decision maker, a METSAT in a particular geostationary orbit does not see all points equally. The shell at the satellite subpoint is imaged head-on, and so the perceived area is equivalent to the actual area of the shell. For all other shells, however, the curvature of the earth causes the area imaged by the satellite to appear smaller than it actually is. This effect becomes more extreme with greater angle, until the perceived area vanishes at the limb of the earth. Thus, another weighting factor is included in the model to account for this phenomenon.

3.7.1.1 *Perceived area.* Figure 3.8 shows a view of the earth and a geostationary satellite (not to scale) from above the plane of the ecliptic, looking down onto the north pole. If a vector from the satellite to the subpoint is dotted with a vector normal to the surface at the same point, the normalized dot product is -1 , because the two vectors are antiparallel. At the other extreme (Figure 3.9), a vector may be drawn from the satellite, tangent to the surface of the earth. By definition, this vector is perpendicular to the local surface normal at that point. Thus the dot product of these two vectors is identically zero. At all points between these extremes, the normalized dot product of the range vector from the satellite and the local surface normal yields a number between 0 and -1 , which scales the actual area to the perceived area. All points which are not visible to the METSAT, due to their being on the "other side" of the ellipsoid, will have a positive value for the dot product. Mathematically, if $\vec{\rho}_{i,j}$ and $\vec{n}_{i,j}$ are the range vector and normal vectors, respectively, to a point $p_{i,j}$, then let the area scaling factor $SF_{i,j}$ be given by

$$SF_{i,j} = -\frac{\vec{\rho}_{i,j} \cdot \vec{n}_{i,j}}{\|\vec{\rho}_{i,j}\| \|\vec{n}_{i,j}\|} \quad (3.24)$$

with the stipulation that if $SF \leq 0$, we set $SF = 0$. Then if the actual area of shell $s_{i,j}$ as calculated in Section 3.4.2.3 is $ActArea_{i,j}$, then the perceived area $PerArea_{i,j}$ is found by

$$PerArea_{i,j} = SF_{i,j} \cdot ActArea_{i,j} \quad (3.25)$$

Using a slightly modified version of our previous change of coordinates (Equations 3.11 through 3.14) which allows for points at an altitude h above the ellipsoid, we have

$$x(\phi, \lambda, h) = \left[\frac{a}{\sqrt{1-e^2 \sin^2 \phi}} + h \right] \cos \phi \cos \lambda \quad (3.26)$$

$$y(\phi, \lambda, h) = \left[\frac{a}{\sqrt{1-e^2 \sin^2 \phi}} \right] \cos \phi \sin \lambda \quad (3.27)$$

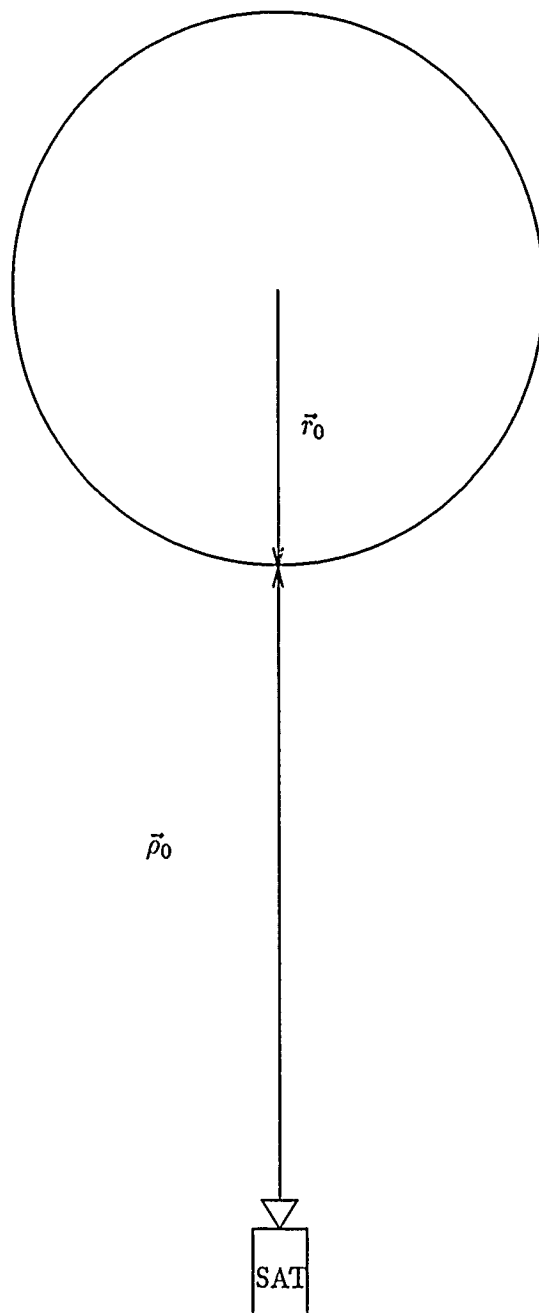


Figure 3.8. Vector from satellite to earth location at subpoint is antiparallel to local surface normal.

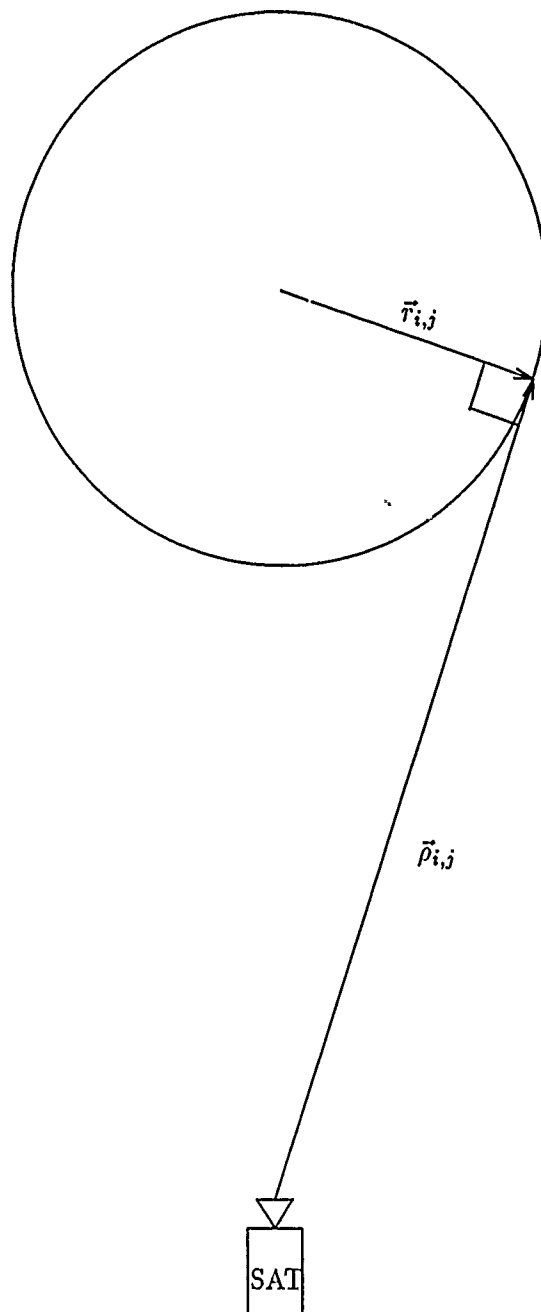


Figure 3.9. Tangent vector from satellite to earth location is perpendicular to local surface normal.

$$z(\phi, \lambda, h) = \left[\frac{a(1-e^2)}{\sqrt{1-e^2 \sin^2 \phi}} + h \right] \sin \phi \quad (3.28)$$

A vector normal to any point on the surface does not, in general, pass through the geocenter and thus is not parallel to the radius vectors computed earlier. However, such a vector may be generated by taking the cross product of the vectors of partial derivatives of $x(\phi, \lambda)$, $y(\phi, \lambda)$, and $z(\phi, \lambda)$ with respect to ϕ and λ . We do not need to include the variable h in these calculations yet, since all of the normal vectors will be calculated for points $p_{i,j}$ on the surface. The necessary partial derivatives are

$$\frac{\partial x}{\partial \phi} = \left[\frac{ae^2 \sin \phi \cos^2 \phi \cos \lambda}{(1-e^2 \sin^2 \phi)^{\frac{3}{2}}} \right] - \left[\frac{a \sin \phi \cos \lambda}{\sqrt{1-e^2 \sin^2 \phi}} \right] \quad (3.29)$$

$$\frac{\partial x}{\partial \lambda} = - \left[\frac{a \cos \phi \sin \lambda}{\sqrt{1-e^2 \sin^2 \phi}} \right] \quad (3.30)$$

$$\frac{\partial y}{\partial \phi} = \left[\frac{ae^2 \sin \phi \cos^2 \phi \sin \lambda}{(1-e^2 \sin^2 \phi)^{\frac{3}{2}}} \right] - \left[\frac{a \sin \phi \sin \lambda}{\sqrt{1-e^2 \sin^2 \phi}} \right] \quad (3.31)$$

$$\frac{\partial y}{\partial \lambda} = \left[\frac{a \cos \phi \cos \lambda}{\sqrt{1-e^2 \sin^2 \phi}} \right] \quad (3.32)$$

$$\frac{\partial z}{\partial \phi} = \left[\frac{ae^2(1-e^2) \sin^2 \phi \cos \phi}{(1-e^2 \sin^2 \phi)^{\frac{3}{2}}} \right] + \left[\frac{a(1-e^2) \cos \phi}{\sqrt{1-e^2 \sin^2 \phi}} \right] \quad (3.33)$$

$$\frac{\partial z}{\partial \lambda} = 0 \quad (3.34)$$

Now for any point $p_{i,j}$ and its associated ϕ_i and λ_j as determined from Equation 3.7, a normal vector to the surface of the geoid can be found by the relation

$$\vec{n}_{i,j} = \begin{bmatrix} \frac{\partial y(\phi_i, \lambda_j)}{\partial \phi} \frac{\partial z(\phi_i, \lambda_j)}{\partial \lambda} - \frac{\partial z(\phi_i, \lambda_j)}{\partial \phi} \frac{\partial y(\phi_i, \lambda_j)}{\partial \lambda} \\ \frac{\partial z(\phi_i, \lambda_j)}{\partial \phi} \frac{\partial x(\phi_i, \lambda_j)}{\partial \lambda} - \frac{\partial x(\phi_i, \lambda_j)}{\partial \phi} \frac{\partial z(\phi_i, \lambda_j)}{\partial \lambda} \\ \frac{\partial x(\phi_i, \lambda_j)}{\partial \phi} \frac{\partial y(\phi_i, \lambda_j)}{\partial \lambda} - \frac{\partial y(\phi_i, \lambda_j)}{\partial \phi} \frac{\partial x(\phi_i, \lambda_j)}{\partial \lambda} \end{bmatrix} \quad (3.35)$$

The range vector from the satellite to the point on the geoid also does not originate at the geocenter. However, a parallel vector can be found as the third leg of the triangle formed by the geocentric radius vectors to the satellite and the point $p_{i,j}$ (Figure 3.10). The ECF coordinates of $p_{i,j}$ are already known. It is a simple matter

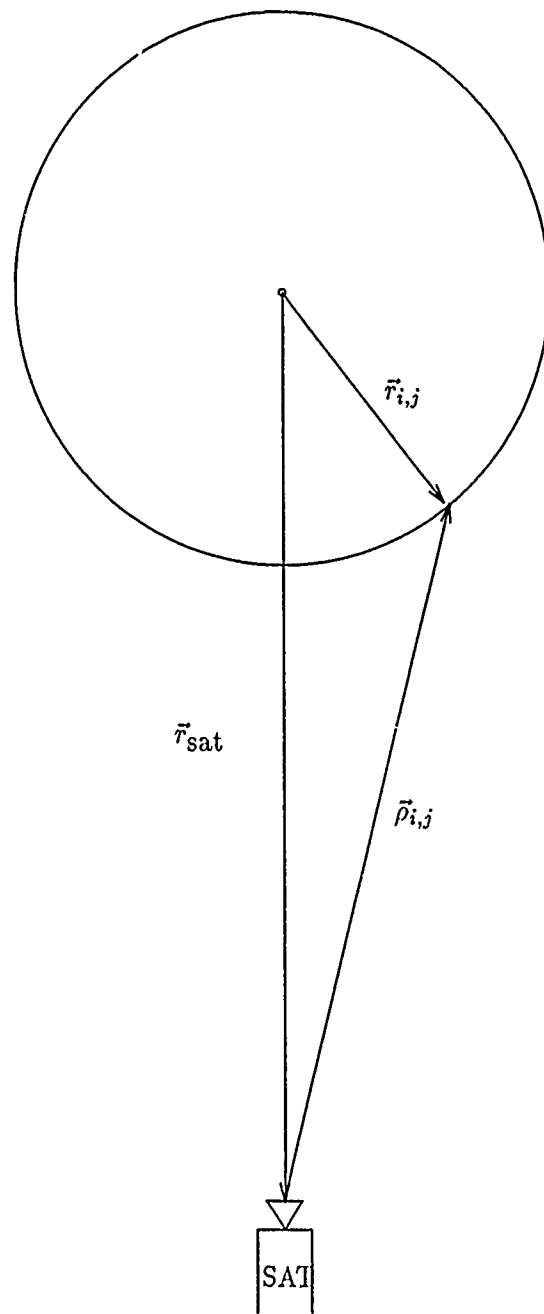


Figure 3.10. Range vector from METSAT to earth point, $\rho_{i,j}$ is the third leg of triangle including radius vectors to satellite and earth location $p_{i,j}$

to calculate the ECF coordinates of the satellite using Equations 3.26, 3.27, and 3.28. Substituting the satellites' nominal operational altitude ($h = 35,862.977$ km ideally, at geostationary altitude), a latitude of $\phi = 0^\circ$, and a longitude of the satellite's subpoint makes these functions of ϕ only, as shown below:

$$x(\phi) = (a + h) \cos \lambda \quad (3.36)$$

$$y(\phi) = a \sin \lambda \quad (3.37)$$

$$z(\phi) = 0 \text{ km} \quad (3.38)$$

Labeling this vector \vec{r}_{sat} , and the geocentric radius to the point $\vec{r}_{i,j}$, the slant range vector $\vec{\rho}_{i,j}$ is given as

$$\vec{\rho}_{i,j} = \vec{r}_{i,j} - \vec{r}_{\text{sat}} \quad (3.39)$$

Expanding the vectors gives

$$\vec{\rho}_{i,j} = \begin{bmatrix} (a + h) \cos \lambda \\ a \sin \lambda \\ 0 \text{ km} \end{bmatrix} - \begin{bmatrix} \frac{a \cos \phi \cos \lambda}{\sqrt{1 - e^2 \sin^2 \phi}} \\ \frac{a \cos \phi \sin \lambda}{\sqrt{1 - e^2 \sin^2 \phi}} \\ \frac{a(1 - e^2) \sin \phi}{\sqrt{1 - e^2 \sin^2 \phi}} \end{bmatrix} \quad (3.40)$$

or

$$\vec{\rho}_{i,j} = \begin{bmatrix} \left[(a + h) - \frac{a \cos \phi}{\sqrt{1 - e^2 \sin^2 \phi}} \right] \cos \lambda \\ \left[a - \frac{a \cos \phi}{\sqrt{1 - e^2 \sin^2 \phi}} \right] \sin \lambda \\ \left[\frac{-a(1 - e^2)}{\sqrt{1 - e^2 \sin^2 \phi}} \right] \sin \phi \end{bmatrix} \quad (3.41)$$

Now Equation 3.25 may be solved completely. It is expanded below to incorporate the derivation given above.

$$SF_{i,j} = - \frac{\begin{bmatrix} \left[(a+h) - \frac{a \cos \phi}{\sqrt{1-e^2 \sin^2 \phi}} \right] \cos \lambda \\ \left[a - \frac{a \cos \phi}{\sqrt{1-e^2 \sin^2 \phi}} \right] \sin \lambda \\ \left[\frac{-a(1-e^2)}{\sqrt{1-e^2 \sin^2 \phi}} \right] \sin \phi \end{bmatrix} \cdot \begin{bmatrix} \frac{\partial y(\phi_i, \lambda_j)}{\partial \phi} \frac{\partial z(\phi_i, \lambda_j)}{\partial \lambda} - \frac{\partial z(\phi_i, \lambda_j)}{\partial \phi} \frac{\partial y(\phi_i, \lambda_j)}{\partial \lambda} \\ \frac{\partial z(\phi_i, \lambda_j)}{\partial \phi} \frac{\partial x(\phi_i, \lambda_j)}{\partial \lambda} - \frac{\partial x(\phi_i, \lambda_j)}{\partial \phi} \frac{\partial z(\phi_i, \lambda_j)}{\partial \lambda} \\ \frac{\partial x(\phi_i, \lambda_j)}{\partial \phi} \frac{\partial y(\phi_i, \lambda_j)}{\partial \lambda} - \frac{\partial y(\phi_i, \lambda_j)}{\partial \phi} \frac{\partial x(\phi_i, \lambda_j)}{\partial \lambda} \end{bmatrix}}{\left\| \begin{bmatrix} \left[(a+h) - \frac{a \cos \phi}{\sqrt{1-e^2 \sin^2 \phi}} \right] \cos \lambda \\ \left[a - \frac{a \cos \phi}{\sqrt{1-e^2 \sin^2 \phi}} \right] \sin \lambda \\ \left[\frac{-a(1-e^2)}{\sqrt{1-e^2 \sin^2 \phi}} \right] \sin \phi \end{bmatrix} \right\| \left\| \begin{bmatrix} \frac{\partial y(\phi_i, \lambda_j)}{\partial \phi} \frac{\partial z(\phi_i, \lambda_j)}{\partial \lambda} - \frac{\partial z(\phi_i, \lambda_j)}{\partial \phi} \frac{\partial y(\phi_i, \lambda_j)}{\partial \lambda} \\ \frac{\partial z(\phi_i, \lambda_j)}{\partial \phi} \frac{\partial x(\phi_i, \lambda_j)}{\partial \lambda} - \frac{\partial x(\phi_i, \lambda_j)}{\partial \phi} \frac{\partial z(\phi_i, \lambda_j)}{\partial \lambda} \\ \frac{\partial x(\phi_i, \lambda_j)}{\partial \phi} \frac{\partial y(\phi_i, \lambda_j)}{\partial \lambda} - \frac{\partial y(\phi_i, \lambda_j)}{\partial \phi} \frac{\partial x(\phi_i, \lambda_j)}{\partial \lambda} \end{bmatrix} \right\|} \quad (3.42)$$

The MathStation file which generated the scaling factors and perceived areas for each shell, given an example METSAT subpoint of 5°E, are given in Appendix H.

3.7.2 Sampling rate. Sampling rates for various operational METSATS are given in Table 3.3. Of the five satellites for which data was available, three were geostationary: Geostationary Operational Environmental Satellite (GOES), Japan's Geostationary Meteorological Satellite (GMS), and TIROS-N. The other two, the Defense Meteorological Satellite Program (DMSP), and Europe's METEOSAT, are polar-orbiting.

Satellite System	Sampling Rate (samples/day)	Reference
GOES	48	(1)
DMSP	2	(19:46)
TIROS-N	2	(19:46)
METEOSAT	48	(13:D-14)
GMS	52.4	(13:E-7)

Table 3.3. Sampling rates of various operational METSATS

Based on this information, an upper limit of 96 images per day (one sample

every fifteen minutes) and a lower limit of 0 samples per day (no samples at all) were arbitrarily chosen by the analyst as being logical limits for METSAT sampling rates of any given location. Samples received more often than every quarter hour are unlikely to provide any more information, even in rapidly changing weather conditions. Similarly, no value whatsoever is received from a METSAT that does not send any images, for example, an inoperational METSAT. Also, those shells not in the field of view of a geostationary METSAT provide no information either.

The decision maker was then queried regarding the relative value of several sampling rate levels along this range, as shown in Table 3.4. This data was then fitted to a continuous preference function. The precise form of this function is determined in Chapter 4.

Sampling_Rate (samples/day)	Relative Value
0	0.00
1	0.60
2	0.75
3	0.80
4	0.85
6	0.90
12	0.95
24	0.96
48	0.98
96	1.00

Table 3.4. Relative values of various levels of sampling rate

3.7.3 Timeliness. Much less data regarding the Timeliness attribute was available than for Sampling_Rate. The 4th Weather Wing (4WW) relies primarily on only two systems, GOES and DMSP for its operational data. GOES data is consistently received by 4WW personnel approximately 30 minutes after collection,

according to the decision maker. This equates to a value of timeliness of 2/hr, the units selected by the decision maker in Section 3.3.3.

The timeliness of DMSP data varies widely, with delay times demonstrating a marked dependence on the geographical location imaged and the time of imaging. This is probably due to the fact that DMSP satellites must wait until they are over one of several tactical ground terminals in order to downlink their data (13:A-14). Data was collected by 4WW personnel on the receipt times for a single 24-hour period, and is displayed in Table 3.5. The values ranged from a "high" of 10 minutes, or 6/hr to a "low" of 105 minutes, or 0.571/hr.

Geographical Location	Shift Received	Timeliness (1/hr)
Europe	days	0.845
North Pole	days	0.698
North America 1	days	0.741
North America 2	days	0.800
Atlantic A	days	0.741
Atlantic B	days	0.741
Asia	days	2.308
Indian Ocean	mids	1.017
Far East	mids	5.455
Atlantic A	mids	6.000
Atlantic B	mids	6.000
North America 1	mids	3.750
North America 2	mids	0.571
Australia	mids	0.909
Europe	mids	0.845
Asia	mids	0.789
Atlantic	mids	1.304
North Pole	mids	0.845
Hawaii	mids	0.845
Mid East	mids	1.304

Table 3.5. Timeliness values for DMSP imagery received on 8 Nov 1990
(31)

The minimum value for timeliness was selected to be 0/hr. This is equivalent to saying that an infinite amount of time passes between receipt of successive images of any location, or that the images are not received at all. The maximum value cannot be bounded, since both the decision maker and analyst could foresee the possibility of real-time data transmission in the future.

The decision maker provided inputs reflecting his perception of the relative values of different levels of timeliness, which are displayed in Table 3.6. A continuous function approximating this data was created and is described in Chapter 4.

Timeliness (1/hr)	Relative Value
1/24	0.10
1/12	0.30
1/8	0.50
1/6	0.60
0.25	0.70
0.50	0.80
1.00	0.85
2.00	0.90
4.00	0.95

Table 3.6. Relative values of various levels of timeliness

3.7.4 Resolution. If the resolution, in kilometers per pixel, is known at a geostationary METSAT's subpoint, it may be calculated for any other point $p_{i,j}$ in the field of view. In this derivation we will assume all pixels are of the same size, and have a square shape on a flat image plane. Then the mapping of an individual pixel onto the METSAT's subpoint is shown in Figure 3.11. Note that there is an angle β_0 which is the angle between the line joining the center of the pixel with the center of its ground projection and the plane surface joining an edge of the pixel to its surface image. Since the distance between object plane and image plane is very large, and the pixel size is very small, we can approximate the linear length of one

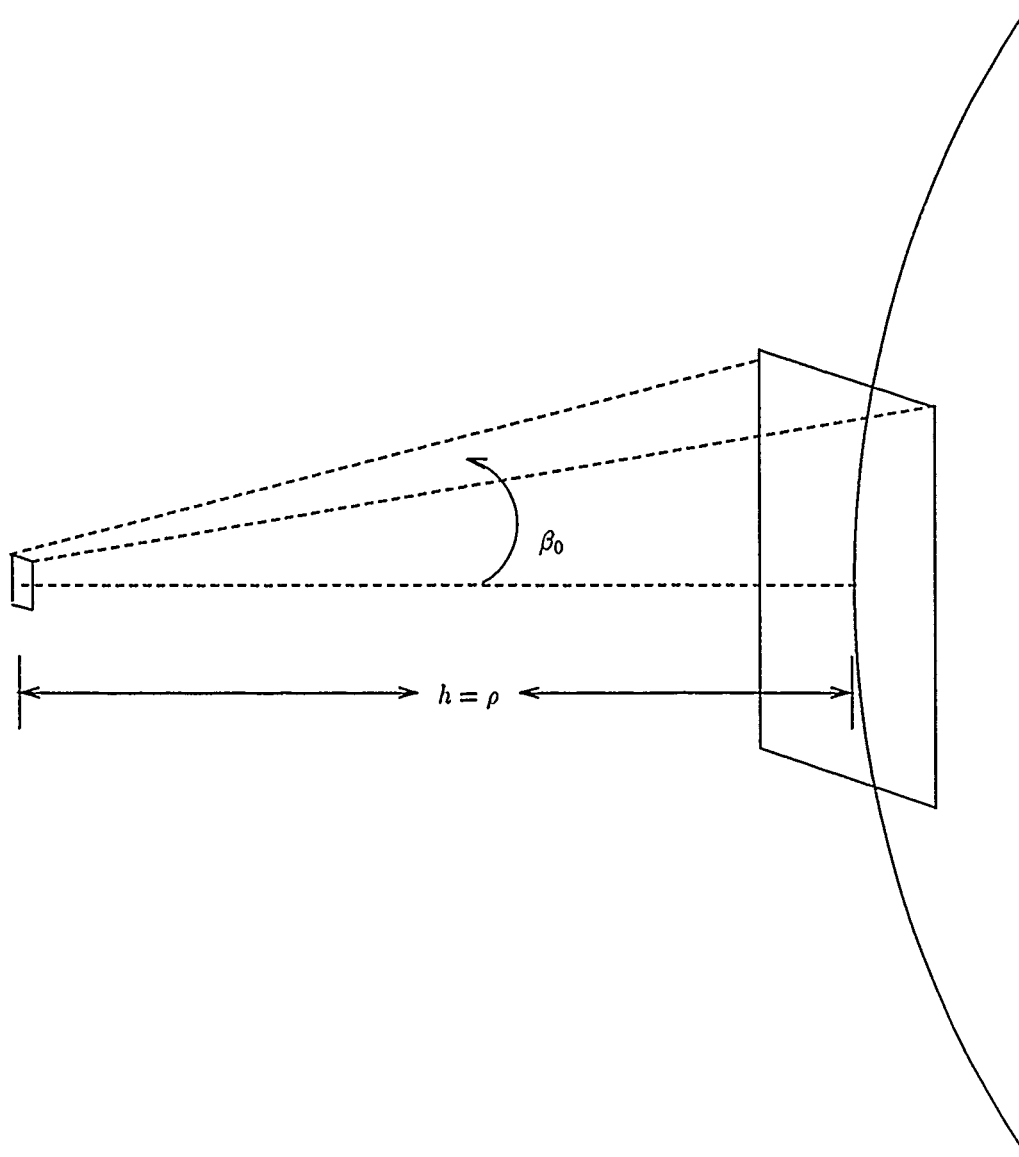


Figure 3.11. Resolution of a Pixel at the Satellite Subpoint

side of the pixel's projection onto the surface, RES_0 as

$$RES_0 = 2h \sin \beta_0 \quad (3.43)$$

Figure 3.12 shows the general case of a point $p_{i,j}$ being imaged by the same pixel. Here, the distance from the METSAT to the object plane is now the slant range $\rho_{i,j}$, which is the magnitude of the vector $\vec{\rho}_{i,j}$ calculated in Equation 3.41. The resolution at that point is then given by

$$RES_{i,j} = 2\rho_{i,j} \sin \beta_{i,j} \quad (3.44)$$

If we assume that the solid angle imaged by each pixel remains constant regardless of look angle, then

$$RES_{i,j} = \frac{\rho_{i,j}}{h} RES_0 \quad (3.45)$$

However, these calculations will give positive values of resolution for shells which are actually invisible to the METSAT, due to their being on the side of the earth facing away from the satellite. This can be corrected by checking the scale factors calculated in Section 3.7.1.1. If the value of the scale factor is zero, then the shell is not visible to the METSAT, and the value for local resolution should also be set to zero.

The MathStation file which generated the $RES_{i,j}$ values for an example METSAT subpoint of 5°E is included in Appendix I.

3.7.4.1 Conversion of raw resolution values. Values of advertised resolution for various operational METSATS are given in Table 3.7. They range from a minimum value of 2.8 km/pixel (noting that lower values bring more value) to a maximum value of 1 km/pixel.

When asked, the decision maker responded that no value of resolution worse

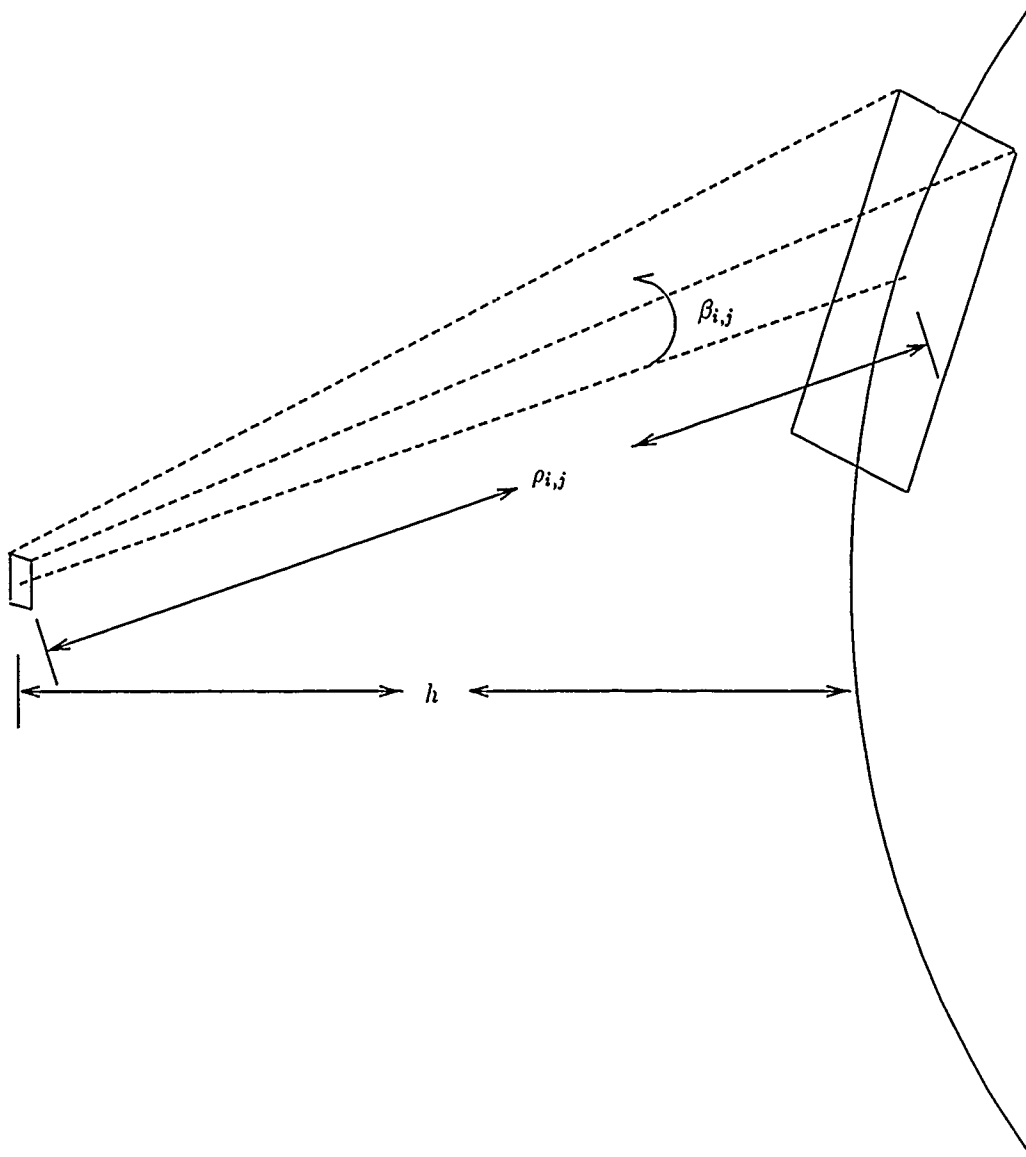


Figure 3.12. Resolution of a Pixel at Point $p_{i,j}$

Satellite System	Resolution (km/pixel)	Reference
GOES	1.00	(13:C-20)
DMSP	2.78	(13:A-2)
TIROS-N	1.10	(13:B-4)
METEOSAT	2.50	(13:D-14)
GMS	2.50	(13:E-7)

Table 3.7. Subpoint resolutions of various operational METSATS

than 10 km/pixel would add much value towards forecasting weather patterns, nor would it be likely that such poor resolution would ever be incorporated in any future METSAT. Therefore, 10 km/pixel was arbitrarily chosen by the analyst as the lower limit for value of resolution. Similar questioning of the decision maker revealed that no advances in resolution beyond 0.5 km/pixel would increase mission effectiveness, as it is the broader weather patterns that are of interest to the mission.

These values were presented to the decision maker, who provided the data necessary to construct a preference curve for resolution. This data is summarized in Table 3.8. The preference function generated as a best fit to this data is derived in Chapter 4.

Resolution (kilometers)	Relative Value
0.0	1.00
0.5	0.80
1.0	0.75
1.5	0.50
2.0	0.35
2.5	0.30
3.0	0.25
4.0	0.20
5.0	0.10

Table 3.8. Relative values of various levels of resolution

IV. Results and Analysis

4.1 Introduction.

This chapter applies the methodology developed in Chapter 3 to the analysis of current and hypothetical METSAT systems. The first analysis entailed measuring the MOE for a single satellite system, varying only the satellite subpoint. The data obtained was extrapolated and a simple relationship was found to relate the subpoint and MOE for that case. Next, the subpoint was fixed at a single value, and the effect of varying the other attributes was tested.

4.2 Relative Value curves.

Several functional forms were considered in modeling the data supplied by the decision maker in terms of continuous value functions. In each case, a two-parameter nonlinear least-squares approximation was used to determine the parameters of best fit. The results of each approximation were then plotted and empirically analyzed, and the form which best resembled the input data in both shape and error minimization was selected. In cases where more than one form gave good results, the form which most closely matched the data in the regions for which operational data was available was chosen, the rationale being that data in this range would be more likely to be encountered in test cases. Each form considered for an attribute will be listed, but only the one chosen is shown graphically.

4.2.1 Sampling rate. The data from Table 3.4 were plotted, with Sampling-Rate as the independent variable. This plot is shown in Figure 4.1.

Because the relative values increase very quickly over a short domain, and then remain very close to one, two types of exponential functions were considered. They were

$$y = 1 - ae^{-bx} \quad (4.1)$$

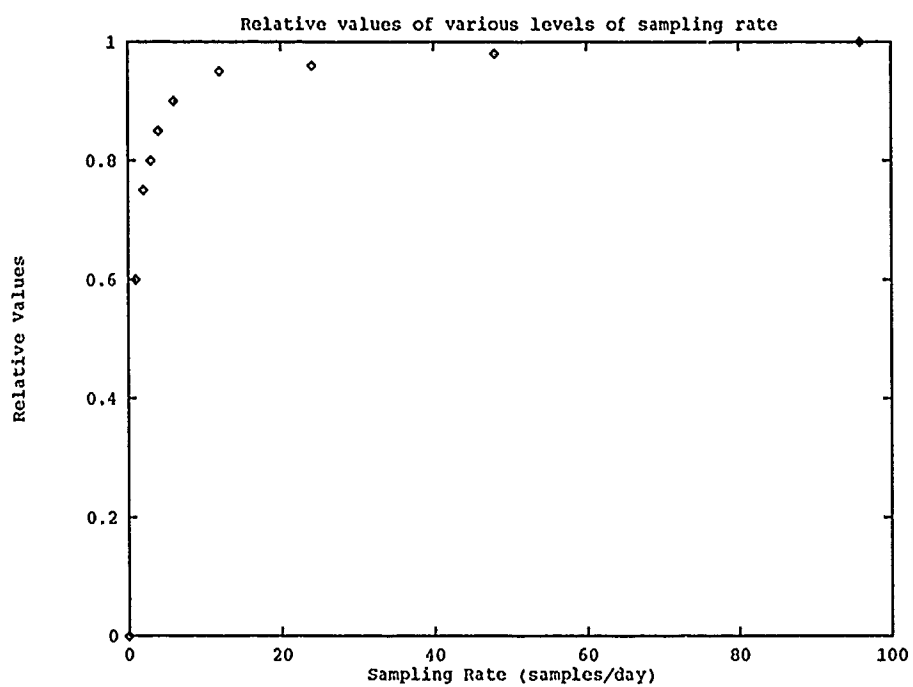


Figure 4.1. Graphic representation of sampling rate data provided by the decision maker.

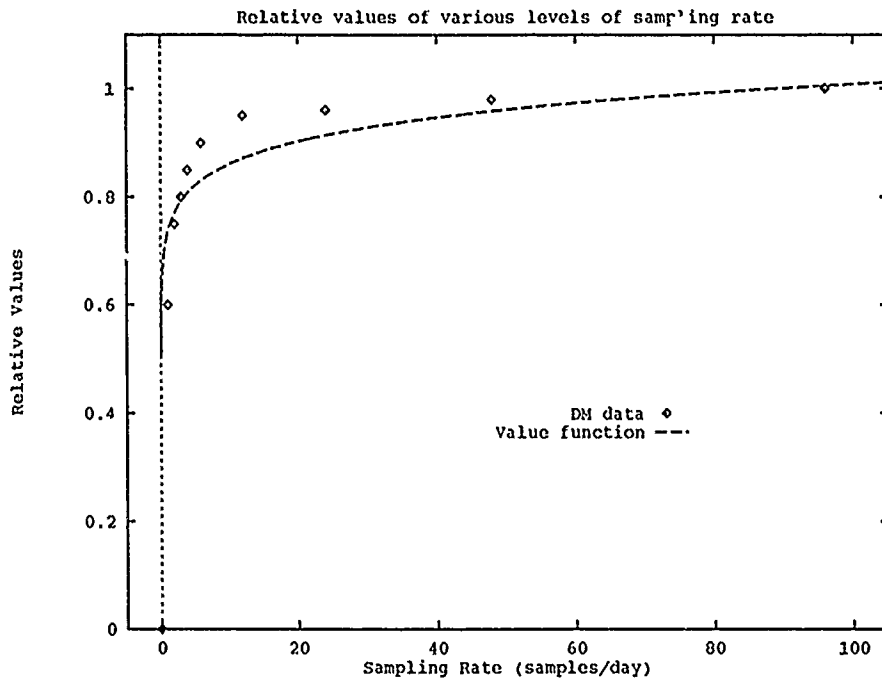


Figure 4.2. Relative Values of Various Sampling Rates

and

$$y = ax^b \quad (4.2)$$

Both equations gave least-squares approximations with variances of 0.004, but Equation 4.2 more closely fit the input data near a sampling rate of 48 samples/day, which is the most likely value to be observed from a geostationary METSAT. The best fit equation, as generated by the MathCad file in Appendix J, is

$$R_{\text{Sampling Rate}} = (0.734) \text{ Sampling Rate}^{(0.069)} \quad (4.3)$$

From Equation 4.3, the relative value of sampling rate for any METSAT, normalized to a maximum value of 1, can be found. The function is plotted along with the data supplied by the decision maker in Figure 4.2. This function, it should be noted, is only an approximation, or model, for the decision maker's preference

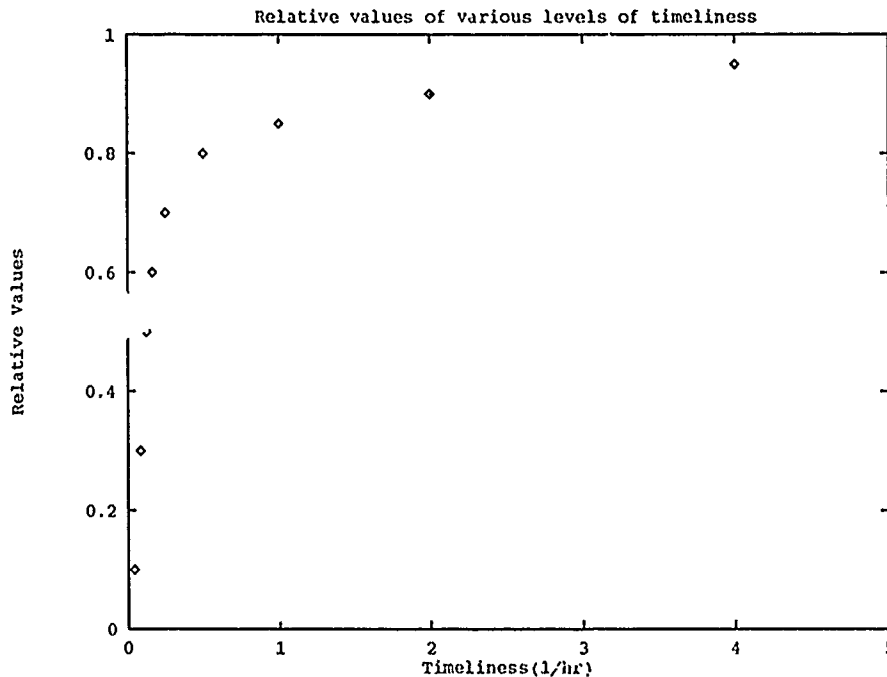


Figure 4.3. Graphic representation of timeliness data provided by the decision maker.

structure. Since the decision maker provided an exact relative value of 0.98 for the operational sampling rate level of 48 samples per day found in geostationary MET-SATs, this value will be used to generate MOEs, rather than the approximate value yielded by Equation 4.3. That equation would be used only for a case where the sampling rate was variable over different shells in the model. The MathStation file which generated the proper value for each point in the model is given in Appendix K.

4.2.2 Timeliness. A preference curve was next constructed for the timeliness data, which is given in Figure 4.3.

Because of the similarity of this data to the sampling rate data, Equations 4.1 and 4.2 were again the candidate forms. In this instance, Equation 4.1 gave the best results, with a variance of 0.008 over the nine points plotted. No coefficients could be found which would give Equation 4.2 a smaller variance than 0.034. The function

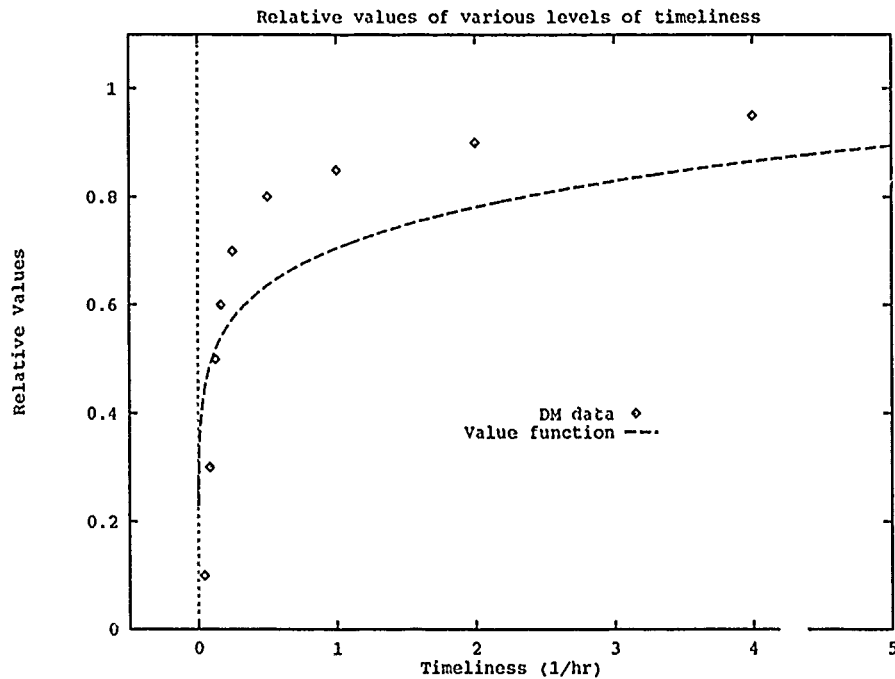


Figure 4.4. Relative Values of Timeliness

to convert raw measures of timeliness to relative value, as generated by the MathCad file in Appendix L, is

$$R_{\text{Timeliness}} = 1 - (1.03)e^{(-4.891) \cdot \text{Timeliness}} \quad (4.4)$$

This function, superimposed on the input data, is given in Figure 4.4. As was the case for the sampling rate data, the decision maker provided an exact value for the only level of timeliness considered in the current model. The geostationary GOES satellite system has an operational timeliness average of 2 hr^{-1} , which equates to a relative value of 0.90, as shown in Table 3.6. This is the value which will be used in all of the data runs. The MathStation file which placed this value into all of the shells is given in Appendix M.

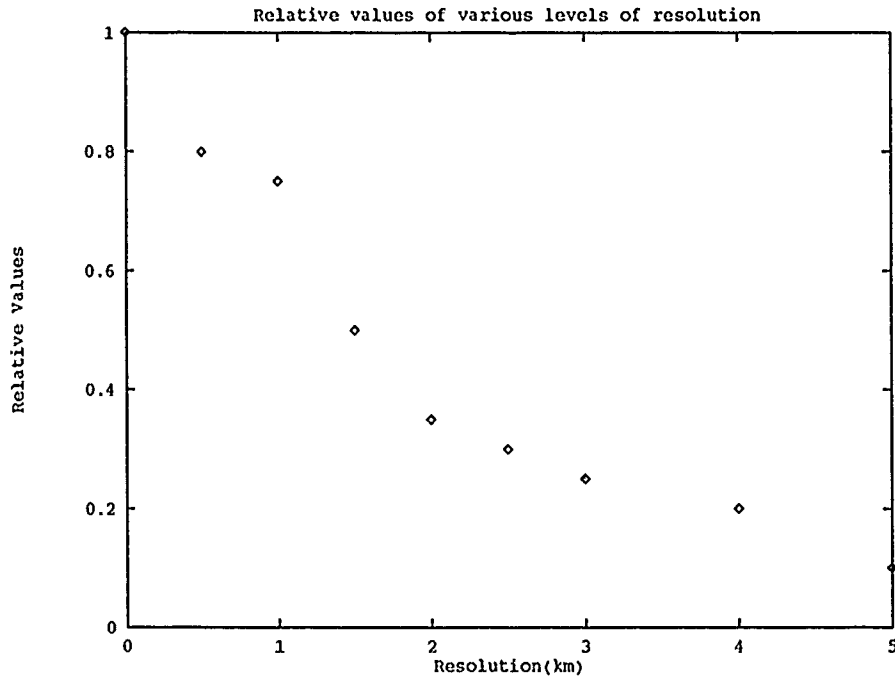


Figure 4.5. Graphic representation of resolution data provided by the decision maker.

4.2.3 Resolution. The data received from the decision maker regarding the relative value of different levels of resolution are presented in Figure 4.5.

The form of this preference function is clearly different than that for the other two attributes. The sloping decrease of value with increasing resolution levels (poorer resolution) indicated that a decaying exponential function of the form

$$y = ae^{bx} \quad (4.5)$$

may have been appropriate. In fact, good agreement w'th the input data was obtained with fit parameters of $a = 1.001$ and $b = -0.448$ (see MathCad file, Appendix N), yielding a value function of

$$R_{\text{Resolution}} = (1.001)e^{(-0.448) \cdot \text{Resolution}} \quad (4.6)$$

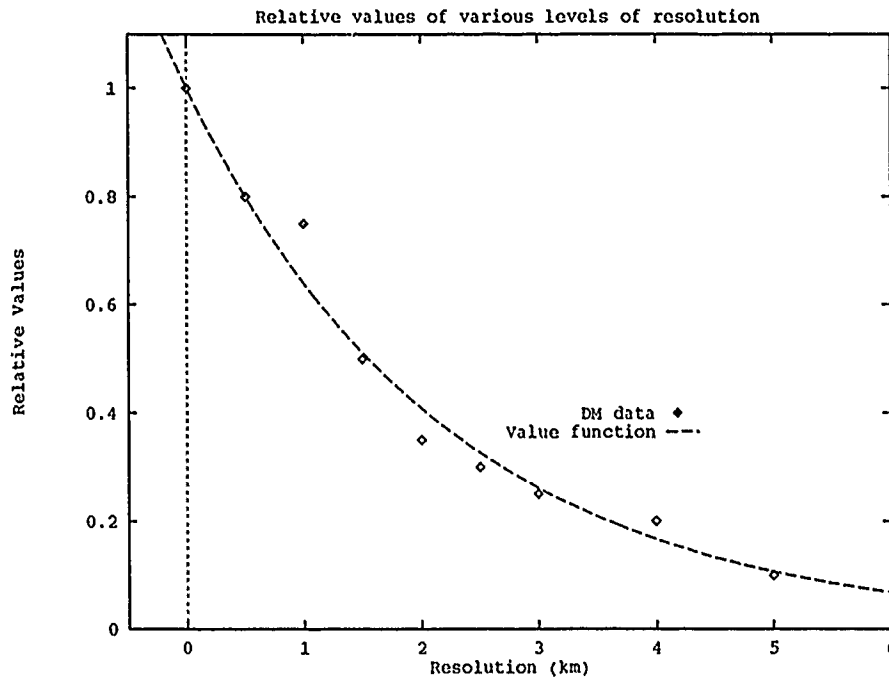


Figure 4.6. Relative Values of Resolution

A plot of this function, with the data from Table 3.8, is shown in Figure 4.6. In this instance, the level of resolution for a particular shell is dependent on that shell's location on the ellipsoid. Therefore, Equation 4.6 will be used in the model to calculate the relative values for each shell. The nominal value of GOES subpoint resolution, 1 kilometer per pixel (13:C-20), will be used.

4.3 MOEs for various subpoints.

The MOE described in Chapter 3 was generated for geostationary orbits with various subpoints as shown in Figure 4.1, using the nominal operational levels of GOES satellites for each attribute. This data is plotted graphically in Figure 4.7.

Subpoint (°E)	MOE	Subpoint (°E)	MOE	Subpoint (°E)	MOE
000	291.226	005	287.425	010	286.573
015	288.516	020	292.952	025	299.522
030	308.097	035	318.828	040	331.707
045	346.067	050	361.310	055	377.253
060	393.677	065	410.303	070	426.713
075	442.568	080	457.215	085	468.879
090	473.799	095	469.477	100	458.194
105	444.172	110	429.226	115	414.080
120	399.203	125	385.061	130	371.930
135	359.972	140	349.276	145	339.881
150	331.882	155	325.629	160	321.594
165	319.870	170	320.496	175	323.616
180	329.381	185	337.846	190	349.114
195	362.843	200	474.887	205	400.631
210	423.234	215	448.078	220	474.887
225	503.177	230	532.228	235	561.720
240	591.470	245	620.813	250	648.856
255	674.820	260	697.432	265	713.898
270	717.761	275	704.429	280	679.144
285	648.860	290	616.439	295	583.035
300	549.464	305	516.312	310	484.031
315	453.367	320	424.801	325	398.545
330	374.827	335	353.790	340	334.742
345	320.251	350	307.699	355	297.981

Table 4.1. Calculated values of the MOE for geostationary METSATs as a function of satellite subpoint

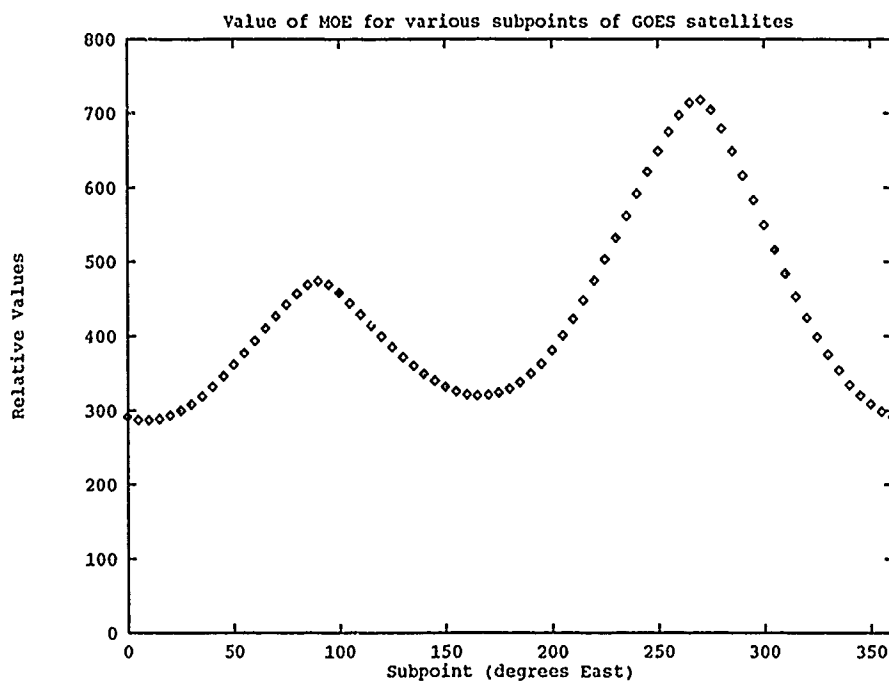


Figure 4.7. Graphic representation of calculated values of the MOE as a function of satellite subpoint.

4.4 Significance of the MOE.

4.4.1 *Unit analysis.* The equation developed in Chapter 3 for the MOE contribution of a single shell is

$$\text{MOE}_{i,j} = \text{GeoWt}_{i,j} \cdot \text{PerArea}_{i,j} \cdot (R_{\text{Sampling Rate}}^{(1-0.381)} \cdot R_{\text{Timeliness}}^{(1-0.333)} \cdot R_{\text{Resolution}}^{(1-0.286)})_{i,j} \quad (4.7)$$

Analyzing this equation, it is seen that the product of the terms involving the attributes sampling rate, timeliness, and resolution are unitless. Another interpretation would be to infer a unit of "value" on the terms, but that makes no sense here. The exponents of the terms are also unitless. The geographical area importance weights are similar in interpretation to the values of the attributes. They simply represent a measure of the relative importance of that shell to all other shells. However, the "value" terms, taken together, relate the goodness or quality of the imagery received by the decision maker. The exact nature of the individual contributions of the attributes is too complex to be easily understood (hence this thesis), yet it is known that all three, taken together, are a measure of the merit of the imagery. Therefore, we assigned the term *quality* to describe the units of the three when multiplied together.

The only term to have a definite physical interpretation is the perceived area term. It has the same units as area, km². Thus, the value calculated for each shell has units of *quality-km²*, or *quality area*. This term reflects the duality of what the decision maker wishes to maximize; not only does he need imagery of a large portion of the earth, it must be of sufficient quality to be useful. Either one alone is not acceptable.

Equation 3.23 takes the average of the *quality area* values over all shells in the model. This implies that the final MOE should have units of *average quality area* (AQA).

4.4.2 Limits of MOE. The minimum value of the MOE is reached when any single attribute has a relative value of zero over all points in the model. The *same* attribute in each shell need not have zero value; it is sufficient that *any* attribute does. As mentioned earlier, this drives the total MOE to 0 AQA.

The maximum limit of the MOE occurs when, for every shell, the relative value of each attribute is identically one, and the perceived area equals the actual area. The value obtained in this situation is 3299.7 AQA. Note that this value is independent of the METSAT subpoint. In effect, it implies that the satellite can see every point on the earth at all times and with perfect resolution, and can get this imagery to the user instantaneously. The one value in the model that the maximum is dependent on is the geographical area importance weights. Changing the distribution of these weights changes the maximum AQA possible. This is regarded as a weakness in the current model, and a proposed solution is offered in Chapter 5, Section 5.2.

4.5 Sensitivity to changes in sampling rate attribute.

Next, the MOE was tested to determine the results of varying degrees of sampling rate. The METSAT subpoint was fixed at the value 265°E, near the current operational subpoint (262°E) of the only GOES satellite at the time of this writing, and also near the maximum value for all the subpoints examined. The value of sampling rate was then varied across the range of likely levels specified in Chapter 3, Table 3.4. The data gathered is presented in tabular form in Table 4 2, and graphically in Figure 4.8.

4.6 Sensitivity to changes in timeliness attribute.

A similar analysis was then run, fixing all variables except for the timeliness attribute. The attribute was allowed to take on all values provided by the decision maker in Chapter 3, Table 3.6.

Sampling Rate (samples/day)	$R_{\text{Sampling_Rate}}$	MOE (AQA)
0	0.00	0.000
1	0.60	526.919
2	0.75	604.965
3	0.80	629.625
4	0.85	653.701
6	0.90	677.241
12	0.95	700.290
24	0.96	704.845
48	0.98	713.898
96	1.00	722.884

Table 4.2. Calculated values of the MOE for geostationary METSATs at 265E, as a function of sampling rate

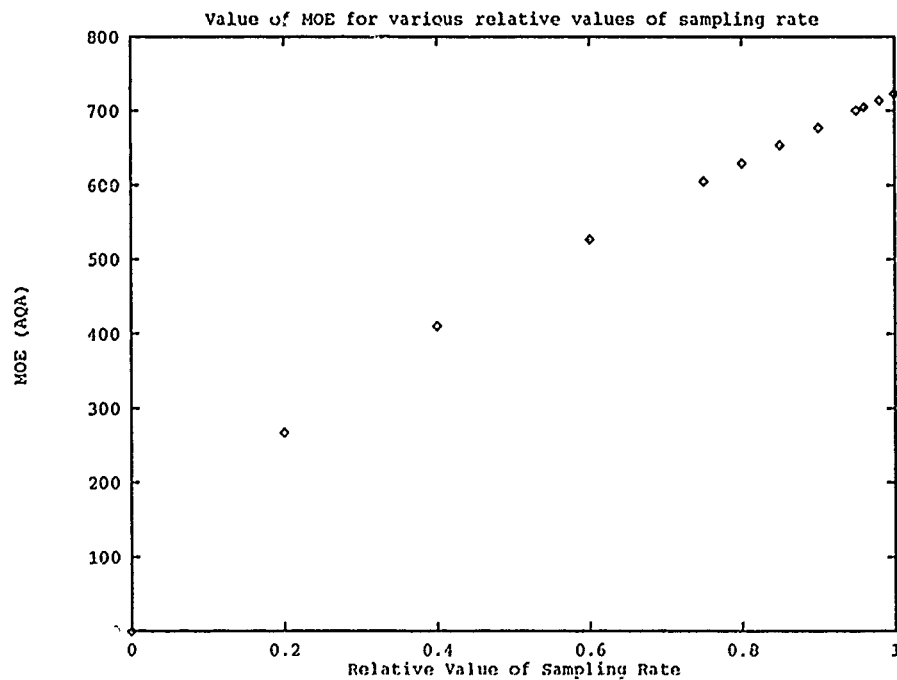


Figure 4.8. Graphic representation of sensitivity of MOE to changes in sampling rate attribute

Timeliness (hr ⁻¹)	$R_{\text{Timeliness}}$	MOE (AQA)
1/24	0.10	164.876
1/12	0.30	343.082
1/8	0.50	482.358
1/6	0.60	544.732
0.25	0.70	603.722
0.50	0.80	659.961
1.00	0.85	713.898
2.00	0.90	740.114
4.00	0.95	765.874

Table 4.3. Calculated values of the MOE for geostationary METSATS at 265E, as a function of timeliness

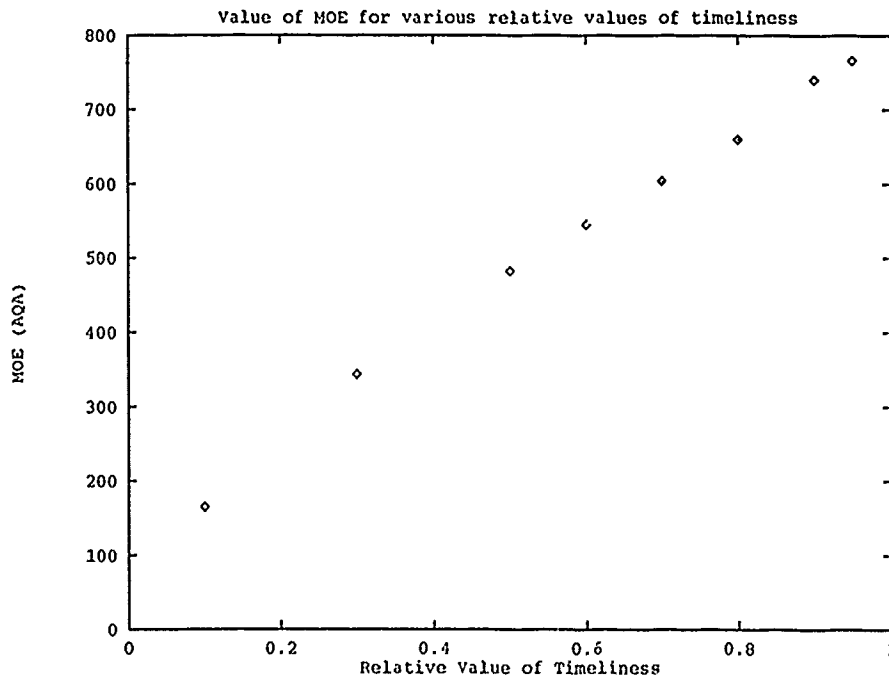


Figure 4.9. Graphic representation of sensitivity of MOE to changes in timeliness attribute

4.7 Sensitivity to changes in resolution attribute.

The third experiment run on the MOE examined its sensitivity to changes in the resolution attribute. The subpoint was fixed at 265°E, and the variable $R_{\text{Resolution}}$ was allowed to take on the values from Table 3.8. The results are shown in Table 4.4 and Figure 4.10.

Resolution (kilometers)	$R_{\text{Resolution}}$	MOE (AQA)
0.0	1.00	749.166
0.5	0.80	731.556
1.0	0.75	713.898
1.5	0.50	696.719
2.0	0.35	679.995
2.5	0.30	663.724
3.0	0.25	647.886
4.0	0.20	617.464
5.0	0.10	465.418

Table 4.4. Calculated values of the MOE for geostationary METSATS at 265E, as a function of resolution

4.8 Summary.

This chapter presented the results of several sample runs using the MOE developed previously. The proper interpretation of the MOE was given, and the units AQA were introduced and described. Three experiments to determine the marginal value of each of the attributes for a single geostationary METSAT were performed, and the results analyzed. The next chapter ties together these concepts and provides recommendations for further research.

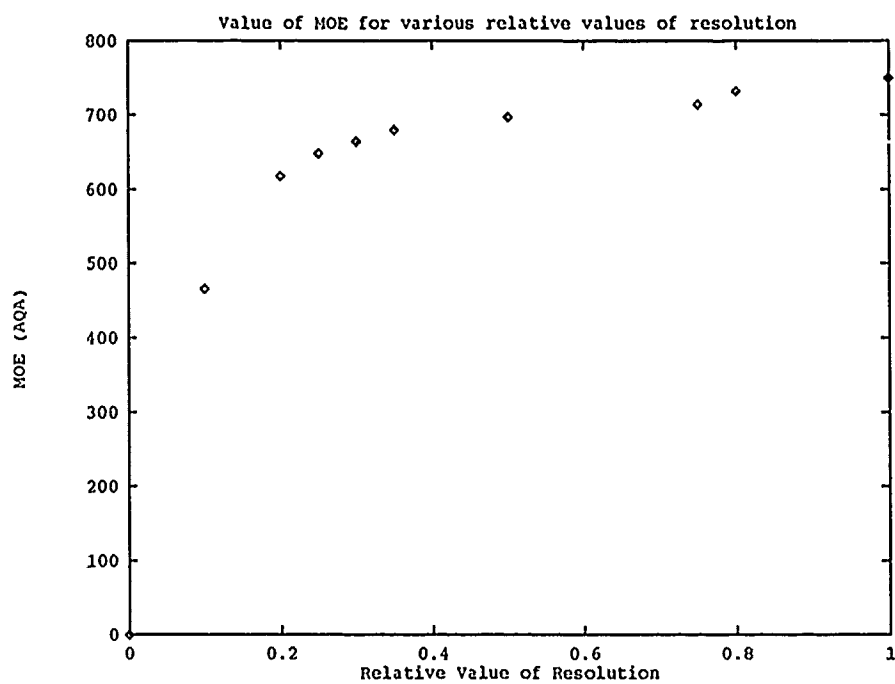


Figure 4.10. Graphic representation of sensitivity of MOE to changes in resolution attribute

V. Conclusion and Recommendations

5.1 Conclusion.

Based on the assumptions made, the measure of effectiveness created in this document is a useful method for measuring the mission effectiveness of satellite meteorological systems. It can determine the optimal subpoint at which to locate a single geostationary METSAT for a given set of performance parameters. In addition, the marginal value of each of the attributes addressed in the model may be reduced to simple linear relations over the ranges of those attributes found in most operational systems.

5.2 Shortcomings of the model and recommendations for further research.

- Link the modules in the appendices for MOE generation so that only one run is required for a given set of conditions. Memory management will need to be addressed. The modules presented were run on a Sun 4/260, a 15 million instructions per second (Mips) workstation with 32 Megabytes of random access memory (RAM). With no other users on the system, the calculation of resolution values nonetheless took over five minutes of central processing unit (CPU) time, at 100% CPU utilization. One complete cycle of modules to obtain a single MOE took approximately forty continuous minutes of CPU and operator input time.
- Generate a user-friendly "front end" code so that the decision maker could easily use the model. For example, the decision maker, after providing his or her preference information, could simply respond to prompts asking the type of METSAT, subpoint, and other features, and the model would generate the MOE without further input. It should be noted that MathStation generates Fortran 77 source code. This would be a good place to start.

- Expand the model to include sun-synchronous METSATS. To do so will require addressing time in some fashion. One approach would be to integrate the area covered by a METSAT over some standard period, such as one day. The 4th Weather Wing relies heavily on DMSP (a sun-synchronous METSAT) data for its forecasting (31). Inclusion of this system into the model should help provide some understanding of the tradeoffs between sun-synchronous and geostationary METSATS.
- Develop a means to include multiple METSATS in the model. The value (or utility) obtained by, say, two GOES satellites at different subpoints (such as in the nominal operational configuration) will not necessarily be the sum of the individual values (1). The area of coverage overlap would be of particular interest. There, some the value realized would likely be greater than the value of either satellite taken singly, but less than the strict sum of the values over that region.
- Include in the model those attributes identified by the decision maker as important, but not considered as part of the value function.
- Examine the effect of using different functional forms for the value of a particular shell, as opposed to Equation 3.22.
- Improve the functions used to calculate relative value from the raw levels of the attributes. High-order polynomials might give good results. Another approach would be to generate a preference "surface," using the axioms in Chapter 2 to determine the decision maker's preference among all attributes.
- Obtain greater fidelity data for the importance weights of the shells. The data used was provided in blocks of ten-by-ten shells for the decision maker's convenience. The decision maker also noted that the data provided did not reflect the importance of locations within the Soviet Union (31).

- Write a procedure which would plot the value of perceived area, graphically, on a projection of the reference ellipsoid. The edge of this calculated field of view should be the projection of a circle onto an ellipsoid. Compare this to the published usable field of view for GOES satellites, which is given as a circle.
- Include reliability data for the METSATS. The addition of this probabilistic element would change the value functions generated in this work to true utility functions.
- Near the end of this research, we realized that a more appropriate method of handling the geographical importance weights would be to normalize them such that they would sum to 1.0 over the model. This would have the effect of making the maximum possible AQA value independent of the distribution of area weights. The maximum AQA value would then be simply the average actual area of all shells in the model, or 7871.668 km².

Appendix A. *Meteorological Satellite (METSAT) Utility Survey*

(This page intentionally left blank)

METSAT Utility Survey

Captain Steven T. Wilson

15 Oct 1990

1 Introduction

The results of this survey will be used to construct functions to measure the utility of various METSATs. Fundamental to the methodology used is the fact that you, as an operational decision maker in this area, have a knowledge base and expertise unmatched by others without your credentials. It is that knowledge base and preference structure that this study attempts to capture. For this reason, any answer that you provide is necessarily the correct one for this study. Please feel free to make comments throughout the survey regarding your interpretation of the material, or explanation of the opinions you express. Thank you very much for your time.

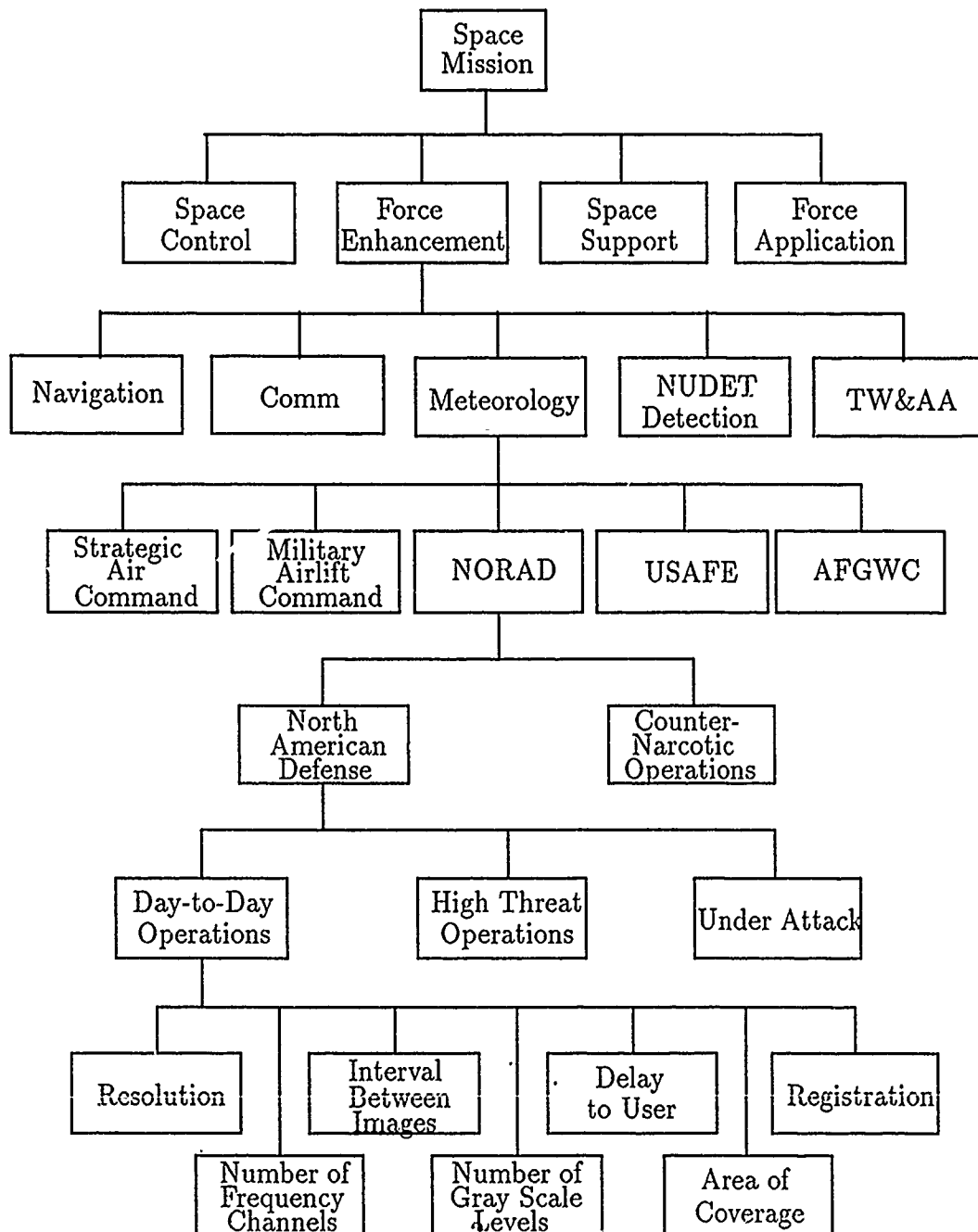
2 Background

The scenario you are asked to consider while making decisions for this study is shown graphically on the next page. That is, the study focuses on day-to-day peacetime weather reporting over the NORAD defended area in support of military aircraft operations. General and specific weather support requirements are referenced in NORAD Regulation 105-1, dated 16 September 1988.

3 Step One

With this scenario in mind, please turn to the page labeled *Attribute Definitions*. There you will see a series of terms for operating parameters of

Figure 1: Mission Hierarchy for the Satellite Meteorological Mission



METSATs, along with sample definitions. Preliminary research indicates that these attributes are those which directly affect mission effectiveness, or the accomplishment of the NORAD mission outlined above.

Please consider each item on the list in turn and decide whether or not it belongs on the list. An item does not belong on the list if, in your opinion, that parameter does not significantly contribute to mission accomplishment. Cross out any items that do not belong on the list, and briefly note why they should not be included.

Some items on the list may be *completely* described by one or more other variables. For example, if you were given the list "apogee, perigee, and orbital period," you might cross out "orbital period" because a satellite's period is completely described if both apogee and perigee are known. Eliminate any items from the list which meet this criterion.

Next, add any variables that have been omitted from the list. This includes any attribute of METSATs which significantly influence their operational effectiveness. Write these in at the bottom of the page, leaving room for short definitions.

If any of the definitions given disagree with your own interpretation, make whatever corrections are necessary. If possible, include any references you use. Also, please give a brief definition for any variables you added to the list.

4 Step Two

In this step, you will rank order the variables. To the left of each of the terms is a blank space. In that space, put the number of that term's relative ranking in terms of impact on mission effectiveness. Assign the most important variable the number 1. Be sure to rank any variables you've added to the list as well. Ties in importance are allowed.

5 Step Three

Now please turn to the page labeled *Rating Scale*. On this page you will assign relative weights to the variables. On the right-hand side of the page is a scale of value, ranging from "00" (completely unimportant to mission effectiveness)

to "100" (most important). Using your rankings from the previous step, first write in the names of the variables, in order, onto the page. The attribute you assigned rank 1 to will thus be listed at the top of the page.

Now you may proceed in either of two ways. You may:

- Draw a line from each variable to the appropriate place on the scale where it belongs in relative importance to the others. Ties are allowed. To help you decide, consider whether the higher-ranking variables are more important than some combination of lower-ranking variables. If so, the ratings should reflect that. When you are done, write the approximate numerical rating for each of the points you marked on the line, and circle it.
- Simply using the scale as a guideline, write the relative weight or rating for each variable to the right of that variable and circle it. Use the decision technique described in the previous paragraph.

6 Step Four

In this step you will identify dependence relations among the variables. Turn to the page marked *Dependence Relations*. It should be blank except for the title. Write the name of the first attribute, followed by the names of those attributes that affect or are affected by changes in that attribute. Farther down on the page, list the next (unused) attribute along with those others that are dependent on it. Continue this process until all attributes are accounted for.

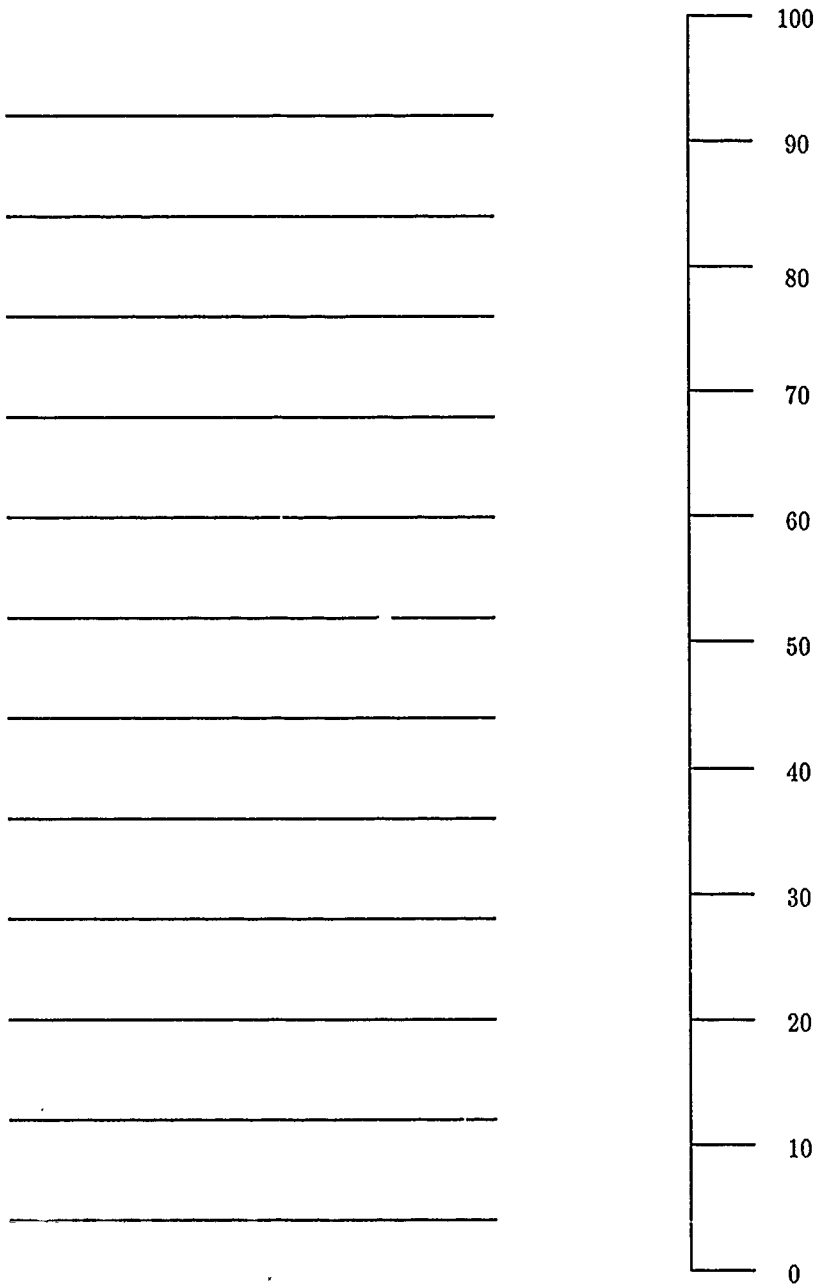
7 Step Five

Return the three pages marked *Attribute Definitions*, *Rating Scale*, and *Dependence Relations* to Capt Steve Wilson, AFIT/ENA432, Wright-Patterson AFB, OH 45433, or by the method given in the cover letter. Again, sir, your patience and cooperation are much appreciated.

Proposed Attribute Definitions

- Resolution/spot size/lines per inch: Length in kilometers of one side of a picture element's (pixel's) field of view at the satellite's sub-point.
- Orbital Parameters: If geostationary, satellite's sub-point in degrees West longitude. If sun-synchronous, solar angle in hours since local midnight.
- Registration Error: Maximum error between a pixel's actual and calculated geographical location.
- Interval between images: During normal operations, the time (in minutes) that elapses between consecutive scans of the same geographical error. If variant, the average value of all intervals.
- Time Delay to User: Average time, in minutes, that elapses between scanning an area and receipt of that imagery by 4th Weather Wing/NORAD Weather Directorate personnel.
- Area of Coverage: Percentage of earth's surface covered by satellite in one orbital period.
- Number of gray scale levels: Number of levels available for visual and/or infrared imagery.
- Number of frequency channels: 1, 2, or 3, depending on the number of the following bands represented — visible, near infrared (vapor), far infrared.

Rating Scale



Dependence Relations

Attribute:

Is dependent with:

Attribute:

Is dependent with:

Attribute:

Is dependent with:

Attribute:

Is dependent with:

Attribute:

Is dependent with:

Appendix B. *User Response to METSAT Utility Survey*

(This page intentionally left blank)

DEPARTMENT OF THE AIR FORCE
Headquarters 4th Weather Wing (MAC)
Peterson Air Force Base, Colorado 80914-5000

FROM: CV

26 Oct 90

SUBJECT: METAT Utility Survey

TO: Capt Steven Wilson


1. We have answered your survey. This looks like a good, but somewhat complex thesis topic. We reviewed your list of attributes and were able to combine some of them. However, we identified several new attributes that contribute to the overall utility of the METSAT imagery system used to support NORAD military aircraft operations.

2. We have identified seven basic attributes of a METSAT imagery system. These attributes, together with the variables that determine each attribute, are listed in Atch 1. Note that several of these attributes vary with geographic location. Therefore, many of the attributes depend on variables such as the elevation angle of the satellite relative to a particular location on the earth.

3. All of the attributes we identified act as utility multipliers. Therefore, any one of these attributes, if set to zero, will render the specific METSAT system useless. In spite of this, we were able to rank order the attributes according to whether or not they have reached the point of diminishing return with respect to utility. The state of the art of METSAT imagery systems is such that some attributes are more than adequate in contributing to the overall system utility. However, other attributes act as 'Achilles heels' to the overall utility and are still in great need of improvement. Therefore, we have rank-ordered the attributes according to their deficiency; attributes having the greatest need for improvement are ranked highest (Atch 2).

4. It seems this project could lead to some valuable results that would help decision-makers determine the best way to enhance the present METSAT imagery systems. Therefore, from a Total Quality Management standpoint, this project is very worthwhile.

5. If you have any further questions, contact Mr. Norman Baker (719-554-4856) or Capt Mark Storz (719-554-4856). Good luck with your research.



WILLIAM B. FREEMAN Jr., Col, USAF
Vice Commander

- 2 Atchs
1. Attributes and Determining Variables
2. Utility of Attributes (rank-ordered by deficiency)

ATTRIBUTES AND DETERMINING VARIABLES

<u>ATTRIBUTE</u>	<u>DETERMINING VARIABLES</u>
<p>1. SAMPLING RATE</p> <p>(Number of images per day)</p> <p>The sampling rate varies with geographic location.</p>	<ul style="list-style-type: none">- Elevation angle of satellite *- Elevation angle of the sun * (visual only)- Slant range of satellite *- Inherent sampling rate of the system- Angular coverage of camera field of view <p>* Note: An asterisk indicates a variable that depends on geographic location</p>
<p>2. TIMELINESS</p> <p>(Processing time intervals per hour)</p> <p>eg. If a particular image gets to the user in 30 minutes, TIMELINESS = 2 hr^{-1}</p>	<ul style="list-style-type: none">- Inherent sample (image) processing time- Location of segment of earth (latitude and longitude) <p>Note: certain locations can be processed quicker if their imagery is collected immediately before the data is downloaded.</p>
<p>3. RESOLUTION</p> <p>(Pixels/km²)</p> <p>The resolution of the GOES imagery system varies with geographical location.</p>	<ul style="list-style-type: none">- Angular resolution (Pixels/steradian)- Elevation angle of satellite *- Slant range of satellite *
<p>4. SPECTRAL COVERAGE</p> <p>Frequency range measured in units of (logarithm of the frequency)</p> <p>This is complicated by the fact that certain parts of the electromagnetic spectrum are more useful than others for meteorological interpretation.</p>	<ul style="list-style-type: none">- This is an intrinsic characteristic of the particular system

5. REGISTRATION ERROR
(ERROR IN POSITION)

(Standard deviation in km)

- Slant range of satellite *
- Elevation angle of satellite *
- Azimuth of satellite *
- Azimuth of linear measurement on the earth's surface

6. "DYNAMIC" RANGE OF
IMAGERY SYSTEM

- This is an intrinsic characteristic of the particular system

This is the dynamic range of the entire gray scale
Units such as the logarithm of the maximum flux minus the logarithm of the minimum flux could be used.

7. NUMBER OF GRAY SHADES

- This is an intrinsic characteristic of the particular system

This is the number of gray shades per unit dynamic range.

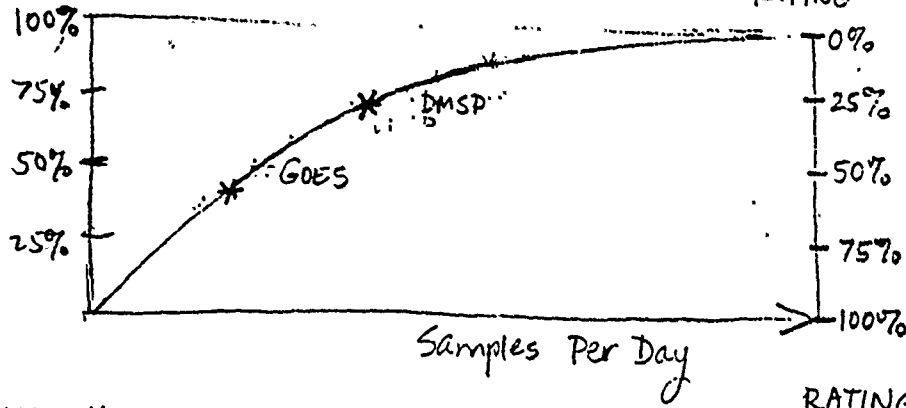
NOTE: Multiplying quantity 6. times quantity 7. gives the total number of gray shades of the system

NOTE: The variables, elevation angle, azimuth, and slant range of the satellite are a function of the satellite orbital parameters, the particular geographic location, and the time.
The variable, solar elevation angle, is a function of geographic location and time.

UTILITY OF ATTRIBUTES

UTILITY

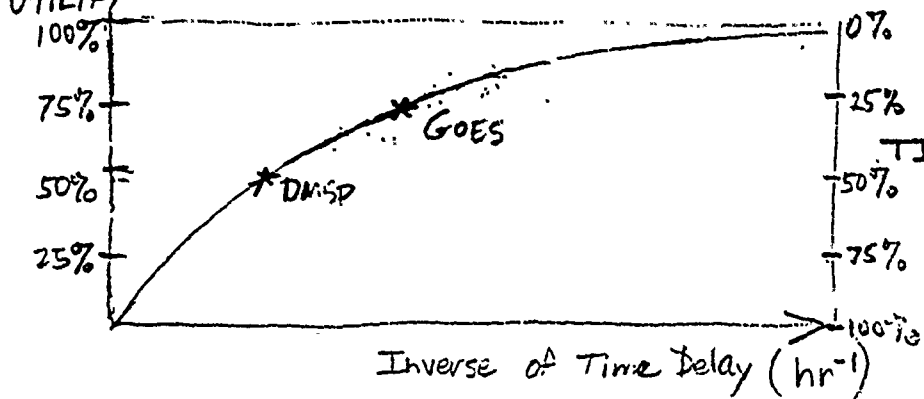
RATING



#1
SAMPLING RATE
40% = RATING

UTILITY

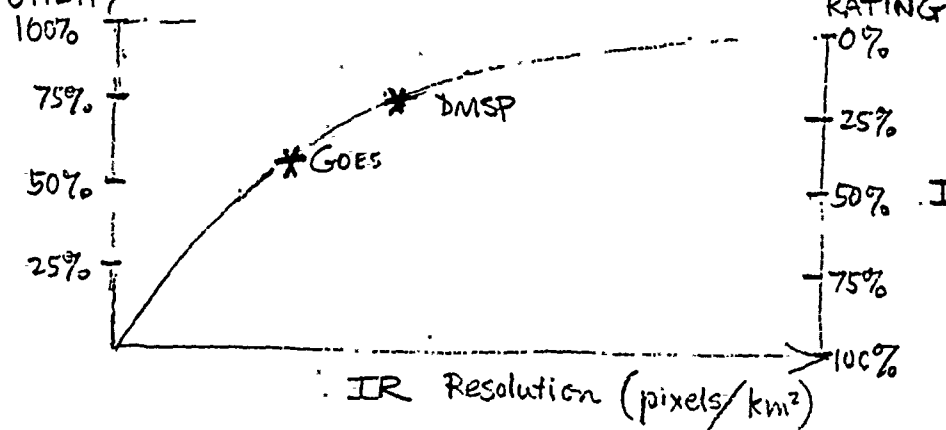
RATING



#2
TIME LINESS
35% = RATING

UTILITY

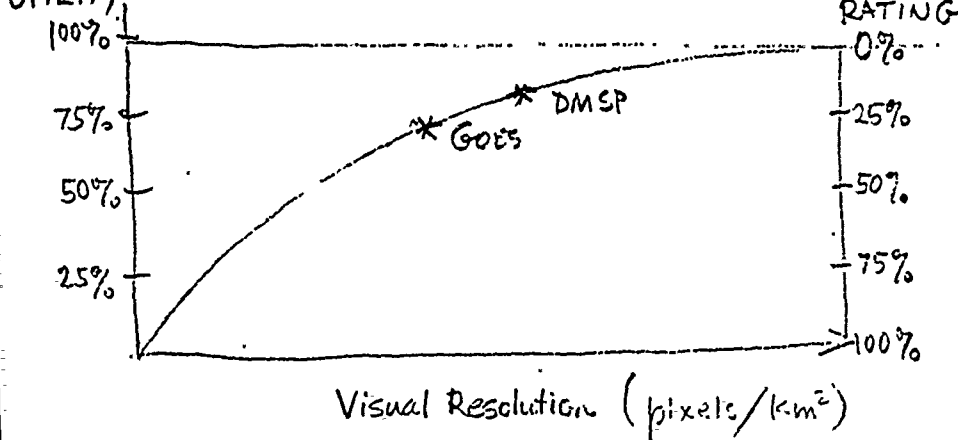
RATING



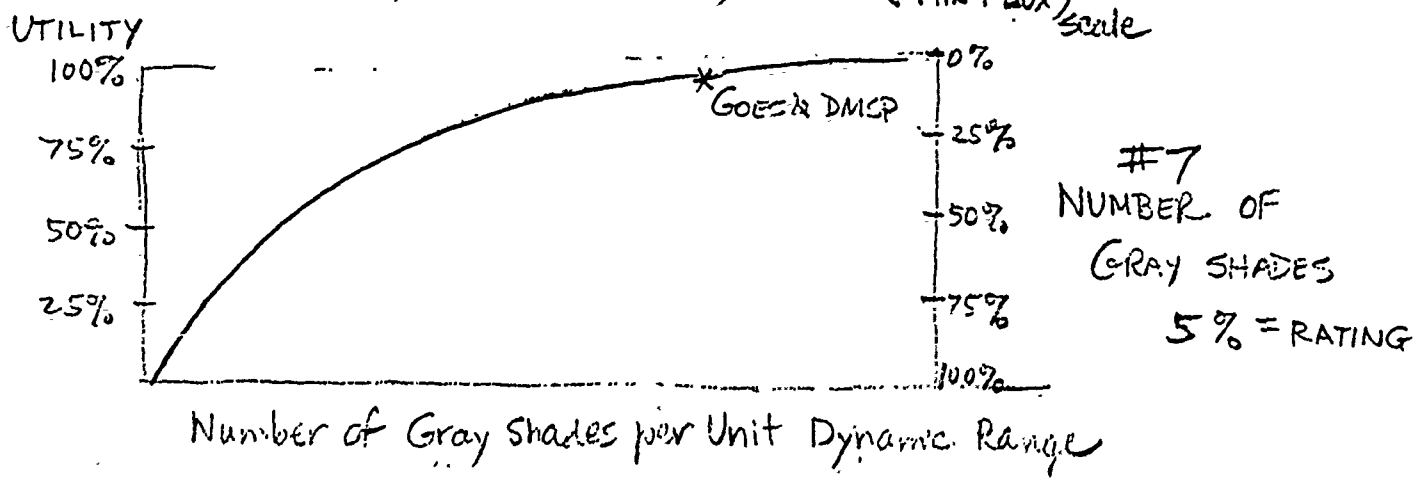
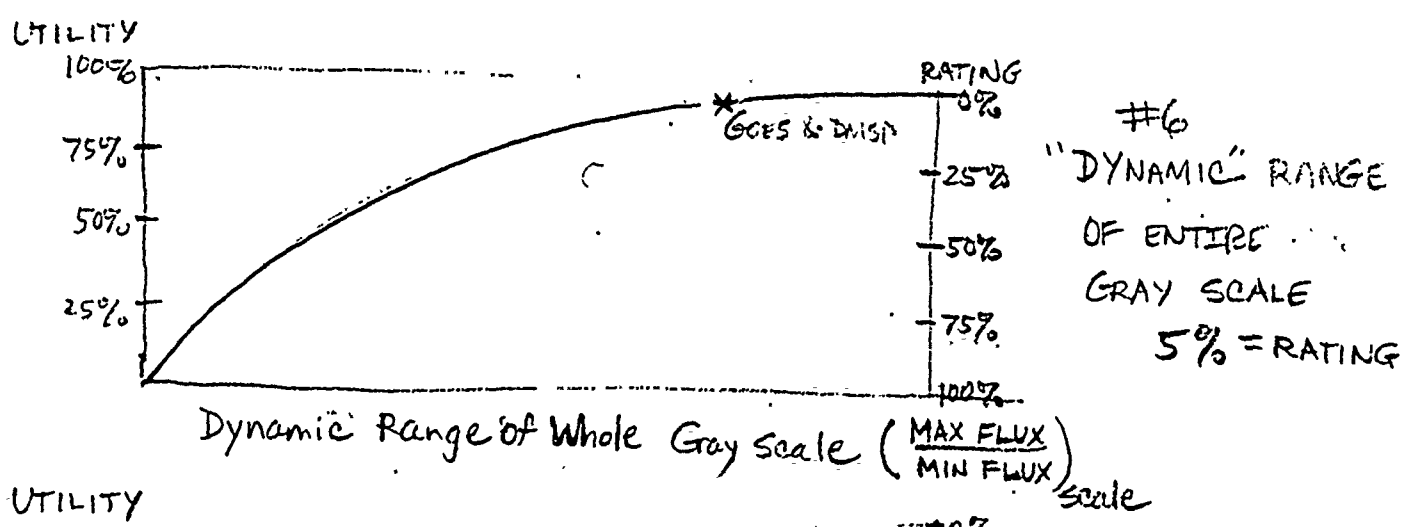
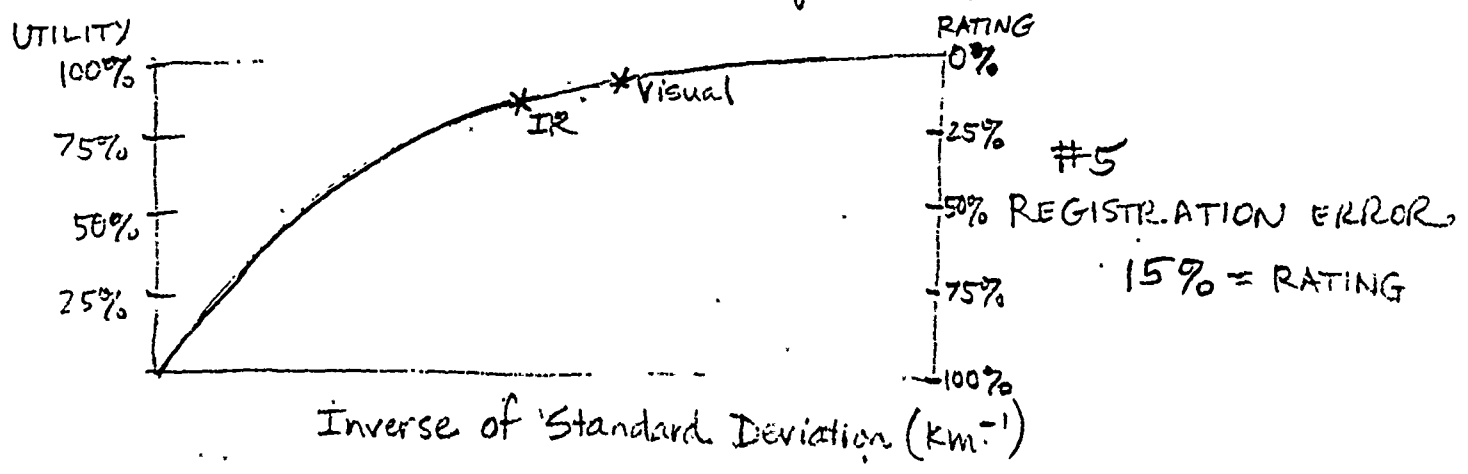
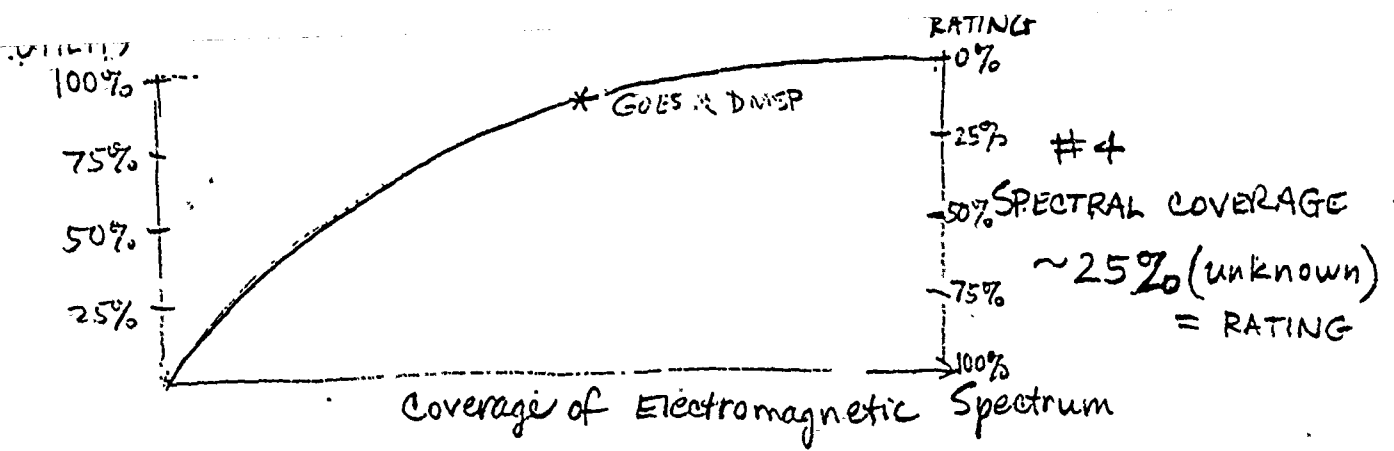
#3-A
INFRARED RESOLUTION
30% = RATING

UTILITY

RATING



#3-B
VISUAL RESOLUTION
20% = RATING



NOTE: $\left(\frac{\text{MAX FLUX}}{\text{MIN FLUX}}\right)_{\text{scale}} = \left(\frac{\text{MAX FLUX}}{\text{MIN FLUX}}\right)_{\text{shade}}^N$ $N \equiv \text{Number of Gray Shades}$

Appendix C. *Shell model generation file*

Generation of Shell Model

This is MAKESHELLS.DOC, a MathStation file which generates shell data files
GEODPOINTS.DAT and ECFPOINTS.DAT

$a, b, e, lat, long \in \text{real}$ Declare variable types

$i, j, k \in \text{integer}$

$\phi, \lambda \in \text{real},$

$geodetic, ecf \in \text{real}, ?$

invoke *setprecision*(12) Instruct MathStation to display real values to 12 digits precision

function *rad*(α) $\in \text{real}$ This function converts degree measures to radian units

on $\alpha \in \text{real}$ is

$$rad := \alpha \cdot \left(\frac{\pi}{180} \right)$$

end

$a := 6378.145$ Earth mean equatorial radius

$b := 6356.785$ Earth mean polar radius

$$e := \frac{\sqrt{(a^2 - b^2)}}{a} \quad \text{Eccentricity factor for oblate ellipsoid model of Earth}$$

$e = 0.08177166432142$ Display value of e calculated

for $i := 1$ to 90 do Generate geodetic latitude (in degrees) for all points in the model

$$\phi_i := 0.5 \cdot (2 \cdot i - 1)$$

end

for $j := 1$ to 360 do Generate earth-fixed longitude for all points in model

$$\lambda_j := 0.5 \cdot (2 \cdot j - 1)$$

end

ECF Coordinates of Points on or Above the Geoid

function $x(\varphi, \lambda, h) \in \text{real}$

on $\varphi, \lambda, h \in \text{real is}$

$$x := \left(\frac{a}{\sqrt{(1 - e^2 \cdot \sin(\varphi)^2)}} + h \right) \cdot \cos(\varphi) \cdot \cos(\lambda)$$

end

Function calculates x-coordinate of ECF position, given geodetic latitude and longitude (in radians), and altitude above the reference ellipsoid in kilometers

function $y(\varphi, \lambda, h) \in \text{real}$

on $\varphi, \lambda, h \in \text{real is}$

$$y := \left(\frac{a}{\sqrt{(1 - e^2 \cdot \sin(\varphi)^2)}} \right) \cdot \cos(\varphi) \cdot \sin(\lambda)$$

end

Function calculates y-coordinate of ECF position, given geodetic latitude and longitude (in radians), and altitude above the reference ellipsoid in kilometers

function $z(\varphi, \lambda, h) \in \text{real}$

on $\varphi, \lambda, h \in \text{real is}$

$$z := \left(\frac{a \cdot (1 - e^2)}{\sqrt{(1 - e^2 \cdot \sin(\varphi)^2)}} + h \right) \cdot \sin(\varphi)$$

end

Function calculates z-coordinate of ECF position, given geodetic latitude and longitude (in radians), and altitude above the reference ellipsoid in kilometers

Generate files containing all Geodetic and ECF points on geoid

$k := 1$

Initialize counter to create one long index for all points

for $i := 1$ **to** 90 **do**

Iterate over all valid latitudes

for $j := 1$ **to** 360 **do**

Iterate over all valid longitudes

$lat := rad(\varphi_i)$
 $long := rad(\lambda_j)$

Convert latitude to radians

Convert longitude to radians

$geodetic_{1,k} := lat$

Put geodetic latitude into 1st column of array 'geodetic'

$geodetic_{2,k} := long$

Put geodetic longitude into 2nd column of array 'geodetic'

$ecf_{1,k} := x(lat, long, 0.0)$

Put ECF x-coordinate into 1st column of array 'ecf'

$ecf_{2,k} := y(lat, long, 0.0)$

Put ECF y-coordinate into 1st column of array 'ecf'

$ecf_{3,k} := z(lat, long, 0.0)$

Put ECF z-coordinate into 1st column of array 'ecf'

$k := k + 1$

Increment index counter

end

end

Writes Geodetic Coordinates to file GEODPOINTS.DAT

```
invoke open_file(1,"geodpoints.dat","FORMATTED" )  
invoke put_file(1,geodetic,"( G18.10, G18.10)")  
invoke close_file(1)
```

Writes ECF Coordinates to file ECFPOINTS.DAT

```
invoke open_file(2,"ecfpoints.dat","FORMATTED" )  
invoke put_file(2,ecf,"( G18.10, G18.10, G18.10)")  
invoke close_file(2)
```

End of Document

Appendix D. Actual Area of shells $s_{i,j}$ for all Values of i

Computation of Actual Shell Areas

This is ACTAREA.DOC, a MathStation file which calculates the actual area of each shell in the model and writes this information to file ACTAREA.DAT

$a, b, e \in \text{real}$ Declare variable types

$i, j, k \in \text{integer}$

$\varphi, \lambda \in \text{real}_2$

invoke *setprecision*(12) Instruct MathStation to display real values to 12 digits precision

function $\text{rad}(\alpha) \in \text{real}$ This function converts degree measures to radians
on $\alpha \in \text{integer}$ is

$$\text{rad} := \alpha \cdot \left(\frac{\pi}{180} \right) \quad \text{end}$$

$a := 6378.145$ Earth mean equatorial radius

$b := 6356.785$ Earth mean polar radius

$$e := \frac{\sqrt{(a^2 - b^2)}}{a} \quad \text{Eccentricity factor for oblate ellipsoid model of Earth}$$

ECF Coordinates of Points on or Above the Geoid

function $x(\varphi, \lambda, h) \in \text{real}$

on $\varphi, \lambda, h \in \text{real}$ is

$$x := \left(\frac{a}{\sqrt{(1 - e^2 \cdot \sin(\varphi)^2)}} + h \right) \cdot \cos(\varphi) \cdot \cos(\lambda)$$

end

Function calculates x-coordinate of ECF position, given geodetic latitude and longitude (in radians), and altitude above the reference ellipsoid in kilometers

function $y(\varphi, \lambda, h) \in \text{real}$

on $\varphi, \lambda, h \in \text{real}$ is

$$y := \left(\frac{a}{\sqrt{(1 - e^2 \cdot \sin(\varphi)^2)}} + h \right) \cdot \cos(\varphi) \cdot \sin(\lambda)$$

end

Function calculates y-coordinate of ECF position, given geodetic latitude and longitude (in radians), and altitude above the reference ellipsoid in kilometers

function $z(\varphi, \lambda, h) \in \text{real}$

on $\varphi, \lambda, h \in \text{real}$ is

$$z := \left(\frac{a \cdot (1 - e^2)}{\sqrt{(1 - e^2 \cdot \sin(\varphi)^2)}} + h \right) \cdot \sin(\varphi)$$

end

Function calculates z-coordinate of ECF position, given geodetic latitude and longitude (in radians), and altitude above the reference ellipsoid in kilometers

Other functions necessary for area computations

function $r(\varphi) \in \text{real}$
on $\varphi \in \text{real}$ is

Function calculates the geocentric radius
to any point on the geoid as a function
of the point's geodetic latitude

$$r := \frac{a}{\sqrt{1 - e^2 \cdot \sin(\varphi)^2}}$$

end

function $glx(\varphi, \lambda) \in \text{real}$
on $\varphi, \lambda \in \text{real}$ is

Function calculates the partial
derivative of x with respect to
 φ

$$glx := \frac{\left(a \cdot e^2 \cdot \sin(\varphi) \cdot \cos(\varphi)^2 \cdot \cos(\lambda) \right)}{\left(1 - e^2 \cdot \sin(\varphi)^2 \right)^{\left(\frac{3}{2} \right)}} - \frac{a \cdot \sin(\varphi) \cdot \cos(\lambda)}{\sqrt{1 - e^2 \cdot \sin(\varphi)^2}}$$

end

function $glz(\varphi, \lambda) \in \text{real}$
on $\varphi, \lambda \in \text{real}$ is

Function calculates the partial
derivative of z with respect to
 φ

$$glz := \frac{\left(a \cdot e^2 \cdot (1 - e^2) \cdot \sin(\varphi)^2 \cdot \cos(\varphi) \right)}{\left(1 - e^2 \cdot \sin(\varphi)^2 \right)^{\left(\frac{3}{2} \right)}} + \frac{a \cdot (1 - e^2) \cdot \cos(\varphi)}{\sqrt{1 - e^2 \cdot \sin(\varphi)^2}}$$

end

Generate Actual Area of Shells

$Area_at_latitude \in \text{real},$ Declare variables
 $ActArea \in \text{real}, ?$

Integrate area of shell at OE (all others at same latitude have the same area)

for $i := 1$ to 90 do

$$Area_at_latitude_i := \int_{rad(i-1)}^{rad(i)} \int_{rad(0)}^{rad(1)} r(\varphi) \cdot \cos(\varphi) \cdot \sqrt{glx(\varphi, \lambda)^2 + glz(\varphi, \lambda)^2} d\lambda d\varphi$$

end

Write 90 areas for inclusion into appendix
Filename is LATAREA.DAT

$$latarea \in \text{real}_{?,?}$$

Declare variables

```
for i := 1 to 90 do
```

$$latarea_{1,i} := loreal(i)$$

Create list of latitudes (in degrees)

$$latarca_{2,i} := Area_at_latitude_i$$

Append list of areas

end

Write file LATAREA.DAT for inclusion to thesis

```
invoke open_file(1,"latarea.dat" ,"FORMATTED" )
```

```
invoke put_file(1,latarea,"(F8.1 , F22.10 )")
```

```
invoke close_file(1)
```

Generate actual area for all shells

$$k := 1$$

Initialize counter to create index for all points

```
for i := 1 to 90 do
```

Increment over all-valid latitudes

```
for  $j := 1$  to 360 do
```

Increment over all valid longitudes

$$ActArea_k := Area_at_latitude_i$$

Put area into array for all longitudes at that latitude

$$k := k + 1$$

Increment index counter

end**end**

Writes actual areas into file ACTAREA.DAT

```
invoke open_file(2,"actarea.dat" ,"FORMATTED" )
```

```
invoke put_file(2,ActArea,"(F18.10)")
```

invoke *close_file*(2)

End of Document

Actual Area of Shells in Model, Indexed by Latitude

Latitude (deg)	Actual Area (square kilometers)
1.0	12308.5937500000
2.0	12304.9414062500
3.0	12297.6445312500
4.0	12286.6933593750
5.0	12272.1103515625
6.0	12253.8837890625
7.0	12232.0078125000
8.0	12206.5087890625
9.0	12177.3916015625
10.0	12144.6367187500
11.0	12108.2890625000
12.0	12068.3330078125
13.0	12024.7685546875
14.0	11977.6455078125
15.0	11926.9335937500
16.0	11872.6582031250
17.0	11814.8427734375
18.0	11753.5136718750
19.0	11688.6240234375
20.0	11620.2539062500
21.0	11548.4160156250
22.0	11473.0664062500
23.0	11394.2871093750
24.0	11312.0937500000
25.0	11226.4541015625
26.0	11137.4384765625
27.0	11045.0556640625
28.0	10949.3466796875
29.0	10850.2792968750
30.0	10747.9511718750
31.0	10642.2988281250
32.0	10533.4746093750
33.0	10421.3974609375
34.0	10306.0976562500
35.0	10187.7099609375
36.0	10066.1650390625
37.0	9941.4912109375
38.0	9813.8212890625

Actual Area of Shells in Model, Indexed by Latitude

Latitude (deg)	Actual Area (square kilometers)
39.0	9683.0947265625
40.0	9549.3427734375
41.0	9412.6962890625
42.0	9273.0996093750
43.0	9130.5917968750
44.0	8985.3046875000
45.0	8837.1835937500
46.0	8686.2705078125
47.0	8532.7011718750
48.0	8376.4257812500
49.0	8217.4931640625
50.0	8056.0297851562
51.0	7891.9702148438
52.0	7725.4750976562
53.0	7556.5078125000
54.0	7385.1206054688
55.0	7211.4399414062
56.0	7035.4404296875
57.0	6857.1748046875
58.0	6676.7690429688
59.0	6494.2084960938
60.0	6309.5649414062
61.0	6122.9038085938
62.0	5934.2338867188
63.0	5743.7353515625
64.0	5551.3481445312
65.0	5357.1679687500
66.0	5161.2602539062
67.0	4963.6474609375
68.0	4764.4946289062
69.0	4563.7651367188
70.0	4361.5517578125
71.0	4157.9218750000
72.0	3952.9367675781
73.0	3746.6416015625
74.0	3539.1745605469
75.0	3330.5246582031
76.0	3120.7890625000

Actual Area of Shells in Model, Indexed by Latitude

Latitude (deg)	Actual Area (square kilometers)
77.0	2910.0300292969
78.0	2698.3208007812
79.0	2485.7109375000
80.0	2272.3193359375
81.0	2058.1662597656
82.0	1843.3355712891
83.0	1627.9022216797
84.0	1411.9311523438
85.0	1195.4906005859
86.0	978.6734619141
87.0	761.5231323242
88.0	544.1251831055
89.0	326.5453491211
90.0	108.8610305786

Appendix E. Approximate Area of shells $s_{i,j}$ for all Values of i

Trapezoidal Approximation of Shell Areas

This is APPROXAREA.DOC, a MathStation file which calculates a trapezoidal approximation to the area of each shell in the model and writes this information to the file APPROXAREA.DAT

$a, b, e, \varphi \in \text{real}$ Declare variable types
 $i, j \in \text{integer}$

invoke *setprecision*(12) Instruct MathStation to display real values to 12 digits precision

function *torad*(α) $\in \text{real}$ This function converts degree measures to radians
on $\alpha \in \text{real}$ is

$$\text{torad} := \alpha \cdot \left(\frac{\pi}{180} \right) \text{ end}$$

Physical Constants

$a := 6378.145$ Earth mean equatorial radius
 $b := 6356.785$ Earth mean polar radius

$$e := \frac{\sqrt{a^2 - b^2}}{a} \quad \text{Eccentricity factor for oblate ellipsoid model of Earth}$$

Other functions necessary for area computations

function *r*(φ) $\in \text{real}$ Function calculates the geocentric radius
on $\varphi \in \text{real}$ is to any point on the geoid as a function
of the point's geodetic latitude

$$r := \frac{a}{\sqrt{1 - e^2 \cdot \sin(\varphi)^2}}$$

end

function *gcl*(φ) $\in \text{real}$ Function calculates the geocentric
on $\varphi \in \text{real}$ is latitude of any point as a function
of the point's geodetic latitude

$$gcl := \varphi - \text{atan} \left(\frac{e^2 \cdot \sin(\varphi) \cdot \cos(\varphi)}{1 - (e^2 \cdot \sin(\varphi)^2)} \right)$$

end

Generate Approximate Area of Shells

top, side, bottom \in real Declare variables
ApproxArea \in real_{2,90}

Approximate area of shell at 0E (all others at same latitude have the same area)

for *i* := 1 to 90 do

*ApproxArea*_{1,*i*} := *i*

φ := *torad*(*i*)

top := *r*(*torad*(φ))·*torad*(1.0)·*cos*(*gcl*(*torad*(φ)))

side := *r*(*torad*(φ - 0.5))·*torad*(1.0)

bottom := *r*(*torad*(φ - 1.0))·*torad*(1.0)·*cos*(*gcl*(*torad*(φ)))

*ApproxArea*_{2,*i*} := $\frac{(\textit{top} + \textit{bottom})}{2} \cdot \textit{side}$

end

Write file APPROXAREA.DAT for inclusion to thesis
invoke *open_file*(1,"approxarea.dat" ,"FORMATTED")
invoke *put_file*(1,*ApproxArea*,"(F8.1 , F22.10)")
invoke *close_file*(1)

End of Document

Approximate Area of Shells in Model, Indexed by Latitude

Latitude (deg)	Approximate Area (square kilometers)
1.0	12390.2080078125
2.0	12384.6718750000
3.0	12375.4638671875
4.0	12362.5869140625
5.0	12346.0400390625
6.0	12325.8339843750
7.0	12301.9667968750
8.0	12274.4482421875
9.0	12243.2832031250
10.0	12208.4775390625
11.0	12170.0410156250
12.0	12127.9824218750
13.0	12082.3134765625
14.0	12033.0439453125
15.0	11980.1835937500
16.0	11923.7451171875
17.0	11863.7441406250
18.0	11800.1943359375
19.0	11733.1103515625
20.0	11662.5078125000
21.0	11588.4052734375
22.0	11510.8193359375
23.0	11429.7705078125
24.0	11345.2763671875
25.0	11257.3593750000
26.0	11166.0400390625
27.0	11071.3437500000
28.0	10973.2929687500
29.0	10871.9101562500
30.0	10767.2236328125
31.0	10659.2587890625
32.0	10548.0410156250
33.0	10433.6035156250
34.0	10315.9736328125
35.0	10195.1826171875
36.0	10071.2597656250
37.0	9944.2402343750
38.0	9814.1572265625

Approximate Area of Shells in Model, Indexed by Latitude

Latitude (deg)	Approximate Area (square kilometers)
39.0	9681.0449218750
40.0	9544.9384765625
41.0	9405.8769531250
42.0	9263.8945312500
43.0	9119.0332031250
44.0	8971.3310546875
45.0	8820.8291015625
46.0	8667.5712890625
47.0	8511.5976562500
48.0	8352.9541015625
49.0	8191.6845703125
50.0	8027.8349609375
51.0	7861.4531250000
52.0	7692.5869140625
53.0	7521.2851562500
54.0	7347.5971679688
55.0	7171.5756835938
56.0	6993.2705078125
57.0	6812.7363281250
58.0	6630.0263671875
59.0	6445.1958007812
60.0	6258.2993164062
61.0	6069.3940429688
62.0	5878.5410156250
63.0	5685.7915039062
64.0	5491.2114257812
65.0	5294.8579101562
66.0	5096.7924804688
67.0	4897.0766601562
68.0	4695.7739257812
69.0	4492.9443359375
70.0	4288.6562500000
71.0	4082.9711914062
72.0	3875.9570312500
73.0	3667.6791992188
74.0	3458.2023925781
75.0	3247.5959472656
76.0	3035.9260253906

Approximate Area of Shells in Model, Indexed by Latitude

Latitude (deg)	Approximate Area (square kilometers)
77.0	2823.2619628906
78.0	2609.6730957031
79.0	2395.2275390625
80.0	2179.9958496094
81.0	1964.0466308594
82.0	1747.4520263672
83.0	1530.2833251953
84.0	1312.6102294922
85.0	1094.5061035156
86.0	876.0381469727
87.0	657.2823486328
88.0	438.3101501465
89.0	219.1904296875
90.0	-0.0005453200

Appendix F. *MathStation file to assign importance weights of shells*

$s_{i,j}$, for all Values of i at example METSAT subpoint of $5^\circ E$

Transfer Importance Weights from Map to File

This is file IMPWEIGHTS.DOC, a MathStation file which generates data file IMPWEIGHTS.DAT, which contains the relative importance weights of each shell from the map provided by the expert decision maker

$i, j, k \in \text{integer}$

Declare variable types

$IW \in \text{real}_{90, 360}$

for $i := 1$ to 90 do

Initialize all points to minimum weight (0.20)

for $j := 1$ to 360 do

$IW_{i,j} := 0.20$

end

end

for $i := 1$ to 10 do

Input weights for strip of shells between 1 and 10 degrees

for $j := 1$ to 360 do

North latitude (geodetic)

if $((j > 270) \wedge (j \leq 290))$ then

$IW_{i,j} := 0.40$ end

end

end

for $i := 11$ to 20 do

Input weights for strip of shells between 11 and 20 degrees

for $j := 1$ to 360 do

North latitude (geodetic)

if $((j > 230) \wedge (j \leq 320))$ then

$IW_{i,j} := 0.40$ end

end

end

for $i := 21$ to 30 do

Input weights for strip of shells between 21 and 30 degrees

for $j := 1$ to 360 do

North latitude (geodetic)

if $((j > 90) \wedge (j \leq 100)) \vee ((j > 200) \wedge (j \leq 240)) \vee ((j > 300) \wedge (j \leq 320))$ then

$IW_{i,j} := 0.40$ end

if $((j > 100) \wedge (j \leq 120)) \vee ((j > 240) \wedge (j \leq 250)) \vee ((j > 290) \wedge (j \leq 300))$ then

$IW_{i,j} := 0.60$ end

if $((j > 250) \wedge (j \leq 290))$ then

$IW_{i,j} := 0.80$ end

end

end

```

for i := 31 to 40 do          Input weights for strip of shells between 31 and 40 degrees
for j := 1 to 360 do        North latitude (geodetic)
if ((j>40) ^ (j≤50)) ^ ((j>120) ^ (j≤140)) ^ ((j>190) ^ (j≤230)) ^ ((j>310) ^ (j≤330)))
then
IWi,j := 0.40 end
if ((j>50) ^ (j≤120)) ^ ((j>300) ^ (j≤310))) then
IWi,j := 0.60 end
if (j>290) ^ (j≤300) then
IWi,j := 0.80 end
if (j>230) ^ (j≤290) then
IWi,j := 1.00 end
end
end

```

```

for i := 41 to 50 do        Input weights for strip of shells between 41 and 50 degrees
for j := 1 to 360 do        North latitude (geodetic)
if ((j>10) ^ (j≤20)) ^ ((j>140) ^ (j≤220))) then
IWi,j := 0.40 end
if ((j>20) ^ (j≤140)) ^ ((j>220) ^ (j≤230)) ^ ((j>310) ^ (j≤320))) then
IWi,j := 0.60 end
if (j>310) ^ (j≤320) then
IWi,j := 0.80 end
if (j>230) ^ (j≤300) then
IWi,j := 1.00 end
end
end

```

```

for i := 51 to 60 do        Input weights for strip of shells between 51 and 60 degrees
for j := 1 to 360 do        North latitude (geodetic)
if ((j>0) ^ (j≤10)) ^ ((j>340) ^ (j≤360))) then
IWi,j := 0.40 end
if (j>10) ^ (j≤190) ^ ((j>310) ^ (j≤340)) then
IWi,j := 0.60 end
if (j>190) ^ (j≤310) then
IWi,j := 0.80 end
end
end

```

```

for i := 61 to 70 do        Input weights for strip of shells between 61 and 70 degrees
for j := 1 to 360 do        North latitude (geodetic)
if (j>0) ^ (j≤190) then
IWi,j := 0.60 end
if (j>190) ^ (j≤300) then
IWi,j := 0.80 end
end
end

```

```

for i := 71 to 90 do           Input weights for strip of shells between 71 and 90 degrees
for j := 1 to 360 do          North latitude (geodetic)
  IWi,j := 0.60
end
end
end

```

Write all importance weight data to file IMPWEIGHTS.DAT

```

invoke open_file(1,"impweights.dat","FORMATTED" )

```

```

k := 1
for i := 1 to 90 do
for j := 1 to 360 do
  invoke put_file(1,IWi,j,"F5.2")
  invoke newline(1,1)
k := k+1
end
end
end

```

```

invoke close_file(1)

```

NORAD MISSION IMPORTANCE CHART

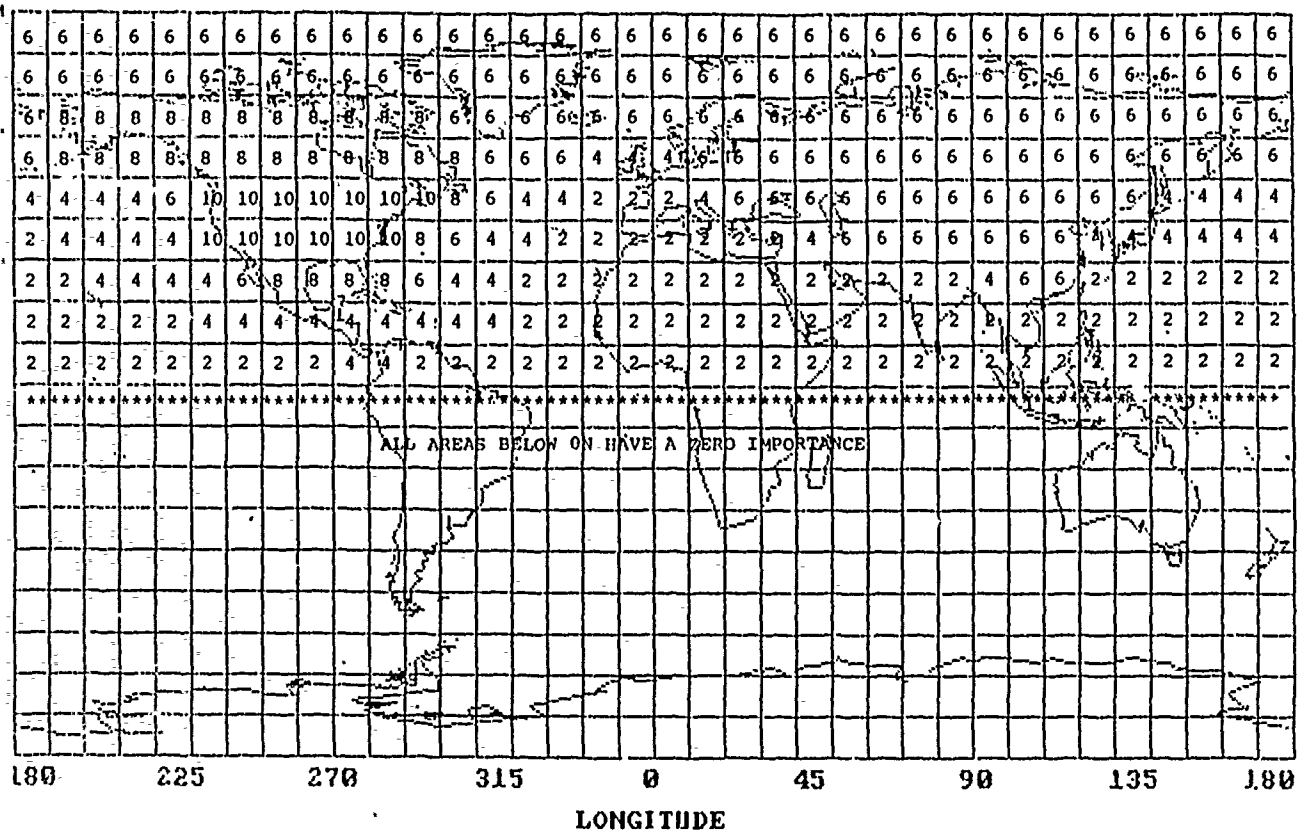


Figure F.1. Reproduction of Geographical Area Importance Data Provided by the Decision Maker

Appendix G. *MOE generation file*

Compile all necessary information for a single case into one file

This is MOE???.DOC, a MathStation file which generates the MOE described in the thesis from the attribute files, including:

1. Geographic area weight (same for all METSAT types and subpoints)
2. Perceived area of shell, for the given METSAT subpoint
3. Value of sampling rate attribute
4. Value of timeliness attribute
5. Value of resolution attribute for the given METSAT subpoint

Open all files

File containing geographic importance weights

invoke *open_file*(1,"impweights.dat","FORMATTED")

File containing perceived areas for the given subpoint

invoke *open_file*(2,"per005.dat","FORMATTED")

File containing sampling rate values

invoke *open_file*(3,"sampling.dat","FORMATTED")

File containing timeliness values

invoke *open_file*(4,"timeliness.dat","FORMATTED")

File containing resolution values for the given subpoint

invoke *open_file*(5,"res005.dat","FORMATTED")

invoke *setprecision*(12)

$i, j, k \in \text{integer}$

Assign variable types

$\text{impweight}, \text{per_area}, \text{sampling}, \text{timeliness}, \text{resolution}, \text{temp}, \text{MOE} \in \text{real}$

$\alpha \in \text{real}_3$

$\alpha := \begin{pmatrix} 0.381 \\ 0.333 \\ 0.286 \end{pmatrix}$ Vector of attribute importance weights

$\text{temp} := 0.0$

Initialize these variables

$\text{MOE} := 0.0$

Obtain the proper values from the various files and write them to ATTSUB.DAT

```
for i := 1 to 90 do
for j := 1 to 360 do
invoke get_file(1,impweight,"F5.2")
invoke get_file(2,per_area,"F14.6")
invoke get_file(3,sampling,"F5.4")
invoke get_file(4,timeliness,"F5.4")
invoke get_file(5,resolution,"F14.9")

temp := (impweight * per_area) * ((sampling(1-α1)) * (timeliness(1-α2)) * (resolution(1-α3))

MOE := MOE + temp

end
end

Close all files
*****
invoke close_file(1)
invoke close_file(2)
invoke close_file(3)
invoke close_file(4)
invoke close_file(5)

MOE :=  $\frac{MOE}{90 \cdot 360}$ 

MOE = 287.4245300293
```

*****End of Document*****

Appendix H. *MathStation file which assigned area scaling factors
and perceived areas of shells $s_{i,j}$ for all Values of i , for example
METSAT subpoint of $5^\circ E$*

Conversion of Actual Area of Shells to Area Perceived by Satellite

This is PERAREA.DOC, a MathStation file which generates data files PER???.DAT
(containing perceived areas of shells at subpoint ???E) and SCALE???.DAT
(containing scale factors for the same subpoint)

$a, b, e \in \text{real}$ Declare variable types
 $i, j, k \in \text{integer}$
 $\phi, \lambda \in \text{real}$

invoke *setprecision*(12) Instruct MathStation to display real values to 12 digits precision

function *rad*(α) $\in \text{real}$ Function converts degree measures to radians
on $\alpha \in \text{real}$ is

$$\text{rad} := \alpha \cdot \left(\frac{\pi}{180} \right)$$

end

Physical Constants

$a := 6378.145$ Earth mean equatorial radius
 $b := 6356.785$ Earth mean polar radius

$$e := \frac{\sqrt{a^2 - b^2}}{a}$$

Eccentricity factor for oblate ellipsoid model of Earth

ECF Coordinates of Points on or Above the Geoid

function $x(\varphi, \lambda, h) \in \text{real}$

on $\varphi, \lambda, h \in \text{real}$ **is**

$$x := \left(\frac{a}{\sqrt{(1 - e^2 \cdot \sin(\varphi)^2)}} + h \right) \cdot \cos(\varphi) \cdot \cos(\lambda)$$

end

Function calculates x-coordinate of ECF position, given geodetic latitude and longitude (in radians), and altitude above the reference ellipsoid in kilometers

function $y(\varphi, \lambda, h) \in \text{real}$

on $\varphi, \lambda, h \in \text{real}$ **is**

$$y := \left(\frac{a}{\sqrt{(1 - e^2 \cdot \sin(\varphi)^2)}} \right) \cdot \cos(\varphi) \cdot \sin(\lambda)$$

end

Function calculates y-coordinate of ECF position, given geodetic latitude and longitude (in radians), and altitude above the reference ellipsoid in kilometers

function $z(\varphi, \lambda, h) \in \text{real}$

on $\varphi, \lambda, h \in \text{real}$ **is**

$$z := \left(\frac{a \cdot (1 - e^2)}{\sqrt{(1 - e^2 \cdot \sin(\varphi)^2)}} + h \right) \cdot \sin(\varphi)$$

end

Function calculates z-coordinate of ECF position, given geodetic latitude and longitude (in radians), and altitude above the reference ellipsoid in kilometers

Functions of Partial Derivatives of x, y, and z

function gx1(φ, λ) \in real
on $\varphi, \lambda \in$ real is

Function calculates the first partial derivative of x(φ, λ) with respect to φ

$$gx1 := \frac{\left(\frac{a \cdot e^2 \cdot \sin(\varphi) \cdot \cos(\varphi)^2 \cdot \cos(\lambda)}{\left(1 - e^2 \cdot \sin(\varphi)^2\right)^{\left(\frac{3}{2}\right)}} \right)}{\left(\frac{a \cdot \sin(\varphi) \cdot \cos(\lambda)}{\sqrt{\left(1 - e^2 \cdot \sin(\varphi)^2\right)}} \right)}$$

end

function gx2(φ, λ) \in real
on $\varphi, \lambda \in$ real is

Function calculates the first partial derivative of x(φ, λ) with respect to λ

$$gx2 := - \frac{\left(\frac{a \cdot \cos(\varphi) \cdot \sin(\lambda)}{\sqrt{\left(1 - e^2 \cdot \sin(\varphi)^2\right)}} \right)}{\left(\frac{a \cdot \sin(\varphi) \cdot \cos(\lambda)}{\sqrt{\left(1 - e^2 \cdot \sin(\varphi)^2\right)}} \right)}$$

end

function gyl(φ, λ) \in real
on $\varphi, \lambda \in$ real is

Function calculates the first partial derivative of y(φ, λ) with respect to φ

$$gyl := \frac{\left(\frac{a \cdot e^2 \cdot \sin(\varphi) \cdot \cos(\varphi)^2 \cdot \sin(\lambda)}{\left(1 - e^2 \cdot \sin(\varphi)^2\right)^{\left(\frac{3}{2}\right)}} \right)}{\left(\frac{a \cdot \sin(\varphi) \cdot \sin(\lambda)}{\sqrt{\left(1 - e^2 \cdot \sin(\varphi)^2\right)}} \right)}$$

end

function gy2(φ, λ) \in real
on $\varphi, \lambda \in$ real is

Function calculates the first partial derivative of y(φ, λ) with respect to λ

$$gy2 := \frac{\left(\frac{a \cdot \cos(\varphi) \cdot \cos(\lambda)}{\sqrt{\left(1 - e^2 \cdot \sin(\varphi)^2\right)}} \right)}{\left(\frac{a \cdot \sin(\varphi) \cdot \sin(\lambda)}{\sqrt{\left(1 - e^2 \cdot \sin(\varphi)^2\right)}} \right)}$$

end

function gz1(φ, λ) \in real
on $\varphi, \lambda \in$ real is

Function calculates the first
partial derivative of $z(\varphi, \lambda)$
with respect to φ

$$gz1 := \left(\frac{\left(a \cdot e^2 \cdot (1 - e^2) \cdot \sin(\varphi)^2 \cdot \cos(\varphi) \right)}{\left(1 - e^2 \cdot \sin(\varphi)^2 \right)^{\left(\frac{3}{2} \right)}} \right) + \left(\frac{\left(a \cdot (1 - e^2) \cdot \cos(\varphi) \right)}{\left(\sqrt{1 - e^2 \cdot \sin(\varphi)^2} \right)} \right)$$

end

function gz2(φ, λ) \in real
on $\varphi, \lambda \in$ real is
gz2 := 0
end

Function calculates the first
partial derivative of $z(\varphi, \lambda)$
with respect to λ

function n(φ, λ) \in real₃
on $\varphi, \lambda \in$ real is

Function returns a vector normal to the
surface at the geoid at the geodetic
coordinates supplied as input

$$n := \begin{pmatrix} gy1(\varphi, \lambda) \cdot gz2(\varphi, \lambda) - gz1(\varphi, \lambda) \cdot gy2(\varphi, \lambda) \\ gz1(\varphi, \lambda) \cdot gx2(\varphi, \lambda) - gx1(\varphi, \lambda) \cdot gz2(\varphi, \lambda) \\ gx1(\varphi, \lambda) \cdot gy2(\varphi, \lambda) - gy1(\varphi, \lambda) \cdot gx2(\varphi, \lambda) \end{pmatrix}$$

end

Generate ECF coordinates to METSAT

sat \in real₃

subpoint_in_degrees := 5
subpoint := rad(subpoint_in_degrees)

$$sat := \begin{pmatrix} x(0.0, subpoint, 35862.977) \\ y(0.0, subpoint, 35862.977) \\ z(0.0, subpoint, 35862.977) \end{pmatrix}$$

Geocentric radius vector to satellite,
in ECF coordinates

function radius(φ, λ) \in real₃
on $\varphi, \lambda \in$ real is

$$radius := \begin{pmatrix} x(\varphi, \lambda, 0.0) \\ y(\varphi, \lambda, 0.0) \\ z(\varphi, \lambda, 0.0) \end{pmatrix}$$

Geocentric radius vector to a point on the geoid,
in ECF coordinates

end

```

function  $\rho(\varphi, \lambda) \in \text{real}_3$ 
on  $\varphi, \lambda \in \text{real}$  is
 $\rho := \text{sat} - \text{radius}(\varphi, \lambda)$ 
end

```

Range vector from satellite to point on geoid,
in ECF coordinates

```

SF, Perarea, ActArea  $\in \text{real}$ 

```

```

invoke open_file(1, "actarea.dat", "FORMATTED")
invoke open_file(2, "scale005.dat", "FORMATTED")
invoke open_file(3, "per005.dat", "FORMATTED")

```

```

for i := 1 to 90 do
for j := 1 to 360 do

```

Increment over all valid latitudes
Increment over all valid longitudes

```

 $\varphi := \text{rad}(0.5 \cdot (2 \cdot i - 1))$ 

```

Find latitude of center of current shell

```

 $\lambda := \text{rad}(0.5 \cdot (2 \cdot j - 1))$ 

```

Find longitude of center of current shell

```

SF :=  $\frac{\rho(\varphi, \lambda) \cdot n(\varphi, \lambda)}{|\rho(\varphi, \lambda)| \cdot |n(\varphi, \lambda)|}$ 

```

Compute scale factor of current shell

```

if SF  $\leq$  0 then SF := 0
end

```

A negative value for SF means the shell is
invisible to the satellite

```

invoke put_file(2, SF, "F18.10")
invoke newline(2, 1)

```

Write scale factors to file SCALE???.DAT,
where ??? is the satellite subpoint in degrees East

```

invoke get_file(1, ActArea, "(F18.10)")

```

Get Actual Area of Shell from file ACTAREA.DAT

```

PerArea := ActArea * SF

```

Compute perceived area of current shell

```

invoke put_file(3, PerArea, "F18.10")
invoke newline(3, 1)

```

Write perceived areas to file PER???.DAT,
where ??? is the satellite subpoint in degrees East

```

end
end
k = *

```

```

invoke close_file(1)
invoke close_file(2)
invoke close_file(3)

```

Close all files

Appendix I. *MathStation file to find resolution values of shells* *$s_{i,j}$, for all Values of i , at example METSAT subpoint of $5^\circ E$*

Computation of local resolution value for all shells at a given METSAT subpoint

This is RES.DOC, a MathStation file which generates data file RES???.DAT
 (containing local resolution values for shells at subpoint ???E)

$a, b, e \in \text{real}$ Declare variable types
 $i, j, k \in \text{integer}$
 $\varphi, \lambda \in \text{real}$

invoke *setprecision*(12) Instruct MathStation to display real values to 12 digits precision

function *rad*(α) $\in \text{real}$ Function converts degree measures to radians
 on $\alpha \in \text{real}$ is

$$\text{rad} := \alpha \cdot \left(\frac{\pi}{180} \right)$$

end

Physical Constants

$a := 6378.145$ Earth mean equatorial radius
 $b := 6356.785$ Earth mean polar radius

$$e := \frac{\sqrt{a^2 - b^2}}{a}$$

Eccentricity factor for oblate ellipsoid model of Earth

ECF Coordinates of Points on or Above the Geoid

function $x(\varphi, \lambda, h) \in \text{real}$

on $\varphi, \lambda, h \in \text{real}$ **is**

$$x := \left(\frac{a}{\sqrt{(1 - e^2 \cdot \sin(\varphi)^2)}} + h \right) \cdot \cos(\varphi) \cdot \cos(\lambda)$$

end

Function calculates x-coordinate of ECF position, given geodetic latitude and longitude (in radians), and altitude above the reference ellipsoid in kilometers

function $y(\varphi, \lambda, h) \in \text{real}$

on $\varphi, \lambda, h \in \text{real}$ **is**

$$y := \left(\frac{a}{\sqrt{(1 - e^2 \cdot \sin(\varphi)^2)}} \right) \cdot \cos(\varphi) \cdot \sin(\lambda)$$

end

Function calculates y-coordinate of ECF position, given geodetic latitude and longitude (in radians), and altitude above the reference ellipsoid in kilometers

function $z(\varphi, \lambda, h) \in \text{real}$

on $\varphi, \lambda, h \in \text{real}$ **is**

$$z := \left(\frac{a \cdot (1 - e^2)}{\sqrt{(1 - e^2 \cdot \sin(\varphi)^2)}} + h \right) \cdot \sin(\varphi)$$

end

Function calculates z-coordinate of ECF position, given geodetic latitude and longitude (in radians), and altitude above the reference ellipsoid in kilometers

Generate ECF coordinates to METSAT

$sat \in \text{real}_3$
 $subpoint_in_degrees, subpoint, RES_at_subpoint \in \text{real}$

$subpoint_in_degrees := 5$
 $subpoint := \text{rad}(subpoint_in_degrees)$

$sat := \begin{pmatrix} x(0.0, subpoint, 35862.977) \\ y(0.0, subpoint, 35862.977) \\ z(0.0, subpoint, 35862.977) \end{pmatrix}$ Geocentric radius vector to satellite,
in ECF coordinates

$RES_at_subpoint := 1.0$ METSAT's resolution at the subpoint,
in kilometers per pixel

function $radius(\varphi, \lambda) \in \text{real}_3$
on $\varphi, \lambda \in \text{real}$ **is**

$radius := \begin{pmatrix} x(\varphi, \lambda, 0.0) \\ y(\varphi, \lambda, 0.0) \\ z(\varphi, \lambda, 0.0) \end{pmatrix}$ Geocentric radius vector to a point on the geoid,
in ECF coordinates

end

function $\rho(\varphi, \lambda) \in \text{real}_3$ Range vector from satellite to point on geoid,
on $\varphi, \lambda \in \text{real}$ **is** in ECF coordinates
 $\rho := sat - radius(\varphi, \lambda)$
end

Generate local resolution values and write to file

```

RES,SF,resvalue ∈ real           Declare variable

invoke open_file(1,"res005.dat","FORMATTED" )
invoke open_file(2,"scale005.dat","FORMATTED" )   Read scale values to see if shell is visible

for i := 1 to 90 do               Increment over all valid latitudes
for j := 1 to 360 do             Increment over all valid longitudes

φ := rad(0.5(2i - 1))           Find latitude of center of current shell
λ := rad(0.5(2j - 1))           Find longitude of center of current shell

RES :=  $\frac{|ρ(φ,λ)|}{35862.977}$  · RES_at_subpoint   Compute local resolution for current shell

resvalue := (1.001) · exp((-0.448) · RES)   Calculate relative value of resolution

invoke get_file(2,SF,"F18.10")             Get scale factor from file SCALE???.DAT,

if (SF ≤ 0) then resvalue := 0              A zero value for SF means the shell is
end                                          invisible to the satellite

invoke put_file(1,resvalue,"F18.10")       Write resolution value to file RES???.DAT,
invoke newline(1,1)                       where ??? is the satellite subpoint in degrees East

end
end

invoke close_file(1)                      Close all files
invoke close_file(2)

```

*****End of Document*****

Appendix J. *MathCad file to generate value function for sampling rate attribute*

This is SAMP.MCD, a MathCad file which finds the best fit function relating levels of METSAT sampling rate with their respective relative values, as provided by the decision maker.

Data Entry *****

ORIGIN := 1

A place setting command to MathCad

Levels of sampling
rate, in samples/day

Relative values

samp :=	$\begin{bmatrix} 0 \\ 1 \\ 2 \\ 3 \\ 4 \\ 6 \\ 12 \\ 24 \\ 48 \\ 96 \end{bmatrix}$	value :=	$\begin{bmatrix} 0 \\ 0.6 \\ 0.75 \\ 0.8 \\ 0.85 \\ 0.9 \\ 0.95 \\ 0.96 \\ 0.98 \\ 1.0 \end{bmatrix}$
---------	--	----------	---

n := length(value)

Number of elements in each vector

i := 1 .. n

Index variable

Define functions *****

$F(\text{samp}, a, b) := a \cdot \text{samp}^b$

General form of the value function, for which we wish to determine the coefficients a, b, and c.

$$SSE(a, b) := \sum_i \left[\text{value}_i - F[\text{samp}_i, a, b] \right]^2$$

A function which gives the sum of the squared errors between the continuous function and the data points

Solve Block

a := 0.5

b := 0.1

Initial guesses for the coefficients

Given

$SSE(a,b) \approx 0$

We want to minimize the sum of the squared errors

$F(96,a,b) \approx 1$

The value function should equal 1 when the sampling rate is infinitely fast

$\begin{bmatrix} a \\ b \end{bmatrix} := \text{Minerr}(a,b)$

The MathCad Minerr function returns a vector of coefficients which minimizes the error in the solve block

Results

a = 0.734

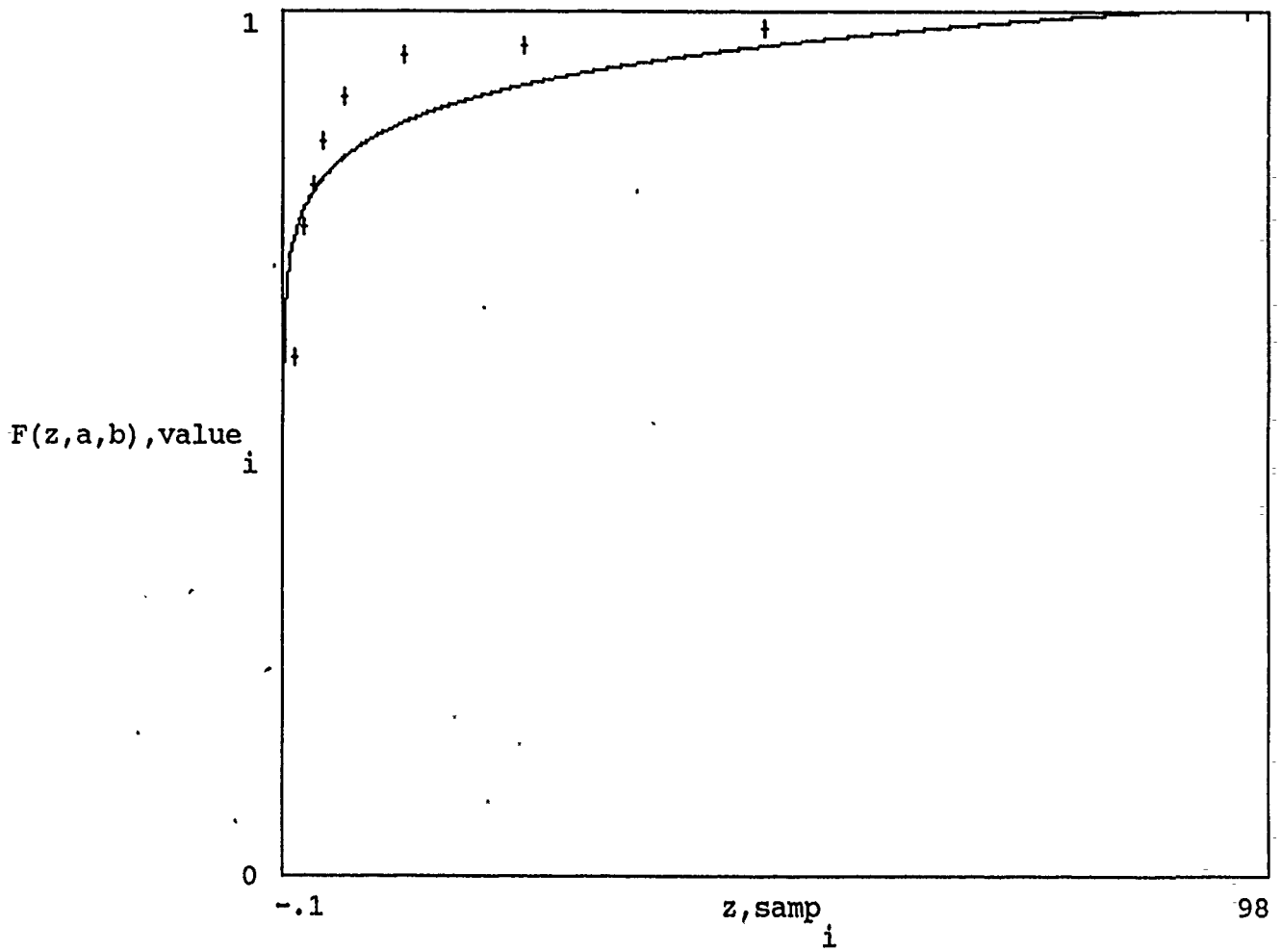
b = 0.069

$\frac{SSE(a,b)}{n - 2} = 0.004$

The variance is a good indicator of the "goodness" of fit

Display Results

$z := 0, 0.1 \dots 96$



Appendix K. *Relative value of sampling rate generation file*

Generate sampling rate values for all shells in the model

This is SAMPLING.DOC, a MathStation file which generates a single file,
SAMPLING.DAT, containing sampling rate values for all shells in the model

Open file

File containing sampling rate values

invoke *open_file*(1,"sampling.dat","FORMATTED")

i,j,k \in integer

Assign variable types

sampling,sampvalue \in real

sampling := 48

for *i* := 1 to 90 do

for *j* := 1 to 360 do

sampvalue := 0.98

invoke *put_file*(1,*sampvalue* ,"F5.4")

invoke *newline*(1,1)

end

end

invoke *close_file*(1)

*****End of Document*****

Appendix L. *MathCad file to generate value function for timeliness*

attribute

This is TIME.MCD, a MathCad file which finds the best fit function relating levels of METSAT timeliness with their respective relative values, as provided by the decision maker.

Data Entry *****

ORIGIN := 1

A place setting command to MathCad

Levels of sampling
rate, in 1/hr

Relative values

time :=
$$\begin{bmatrix} 1 \\ \text{---} \\ 24 \\ 1 \\ \text{---} \\ 12 \\ .125 \\ 1 \\ \text{---} \\ .6 \\ .25 \\ .50 \\ 1.0 \\ 2.0 \\ 4.0 \end{bmatrix}$$

value :=
$$\begin{bmatrix} 0.1 \\ 0.3 \\ 0.5 \\ 0.6 \\ 0.7 \\ 0.8 \\ 0.85 \\ 0.9 \\ 0.95 \end{bmatrix}$$

n := length(value)

Number of elements in each vector

i := 1 ..n

Index variable

Define functions *****

$$F(\text{time}, a, b) := 1 - a \cdot e^{b \cdot \text{time}}$$

General form of the value function, for which we wish to determine the coefficients a, b, and c.

$$\text{SSE}(a, b) := \sum_i \left[\text{value}_i - F[\text{time}_i, a, b] \right]^2$$

A function which gives the sum of the squared errors between the continuous function and the data points

Solve Block

a := 1

b := -4

Initial guesses for the coefficients

Given

$SSE(a,b) \approx 0$

We want to minimize the sum of the squared errors

$F(20,a,b) \approx 1$

The value function should approach 1 as the delay time goes to zero.

$\begin{bmatrix} a \\ b \end{bmatrix} := \text{Minerr}(a,b)$

The MathCad Minerr function returns a vector of coefficients which minimizes the error in the solve block

Results

a = 1.046

b = -4.981

$$\frac{SSE(a,b)}{n - 2} = 0.008$$

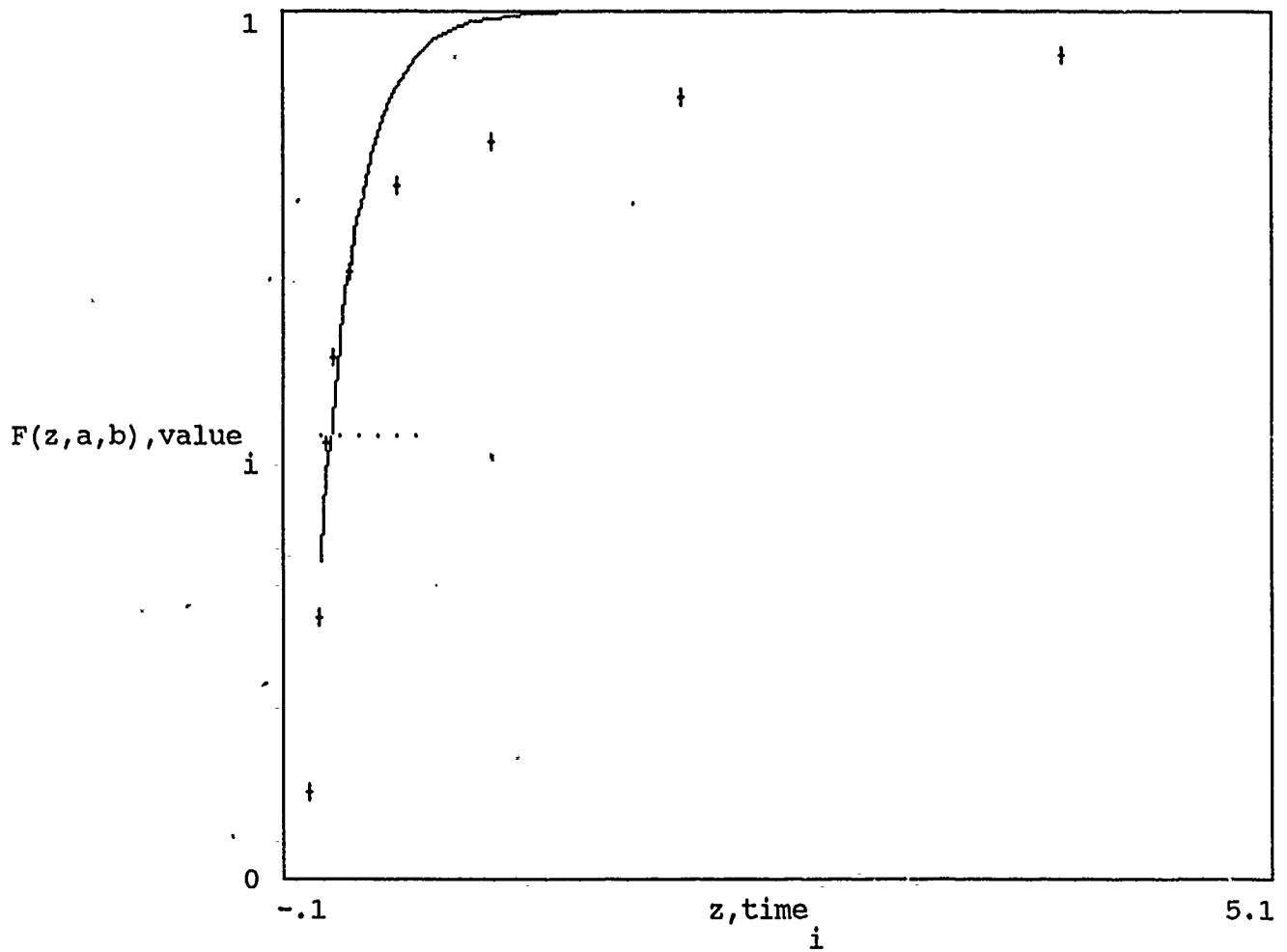
The variance is a good indicator of the "goodness" of fit

Display Results

z := 0,0.1 ..5

Value function: -

Value point: +



Appendix M. *Relative value of timeliness generation file*

Generate sampling rate values for all shells in the model

This is TIMELINESS.DOC, a MathStation file which generates a single file, TIMELINESS.DAT, containing timeliness values for all shells in the model

Open file

File containing sampling rate values

invoke *open_file*(1,"timeliness.dat","FORMATTED")

i,j,k \in integer Assign variable types

timeliness,timevalue \in real

timeliness := 2.0

for *i* := 1 to 90 do

for *j* := 1 to 360 do

timevalue := 0.90

invoke *put_file*(1,*timevalue*,"F5.4")

invoke *newline*(1,1)

end

end

invoke *close_file*(1)

*****End of Document*****

Appendix N. *MathCad* file to generate value function for resolution attribute

This is RESO.MCD, a MathCad file which finds the best fit function relating levels of METSAT resolution with their respective relative values, as provided by the decision maker.

Data Entry

ORIGIN := 1

A place setting command to MathCad

Levels of resolution,
in kilometers

Relative values

```

reso :=
  [ 0
  0.5
  1
  1.5
  2
  2.5
  3
  4
  5 ]

```

```
value := [ 1
           0.8
           0.75
           0.5
           0.35
           0.3
           0.25
           0.2
           0.1
```

```
n := length(value)
```

Number of elements in each vector

$$i := 1 \dots n$$

Index variable

```
Define functions
*****
```

$$F(\text{reso}, a, b) := a \cdot e \quad b \cdot \text{reso}$$

General form of the value function, for which we wish to determine the coefficients a , b , and c .

$$\text{SSE}(a,b) := \sum_i [\text{value}_i - F[\text{reso}_i, a, b]]^2$$

A function which gives the sum of the squared errors between the continuous function and the data points

Solve Block

a := 1

b := -0.5

Initial guesses for the coefficients

Given

$SSE(a,b) \approx 0$

We want to minimize the sum of the squared errors

$F(0,a,b) \approx 1$

The value function should equal 1 when the resolution is infinitely fine

$\begin{bmatrix} a \\ b \end{bmatrix} := \text{Minerr}(a,b)$

The MathCad Minerr function returns a vector of coefficients which minimizes the error in the solve block

Results

a = 1.001

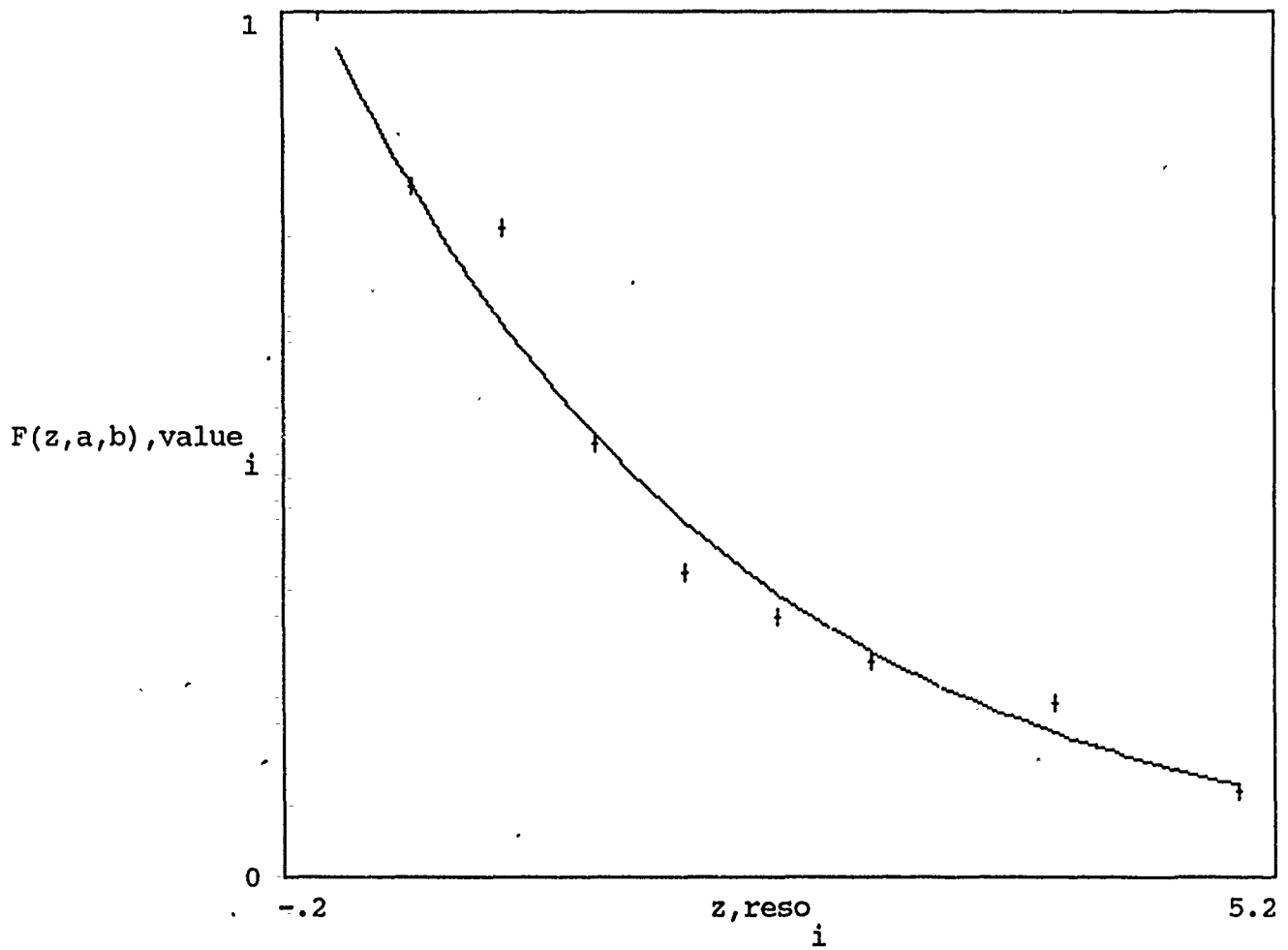
b = -0.448

$\frac{SSE(a,b)}{n - 2} = 0.003$

The variance is a good indicator of the "goodness" of fit

Display Results

z := 0,0.1 ..5



Bibliography

1. Baker, Norman, Deputy Director for Space Analysis. Personal interviews. Fourth Weather Wing (Military Airlift Command), Peterson Air Force Base, CO, 8-10 August, 1990.
2. Bate, Roger R., et al. *Fundamentals of Astrodynamics*. New York: Dover Publications, Inc., 1977.
3. Battilega, John A. and Judith K. Grange, ed. *The Military Applications of Modeling*. Wright-Patterson Air Force Base, OH: Air Force Institute of Technology Press, 1984.
4. Battilega, John A. and Judith K. Grange, ed. *The Military Applications of Modeling*. Washington: Government Printing Office, 1984.
5. Bell, David E. "Consistent Assessment Procedures Using Conditional Utility Functions," *Operations Research* 27:1054-1066 (1979).
6. Boulding, K. E. "The Ethics of Rational Decision," *Management Science*, 12: B-161-B-169 (February 1966).
7. Buede, Dennis M. *The Use of the Reconnaissance/Surveillance Mission Area Analysis by a Program Office*. Final Report PR 77-15-75. McLean, VA: Decisions and Designs, Inc., November 1977.
8. Eckenrode, Robert T. "Weighting Multiple Criteria," *Management Science*, 12:180-192 (November 1965).
9. Epenschade, Edward B., ed. *Goode's World Atlas, 16th Edition*. Chicago: Rand McNally & Company, 1984.
10. Friel, John. "Air Battle Models," *Military Modeling* (Second Edition), edited by Wayne P. Hughes. Alexandria, VA: Military Operations Research Society, 1989.
11. Goicoechea, A. et al. *Multiobjective Decision Analysis with Engineering and Business Applications*. New York: John Wiley & Sons, 1982.
12. Hacking, Ian. *The Emergence of Probability*. Cambridge: Cambridge University Press, 1975.
13. Haig, Thomas O. *The Role of Meteorological Satellites in Tactical Battlefield Weather Support*. Final Report. Hanscom AFB, MA: Air Force Geophysics Laboratory, March 1982(AD-A116936).
14. Helmer, Olaf. *Social Technology*. New York: Basic Books, Inc., 1966.
15. Howard, Ronald A. "An Assessment of Decision Analysis," *Operations Research*, 28:4-27 (1980).

16. Howard, Ronald A. "The Foundations of Decision Analysis," *IEEE Transactions on Systems, Science, and Cybernetics*, SSC4: 211-219 (1968).
17. Hughes, Wayne P. ed. *Military Modeling* (Second Edition). Alexandria, VA: Military Operations Research Society, 1989.
18. Keefer, Donald L. "Approximations and Sensitivity in Multiple Objective Resource Allocation," *Operations Research*, 28: 114-128 (1980).
19. Larcomb, Capt Charles H. *Spatial Registration of TIROS-N Weather Satellite Data*. MS Thesis AFIT/GSO/ENS/89D-10. School of Engineering, Air Force Institute of Technology (AU), Wright-Patterson Air Force Base, OH, December 1989.
20. Markowitz, Harry M. *Portfolio Selection*. New York: John Wiley & Sons, 1959.
21. Matheson, J. E. and R. A. Howard. *An Introduction to Decision Analysis*. Menlo Park, CA: Stanford Research Institute, 1968.
22. Mehlberg, Capt Jerry M. Personal interview. Air Force Institute of Technology, Wright Patterson Air Force Base, OH, 17 November 1990.
23. North, D. Warner. "A Tutorial Introduction to Decision Theory," *IEEE Transactions on Systems, Science, and Cybernetics*, SSC4: 200-210 (1968).
24. Putman, Joe M. *Look Angles and Slant Range Calculations*. Report for the 4950th Test Wing, ARIA Engineering Division, Wright-Patterson AFB, OH., 1977.
25. Quade, E. S. "When Quantitative Models are Inadequate," *Systems Analysis and Policy Planning: Applications in Defense*. New York: Elsevier North-Holland, 1977.
26. Quade, E. S. "Pitfalls and Limitations," *Systems Analysis and Policy Planning: Applications in Defense*. New York: Elsevier North-Holland, 1977.
27. Raiffa, H. *Decision Analysis*. Reading, MA: Addison-Wesley, 1968.
28. Ravindran, A., Don T. Phillips, and James J. Solberg. *Operations Research: Principles and Practice*. New York: John Wiley & Sons, 1987.
29. Seiler, George J. *Strategic Nuclear Force Requirements and Issues*. Maxwell Air Force Base, AL: Air University Press, 1983.
30. Slovic, P., B. Fischhoff, and S. Lichtenstein. "Behavioral Decision Theory," *Annual Review of Psychology*, 28: 1-39 (1977).
31. Storz, Capt Mark, Deputy Director for Space Analysis. Personal interviews. Fourth Weather Wing (Military Airlift Command), Peterson Air Force Base, CO, 8-10 August, 1990.
32. Szidarovsky, F. "Weak and Strong Dominance in Multiobjective Programming," *Class Notes #80-20*, Department of Systems and Industrial Engineering, University of Arizona, Tucson, 1980.

33. Tani, Steven N. "A Perspective on modeling in Decision Analysis," *Management Science*, 24: 1500-1506 (1978).
34. von Winterfeldt, Detlof and Ward Edwards. *Decision Analysis and Behavioral Research*. Cambridge: Cambridge University Press, 1986.
35. Winstead, Captain Curtis L. Personal interviews. Wright-Patterson Air Force Base, OH, 4 September through 8 September 1990.

REPORT DOCUMENTATION PAGE

Form Approved
OMB No. 0704-0188

Public reporting burden for this collection of information is estimated to average 1 hour per response, including the time for reviewing instructions, searching existing data sources, gathering and maintaining the data needed, and completing and reviewing the collection of information. Send comments regarding this burden estimate or any other aspect of this collection of information, including suggestions for reducing this burden, to Washington Headquarters Services, Directorate for Information Operations and Reports, 1215 Jefferson Davis Highway, Suite 1204, Arlington, VA 22202-4302, and to the Office of Management and Budget, Paperwork Reduction Project (0704-0188), Washington, DC 20503.

1. AGENCY USE ONLY (Leave blank)		2. REPORT DATE December 1990		3. REPORT TYPE AND DATES COVERED MS Thesis	
4. TITLE AND SUBTITLE Measuring the Effectiveness of Space: Satellite Weather Systems				5. FUNDING NUMBERS	
6. AUTHOR(S) Steven Trent Wilson, Captain, USAF					
7. PERFORMING ORGANIZATION NAME(S) AND ADDRESS(ES) Air Force Institute of Technology, WPAFB OH 45433-6583				8. PERFORMING ORGANIZATION REPORT NUMBER AFIT/GSO/ENS/90D-18	
9. SPONSORING / MONITORING AGENCY NAME(S) AND ADDRESS(ES)				10. SPONSORING / MONITORING AGENCY REPORT NUMBER	
11. SUPPLEMENTARY NOTES					
12a. DISTRIBUTION / AVAILABILITY STATEMENT Approved for public release; distribution unlimited				12b. DISTRIBUTION CODE	
13. ABSTRACT (Maximum 200 words) Using concepts from multivariate utility theory, basic orbital mechanics, and information regarding operational and planned meteorological satellites, this thesis develops a meaningful MOE to support high-level decision making regarding the allocation, acquisition, and operational deployment of space meteorological satellite (METSAT) assets. Satellite meteorological systems were chosen because of the ready availability of pertinent unclassified data. However, the methodology presented may be applied to any type of space system. <i>Keywords:</i>					
14. SUBJECT TERMS Multiattribute Utility Theory, Measures of Effectiveness, Satellites, Meteorology, Weather, <i>Theses. (JH) /</i>				15. NUMBER OF PAGES 140	
				16. PRICE CODE	
17. SECURITY CLASSIFICATION OF REPORT UNCLASSIFIED	18. SECURITY CLASSIFICATION OF THIS PAGE UNCLASSIFIED	19. SECURITY CLASSIFICATION OF ABSTRACT UNCLASSIFIED	20. LIMITATION OF ABSTRACT UL		